

Investigations on the Radiation Characteristics of CPW-fed Planar Antenna with Superstrates

Thesis submitted by

TONY D.

in partial fulfillment of the requirements for the award of the degree of

DOCTOR OF PHILOSOPHY

Under the guidance of

Dr. K. VASUDEVAN



Department of Electronics
Faculty of Technology
Cochin University of Science and Technology
Cochin - 682 022, Kerala, India

August 2019

Investigations on the Radiation Characteristics of CPW-fed Planar Antenna with Superstrates

Ph.D. Thesis under the Faculty of Technology

Author:

Tony D.

(University Registration Number: 3457)

Department of Electronics

Cochin University of Science and Technology

Cochin - 682 022, Kerala, India.

Email: pdtony@gmail.com

Supervisor:

Dr. K. Vasudevan

Professor

Department of Electronics

Cochin University of Science and Technology

Cochin - 682 022, Kerala, India.

Email:vasudevan@cusat.ac.in

Department of Electronics

Cochin University of Science and Technology

Cochin - 682 022, Kerala, India.

August 2019

Dedicated to All.....



DEPARTMENT OF ELECTRONICS
COCHIN UNIVERSITY OF SCIENCE AND TECHNOLOGY
COCHIN-682 022

Dr. K. Vasudevan
(Supervising Guide)
Professor
Department of Electronics
Cochin University of Science and Technology

Certificate

This is to certify that this thesis entitled “**Investigations on the Radiation Characteristics of CPW-fed Planar Antenna with Superstrates**” is a bonafide record of the research work carried out by Mr. Tony D. under my supervision in the Department of Electronics, Cochin University of Science and Technology. The results embodied in this thesis or parts of it have not been presented for the award of any other degree.

I further certify that the corrections and modifications suggested by the audience during the pre-synopsis seminar and recommended by the Doctoral committee of Mr. Tony D. are incorporated in the thesis.

Cochin - 22
31st August 2019

Dr. K. Vasudevan

Declaration

I hereby declare that the work presented in this thesis entitled “**Investigations on the Radiation Characteristics of CPW-fed Planar Antenna with Superstrates**” is based on the original research work carried out by me under the supervision and guidance of Dr. K. Vasudevan, Professor, Department of Electronics, Cochin University of Science and Technology, Cochin-682 022 and has not been included in any other thesis submitted previously for the award of any degree.

Cochin - 22
31st August 2019

Tony D.
Department of Electronics,
CUSAT,
Cochin-22.

Acknowledgments

I remember with gratitude,

My supervising guide, Dr. K Vasudevan for the invaluable help and guidance given to me, spending his precious time, by discussing ideas, excellent suggestions and constant encouragement with an innovative mind and boundless knowledge.

Prof. James Kurian, Head, Department of Electronics, Cochin University of Science and Technology for his constant encouragement and support..

Prof. P Mohanan, Prof. C K Aanandan, and Prof. Supriya M H, for their help rendered to me in pursuing my research.

Prof. K T Mathew, Prof. P R S Pillai, Prof. Tessamma Thomas and Prof. Gopika Kumari for their valuable help during my research.

Dr. Sarin V P, Assistant Professor, Govt. college Chittur, Palakkad, for the wholehearted help given to me throughout my research by sharing invaluable knowledge, excellent suggestions, fruitful discussions and encouragement.

Faculty members Mr. Arun A Balakrishnan, Mr. Midhun Haridas, Dr. Deepthi Das Krishna, Dr. Nalesh, Dr. Tripti S Warriar and Mrs. Kumari Vidhu for their moral support during research.

Dr. Beena C, Librarian of CUSAT Central Library and Mr. Padamakumar Department Librarian for their very valuable help..

The members of management and staff, Viswajyothi College of Engineering and Technology for their boundless help given to me for completing the research.

Prof Jose P Varghese the former Head of the Department, Dept. of ECE, VJCET for all the valuable help.

My colleagues in the department Cyriac M Odackal, Nelson K J, Neeraj K Pushkaran, Lindo A O, Abhilash A P, Paulbert Thomas, Sruthi Dinesh, Ullas G Kalappura, Prasanth M N, Libimol V A, Sreekala P S, Dibin Mary George and Anju P Mathews.

Research scholars of the department especially, Suraj Kamal, Kurian Thomas, Manoj M, Satheesh Chandran, Aji George, Midhun M S, Athul Thomas, Prasanth P P, Navya Mohan, Ann Varghese, Remsha M, Vivek R, Vinisha C V,

Prakash K C, DrShameena, Anitha, P V,Sangeetha, Deepthi, Suja, Bindhya, Jisha, and Akhil.

Dr. Joe Jacob and Dr. Thomaskutty Mathew for their fruitful discussions and help.

My friends at SOE, CUSAT for their constant encouragement and support.

My friends Dr. Nishamol, Dr. Deepu, Dr. Sujith Raman, Dr. Laila and Dr. Jitha.

Mr. Anil P Y, Mr. Ibrahimkutty P M, Mr. Russel E P , Mr. Pradeep Kumar S and Mrs. Anitha who helped me a lot to complete the research.

My friend, Dr. Rajesh Cherian Roy, for his constant encouragement.

My family and in laws, especially my wife Smitha, children Liz and Jonathan, Mother Mariyamma Devassy, and Mother-in-law, Mary Sebastian for their deep love, care and patience.

Above all I thank Lord Almighty for helping me in each of my steps in my research.

Tony D.

INVESTIGATIONS ON THE RADIATION CHARACTERISTICS OF CPW-FED PLANAR ANTENNA WITH SUPERSTRATES

Coplanar Waveguide(CPW) transmission line consists of a conductor strip at the middle and two ground planes located on either side of the center conductor. The center conductor and the two ground planes lie in the same plane. It combines some of the advantages of microstrip and slot lines. The radiation loss and dispersion of cpw transmission line is less compared to a microstrip line. These transmission lines can be used to feed planar antennas. Planar antennas can be very small so that they are ideal for wireless applications. Radiation characteristics of planar antennas can be modified by the proper selection of superstrates.

Chapter 1 An overview of planar antennas and different methods used for varying antenna parameters are described in this chapter. Superstrate effect on antenna parameters are also discussed. The motivation behind present work is mentioned. Chapter concludes with the description of organization of the thesis.

Chapter 2 Earlier works related to cpw-fed antennas and effects of superstrates on the performance of the antenna characteristics are presented in this chapter.

Chapter 3 A brief account of simulation software used, antenna fabrication process and experimental set up for antenna parameters measurement are described in this chapter.

Chapter 4 Design and analysis of a CPW-fed planar antenna for dual-band operation is described in this chapter. The evolution of the antenna, the effect of varying different parameters on the performance of the antenna and the radiation pattern of the antenna are also discussed.

Chapter 5 For enhancing the radiation characteristics of antennas a superstrate printed with periodic pattern is used. Unit cell analysis of the pattern is performed and the values of relative permeability and relative permittivity are extracted. The effects of superstrate on the performance characteristics of antennas are investigated.

Chapter 6 A brief summary of main topics described in the previous chapters is presented here. Whether any promising paths are present for further improving the techniques presented in the thesis is also considered here.

List of Figures

1.1	Microstrip antenna.	5
1.2	Planar inverted F antenna	6
1.3	Coplanar waveguide transmission line.	6
1.4	CPW fed antenna	7
1.5	CPW line with centre conductor shorted to ground	9
1.6	CPW fed antenna	9
1.7	CPW fed dual band antenna	10
1.8	Antenna loaded with superstrate	10
3.1	E8362B Network analyzer	28
3.2	Anechoic chamber	30
4.1	An open ended CPW transmission line.	35
4.2	Reflection characteristics of an open ended CPW transmission line.	35
4.3	Surface current distribution of an open ended transmission line.	36
4.4	Open ended CPW transmission line with a short at 11.5 mm away from the bottom.	37
4.5	Reflection characteristics of an open ended CPW transmission line with a short at 11.5 mm away from the bottom.	37
4.6	Open ended CPW transmission line with a short at 7.5 mm away from the bottom.	38
4.7	Reflection characteristics of an open ended CPW transmission line with a short at 7.5 mm away from the bottom.	38
4.8	Open ended CPW transmission line with a short at 3.5mm away from the bottom.	39
4.9	Reflection characteristics of an open ended CPW transmission line with a short at 3.5 mm away from the bottom.	39
4.10	Antenna structure formed by carving out a slot and adding a short on an open ended CPW line. $W_f = 3$, $W_g = 16.6$, $g = 0.35$, $L_s = 13$, $S_w = 1$, $L_g = 15$ and $t = 1.5$ (All units are in mm)	40

4.11	Simulated reflection characteristics of the antenna structure formed by carving out a slot and adding a short on an open ended CPW line.	41
4.12	Measured reflection characteristics of the proposed antenna. . .	41
4.13	Impedance plot of the antenna structure formed by carving out a slot and adding a short on a CPW line.	42
4.14	Surface current at resonance frequency of the proposed antenna structure	42
4.15	Simulated 3D radiation pattern of the proposed antenna. . . .	43
4.16	Measured 2D radiation pattern of the proposed antenna in the XZ plane.	44
4.17	Measured 2D radiation pattern of the proposed antenna in the YZ plane.	45
4.18	Measured gain of the proposed antenna.	46
4.19	The configuration of the proposed dual band antenna.(a)Top view and (b)Side view. $L_g = 15$, $W_g = 16.6$, $S_w = 1$, $g = 0.35$, $t = 1.5$, $d = 3.95$, $W_f = 3$, $b = 1.5$, $L_{t1} = 7.5$, $L_{t2} = 5.3$, $h_t = 2$, $h = 1.6$, and $L_s = 15.15$ (Units in mm)	48
4.20	Evolution of the antenna.	49
4.21	Variation in S_{11} with L_s variation.	49
4.22	Variation in S_{11} with L_{t1} variation.	50
4.23	Variation in S_{11} with L_{t2} variation.	51
4.24	Measured and simulated reflection characteristics.	52
4.25	3D radiation pattern at 2.5 GHz.	53
4.26	3D radiation pattern at 5.21 GHz.	54
4.27	Measured 2D radiation pattern (a) at 2.5 GHz and (b) at 5.21 GHz.	55
4.28	Measured gain of the antenna for the lower frequency band. . .	56
4.29	Measured gain of the antenna for the upper frequency band. . .	56
5.1	Geometry of the unitcell. $p=14$, $a=6$ and $b=2$ (units in mm.)	61
5.2	Unitcell between two Floquet ports.	62
5.3	Reflection characteristics when properties of vacuum is assigned to unitcell.	64
5.4	Transmission characteristics when properties of vacuum is assigned to unitcell.	64

5.5	Effective permeability when properties of vacuum is assigned to unitcell.	65
5.6	Effective permittivity when properties of vacuum is assigned to unitcell.	65
5.7	Refractive index when properties of vacuum is assigned to unitcell.	66
5.8	Reflection characteristics for FR-4 equivalent of unitcell. . . .	67
5.9	Transmission characteristics for FR-4 equivalent of unitcell. . .	67
5.10	Refractive index for FR-4 equivalent of unitcell.	68
5.11	Effective permeability for FR-4 equivalent of unitcell.	68
5.12	Effective permittivity for FR-4 equivalent of unitcell.	69
5.13	Reflection and transmission characteristics of FR-4 with periodic pattern.	69
5.14	Refractive index of FR-4 with periodic pattern.	70
5.15	Effective permeability of FR-4 with periodic pattern.	71
5.16	Effective permittivity of FR-4 with periodic pattern.	71
5.17	Reference antenna loaded with 3×3 array periodic pattern. .	72
5.18	Reflection characteristics of reference antenna loaded with 3×3 array periodic pattern.	73
5.19	3D radiation pattern of the reference antenna loaded with 3×3 array periodic pattern.	74
5.20	Reference antenna loaded with 3×4 array periodic pattern. .	74
5.21	Reflection characteristics of reference antenna loaded with 3×4 array periodic pattern.	75
5.22	3D radiation pattern of the reference antenna loaded with 3×4 array periodic pattern.	75
5.23	Reference antenna loaded with 4×4 array periodic pattern. .	76
5.24	Reflection characteristics of reference antenna loaded with 4×4 array periodic pattern.	77
5.25	3D radiation pattern of the reference antenna loaded with 4×4 array periodic pattern.	77
5.26	Effective permittivity when periodicity $p = 15$ mm.	79
5.27	Effective permeability when periodicity $p = 15$ mm.	80
5.28	Refractive index when periodicity $p = 15$ mm.	80
5.29	Reflection/transmission characteristics when periodicity $p = 15$ mm.	81
5.30	Effective permittivity when periodicity $p = 16$ mm.	82

5.31	Effective permeability when periodicity $p = 16$ mm.	82
5.32	Refractive index when periodicity $p = 15$ mm.	83
5.33	Reflection/transmission characteristics when periodicity $p = 16$ mm.	83
5.34	Effective permittivity when periodicity $p = 13$ mm.	84
5.35	Effective permeability when periodicity $p = 13$ mm.	84
5.36	Refractive index when periodicity $p = 13$ mm.	85
5.37	Reflection/transmission characteristics when periodicity $p = 13$ mm.	85
5.38	Photograph of periodic pattern	86
5.39	Antenna loaded with periodic pattern	87
5.40	Reflection characteristics of the antenna with and without superstrate	88
5.41	Measured gain of the reference antenna with and without superstrate	88
5.42	Structure(a), 3D pattern(b), 2D pattern in XZ plane(c) and 2D pattern in YZ plane(d) of the reference antenna	89
5.43	Structure(a), 3D pattern(b), 2D pattern in XZ plane(c) and 2D pattern in YZ plane(d) of the reference antenna loaded with plain superstrate	90
5.44	Structure(a), 3D pattern(b), 2D pattern in XZ plane(c) and 2D pattern in YZ plane(d) of the reference antenna loaded with periodic pattern printed superstrate	91
5.45	Measured two-dimensional co-polarization radiation pattern with and without superstrate for (a)XZ plane and (b)YZ plane . . .	92
5.46	3D radiation pattern of the antenna at 2.5 GHz (a)without superstrate and (b)with superstrate	93
5.47	3D radiation pattern of the antenna at 5.63 GHz (a)without superstrate and (b)with superstrate	93
5.48	Antenna loaded with superstrate from bottom	94
5.49	Radiation pattern at 5.6GHz when superstrate is loaded from bottom	94
5.50	Antenna loaded with two layers of superstrate	95
5.51	Simulated and measured reflection characteristics for antenna loaded with two layers of superstrates	99

5.52	Measured 2D radiation pattern of reference antenna loaded with two layer superstrate at 2.5 GHz for (a) XZ plane and (b) YZ plane	99
5.53	Measured gain of reference antenna loaded with two layer superstrate	100

List of Tables

5.1	Comparison of superstrate size, resonance frequency, bandwidth and gain for different array sizes.	78
5.2	Variation of gain with spacing between antenna and superstrate.	79
5.3	Bandwidth variation with antenna and superstrate spacings h1=spacing between antenna and bottom superstrate in mm h2=spacing between top surfaces of two superstrates in mm	96
5.4	Resonance frequency variation with antenna and superstrate spacings h1=spacing between antenna and bottom superstrate in mm h2=spacing between top surfaces of two superstrates in mm	97
5.5	Gain variation with antenna and superstrate spacings h1=spacing between antenna and bottom superstrate in mm h2=spacing between top surfaces of two superstrates in mm	98

Contents

List of Figures	xi
List of Tables	xii
1 Chapter 1	1
1.1 Introduction	1
1.2 Historical timeline in communication	2
1.3 Planar antennas	4
1.3.1 Microstrip antenna	4
1.3.2 Planar inverted F-antenna	4
1.3.3 Coplanar waveguide fed antenna	5
1.4 Artificially engineered materials	5
1.5 Superstrates	8
1.6 Motivation of the work	8
1.7 Thesis organization	11
References	12
2 Chapter 2	14
2.1 Planar antennas	14
2.2 Superstrate loading of antennas	15
2.3 Parameter extraction	16
References	18
3 Chapter 3	26
3.1 Antenna fabrication method	27
3.2 CST studio suite	27
3.3 Experimental setup for antenna measurement	28
3.3.1 E8362B Network analyzer	28
3.3.2 Anechoic chamber	29
3.3.3 Turn table assembly	29
3.4 Antenna parameter measurements	29
3.4.1 Return loss and bandwidth measurement	29

3.4.2	Radiation pattern measurement	30
3.4.3	Antenna gain measurement	31
3.4.4	Antenna efficiency measurement	31
References	32
4	Chapter 4	33
4.1	Introduction	34
4.2	Open ended CPW transmission line	34
4.3	Transformation of a CPW transmission line into a radiating structure	35
4.4	Analysis of the position of the short on reflection characteristics.	36
4.5	Antenna design	39
4.5.1	Antenna geometry	40
4.5.2	Antenna reflection characteristics	40
4.5.3	Radiation characteristics of the antenna.	43
4.5.4	Gain and efficiency	43
4.6	CPW fed dual-band antenna	47
4.6.1	Antenna Geometry	47
4.6.2	Antenna evolution	47
4.6.3	Parametric analysis	48
4.6.4	Reflection characteristics	50
4.6.5	Radiation pattern	51
4.6.6	Gain and efficiency	52
4.7	Conclusion	57
References	57
5	Chapter 5	58
5.1	Introduction	59
5.2	Formation of unit cell	61
5.3	Antenna array size selection	72
5.3.1	Analysis with 3×3 unit cell periodic array pattern . .	72
5.3.2	Analysis with 3×4 unit cell periodic array pattern . .	73
5.3.3	Analysis with 4×4 unit cell periodic array pattern . .	76
5.4	Gain variation with spacing between antenna and superstrate	78
5.5	Unit cell periodicity selection	78

5.6	Analysis of antenna loaded with periodic pattern printed superstrate	86
5.6.1	Antenna loaded with superstrate	87
5.6.2	Gain	87
5.6.3	Radiation Pattern	89
5.7	Two layer superstrate	95
5.7.1	The effect of spacing variations on bandwidth	95
5.7.2	The effect of spacing variations on resonance frequency	96
5.7.3	The effect of spacing variations on gain	97
5.8	Conclusion	101
	References	101
6	Chapter 6	104
6.1	Thesis Highlights	105
6.2	Inferences from CPW fed single band antenna	105
6.3	Inferences from CPW fed dual band antenna	106
6.4	Inferences from effect of superstrates on performance characteristics of antennas	106
6.5	Suggestions for future work	107
7	List of publications	108
	Journals	108
	Resume	110

Chapter 1

Introduction

Contents

1.1	Introduction	1
1.2	Historical timeline in communication	2
1.3	Planar antennas	4
1.3.1	Microstrip antenna	4
1.3.2	Planar inverted F-antenna	4
1.3.3	Coplanar waveguide fed antenna	5
1.4	Artificially engineered materials	5
1.5	Superstrates	8
1.6	Motivation of the work	8
1.7	Thesis organization	11
	References	12

1.1 Introduction

Communication is undoubtedly the need of the hour. Everyone whom we come across in our daily life will be making use of one or the other of the available communication techniques. People living under the same roof find it easier to communicate with each other using modern gadgets than face to face conversation. All these wireless devices makes use of electromagnetic waves. Communication is made a reality in all these wireless devices by the transmission of electromagnetic waves. Antennas play a pivotal role in transmission of electromagnetic waves between these devices.

In this chapter major inventions and discoveries that had a great impact in the communication field is discussed first. It is followed by an introduction to planar antennas. One of the areas in which active research is going on is about artificially engineered materials. An introduction to artificially engineered materials is given. These materials can be used as a superstrate for antennas. The radiation characteristics of an antenna is greatly influenced by the presence of a superstrate. A brief discussion of various methods used in the design of superstrates is provided. The chapter concludes with the motivation of the work and a brief description of thesis organization.

1.2 Historical timeline in communication

Chronology given below highlights those inventions and discoveries that impacted the development of communications in a significant way.

Circa BC 2800 Greeks report attractive force of magnetite

Circa BC 600 Thales of Miletus describes how rubbing of amber develops a force which could lift certain light objects

AD 1745 German Ewald Georg von Kleist and Dutch scientist Pieter van Musschenbroek independently develop Leyden jar which could store electric charge

1752 By his famous kite experiment Benjamin Franklin proves that lightning is a form of electricity

1785 Charles Augustin de Coulomb formulates mathematical expression for force between two charges

1831 Michael Faraday demonstrates that a changing magnetic field induces an electric field

1873 James Clerk Maxwell introduces his famous equations

1887 Heinrich Hertz proves the existence of electromagnetic waves predicted by James Clerk Maxwell

1888 Nikola Tesla invents the alternating current

1895 Wilhelm Conrad Rontgen discovers X-Rays

1901 Guglielmo Marconi demonstrates wireless transmission across Atlantic Ocean

- 1906** Reginald Aubrey Fessenden invents amplitude modulation for radio transmission and performs first two-way radio telegraphic communication across the Atlantic Ocean
- 1919** Edwin Armstrong develops the superheterodyne radio receiver
- 1926** John Logie Baird demonstrates television working by transmitting TV images over telephone wires
- 1926** Shintaro Uda and Hidetsugu Yagi invents Yagi-Uda antenna
- 1933** Edwin Armstrong invents frequency modulation (FM) radio
- 1935** Robert Watson Watt invents radar
- 1947** American physicists John Bardeen, Walter Brattain and William Shockley at Bell Labs invents junction transistor
- 1957** Sputnik 1, the first artificial earth satellite is launched into an elliptical earth orbit by Soviet Union
- 1969** The Advanced Research Projects Agency Network (ARPANET), which was later evolved into INTERNET is launched by United States Department of Defence
- 1976** Steve Noznaik and Steve Jobs designs and markets APPLE-1, personal computer
- 1989** Tim Berners-Lee and Robert Caillian invents the World Wide Web
- 1991** Global System for Mobile Communications (GSM), a standard developed by European Telecommunications Standards Institute for 2G digital cellular networks is launched
- 1995** Interim Standard 95 (IS-95), first ever CDMA based 2G mobile telecommunications standard is launched
- 2001** Universal Mobile Telecommunications System (UMTS), a third generation mobile cellular system for networks based on the GSM standard is launched
- 2009** Long-Term-Evolution (LTE), a standard for wireless broadband communication for mobile devices and terminals based on GSM/EDGE and UMTS/HSPA is launched
- 2018** 5G NR radio access technology, designed to be the global standard for the air interface of 5G network is launched

1.3 Planar antennas

The term planar antenna can be considered as a quite general term. Antennas like printed microstrip patch antennas, slot antennas, planar inverted F antennas (PIFA), printed monopole antennas and printed dipole antennas come under the category of planar antennas. When we use the term printed antennas, we are referring to the technology used for fabrication of antennas. The term planar implies that the characteristics of the antenna are determined by two dimensions. Microstrip line, slot line, coplanar waveguide etc. are planar transmission lines. Antennas based on these transmission lines can be considered as planar antennas. Their characteristics are almost independent of the third dimension, say, thickness. The technology same as printed circuit board can be used for the manufacture of a large number of antennas all having the same performance characteristics. It is also possible to print these antennas on curved surfaces.

1.3.1 Microstrip antenna

Microstrip antenna is also called a patch antenna. It consists of a patch etched on one side of a substrate and ground plane on the other side. The patch is made of highly conductive material. The patch can assume a variety of shapes. Usually the height of the substrate is much smaller compared to the wavelength of operation. Feeding method for patch antennas include inset feed, quarter wavelength transmission line feed, coaxial cable feed and aperture feed. The advantages of microstrip antenna include low volume, low profile, low fabrication cost and easy integration with integrated circuits. Some of the disadvantages with microstrip antenna include narrow bandwidth, only half plane radiation and comparatively large ground plane. The structure of a microstrip antenna is shown in Fig1.1.

1.3.2 Planar inverted F-antenna

This is one of the antennas that became very popular with mobile phone market. The structure of the antenna looks like an inverted F and that is the reason why it is called planar inverted F antenna. The structure of the antenna consists of a ground plane, a top plate and a feeding wire to feed the top plate.

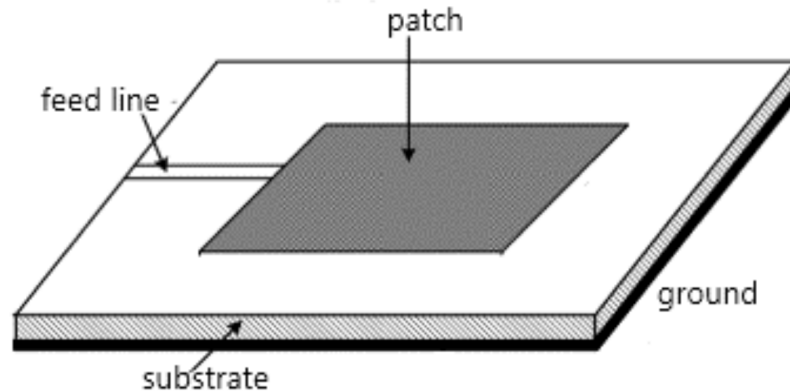


Figure 1.1: Microstrip antenna.

A shorting plate at one end is used to short the ground plane to the top plate. The planar inverted F antenna resonates at a quarter wavelength because of the presence of the shorting plate at one end. We can control the impedance of a PIFA by changing the distance between feed line and shorting plate. The main advantages of PIFA include low profile, omnidirectional pattern, easy integration to mobile phone housing and comparatively low backward radiation. The structure of a planar inverted F antenna is shown in Fig.1.2.

1.3.3 Coplanar waveguide fed antenna

The structure of a coplanar waveguide transmission line is shown in Fig.1.3. A coplanar waveguide transmission line consists of a centre conductor and two ground planes on either side of the centre conductor. Antennas with CPW fed are very popular for a variety of applications due to a lot of advantages like low radiation loss, wide bandwidth, easy integration with MMIC applications. A CPW fed antenna is shown in Fig.1.4.

1.4 Artificially engineered materials

When we apply an external electric or magnetic field, the response of atoms or molecules to this field varies from material to material. Their behaviour to electromagnetic fields may be described using Maxwells equations. To form these equations, we must consider very small volumes where we have enough

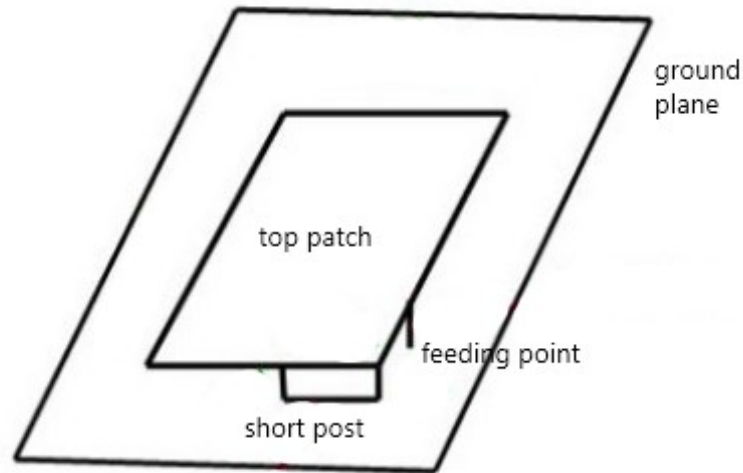


Figure 1.2: Planar inverted F antenna

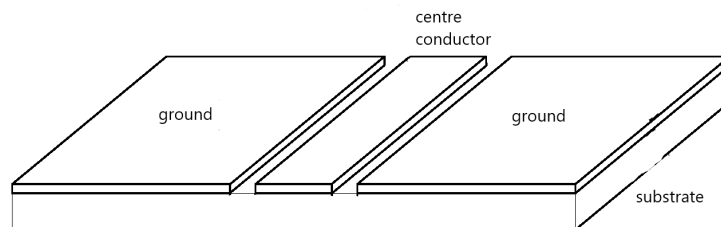


Figure 1.3: Coplanar waveguide transmission line.

number of polarizable or magnetisable atoms or molecules. Over these small volumes, we will consider the average of electric and magnetic fields. Then the permittivity(ϵ) and permeability(μ) can be defined for the material. Materials can be characterized in terms of μ and ϵ . In a similar manner, when we consider artificially engineered materials, we will assume that their structural units are much larger compared with atomic scale but much smaller compared to the operating wavelength. Hence just like ordinary materials, terms similar

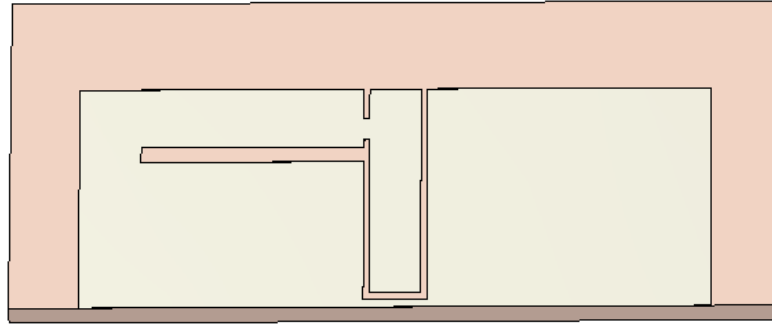


Figure 1.4: CPW fed antenna

to permittivity and permeability can be used to describe such materials. When the operating wavelength is very large, materials consisting of small elements behave as a continuous media. Let us consider an artificially engineered material. When electromagnetic wave falls onto this material, scattering occurs. Now let us replace the artificially engineered material with a new medium such that when EM wave falls onto it, we get the same scattered fields. Then the newly introduced medium can be considered as an effective medium and the medium will be characterized by its effective permittivity and permeability. The reason why we use artificially engineering materials is that in the microwave frequency range, naturally occurring materials may not have the desired value of permittivity or permeability. But an artificial material will have electric and magnetic properties that are not readily available in nature. By proper design we can have an artificially engineered material with desired value of effective permittivity or permeability. One of the methods to engineer artificial materials is to use a periodic pattern in a host medium. One such element in a periodic pattern is called a unit cell. We will design the unit cell such that the size of the unit cell will be very small compared to the operating wavelength. Various combinations of effective permittivity and permeability are possible for an artificially engineered material. We can have dielectric material with a high value of effective permittivity. It is also possible to design a magnetic material with high value of effective permeability. When the artificially engineered materials are polarized both electrically and magnetically when exposed to electromagnetic fields, they are called magneto-dielectric materials. Both effective permittivity and permeability of such materials will be

greater than unity. It is also possible to have materials with both effective permittivity and permeability less than one. Such materials are called DNG materials. All these artificially engineered materials can be used as superstrates for antennas. Radiation properties of antennas can be enhanced by using artificially engineered materials as superstrates.

1.5 Superstrates

A superstrate can be considered as a dielectric or a dielectric with a printed pattern, placed above an antenna. Initially the aim of using a superstrate was to protect antenna from environmental hazards. Later people have started making use of superstrates for improving antenna parameters. By the proper choice of superstrates, it is possible to enhance the gain and radiation resistance of an antenna. If the materials for the superstrates are properly selected, surface waves can be eliminated which will improve antenna efficiency. Mathematical proof of antenna parameter enhancements by superstrates were given by Nicolaos G. Alexopoulos and David R. Jackson. They used transmission line analogy for antenna-superstrate combination. Based on the above analogy high gain occurs when the transmission line act as a resonant circuit. Researchers started showing greater interest in using superstrates for enhancing gain of antennas. Several papers appeared in literature using electromagnetic band gap(EBG) structures as superstrates for enhancing gain of printed antennas. When we use an EBG structure, the gain enhancement is obtained because the EBG array helps in increasing equivalent aperture size of the antenna. Frequency selective surfaces(FSS) were also used for gain enhancement. When we use FSS as superstrate, a Fabry-Perot resonator is created between ground plane and the superstrate. The resonance condition in the Fabry-Perot resonator is the reason for the high gain of antenna-superstrate combination.

1.6 Motivation of the work

Compact antennas are an integral part of devices communicating over WLAN network. Hence designing of compact antennas that follow wireless commu-

nication standards is very important. A coplanar waveguide fed antenna can be made from a coplanar waveguide transmission line by a few modifications. If we short one of the ground of the CPW line to its centre conductor, a resonance can be generated(Fig.1.5).

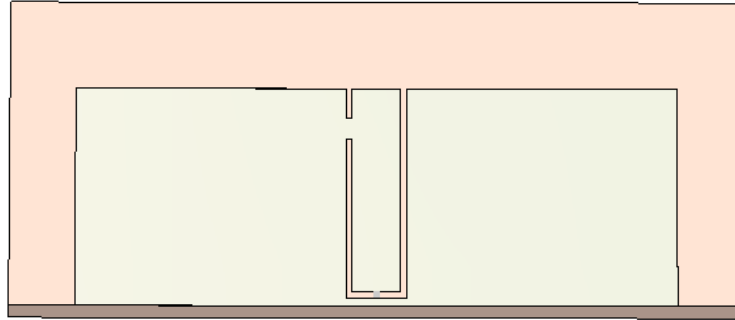


Figure 1.5: CPW line with centre conductor shorted to ground

The resonance can be shifted to lower frequency side by making a slot in the ground plane(Fig.1.6).

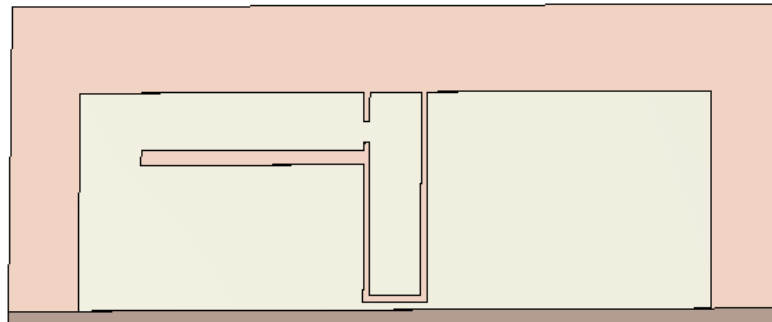


Figure 1.6: CPW fed antenna

The antenna can be made to work in an additional band by adding an asymmetric T shaped strip(Fig.1.7).

Different techniques are available for improving the gain of planar antennas. One of the method is to use a superstrate.

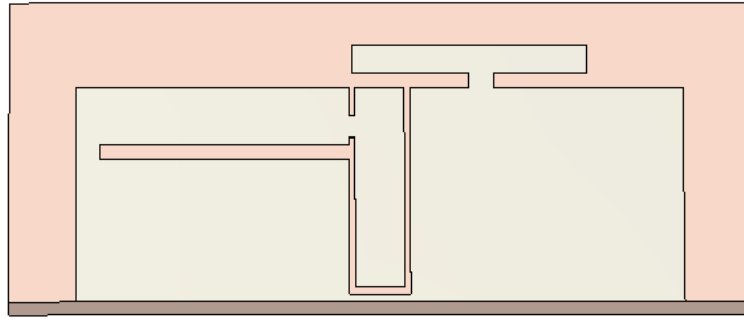


Figure 1.7: CPW fed dual band antenna

The effect of superstrate on radiation properties of an antenna can be further improved if we use an artificially engineered materials a superstrate(Fig.1.8). These artificially engineered materials are formed by printing a periodic pattern on a substrate. Depending upon the design the artificially engineered material will assume different values for its effective permeability and effective permittivity.

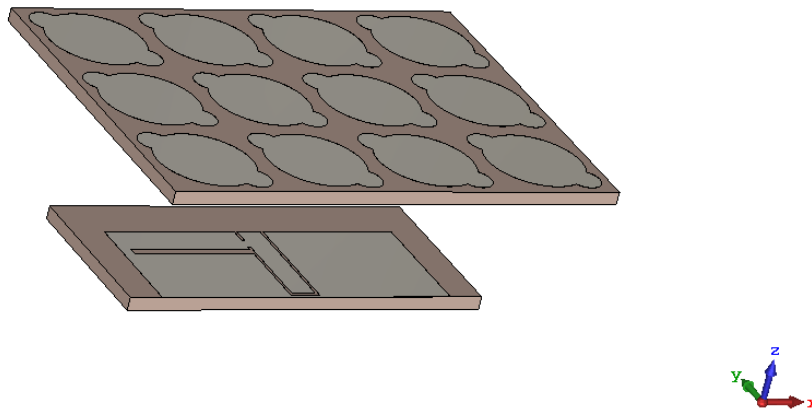


Figure 1.8: Antenna loaded with superstrate

1.7 Thesis organization

The thesis comprises of six chapters.

Chapter 1: Introduction

An overview of planar antennas and different methods used for varying antenna parameters are described in this chapter. Superstrate effect on antenna parameters are also discussed. The motivation behind present work is mentioned. Chapter concludes with the description of organization of the thesis.

Chapter 2: Literature Review

Earlier works related to cpw-fed antennas, effects of superstrates on the performance of the antenna characteristics and parameter extraction techniques are presented in this chapter.

Chapter 3: Methodology

A brief account of simulation software used, antenna fabrication process and experimental set up for antenna parameters measurement are described in this chapter.

Chapter 4: Design and analysis of CPW-fed planar antennas for wireless applications

Design and analysis of CPW-fed planar antennas for single band and dual-band operation is described in this chapter. The evolution of the antenna, the effect of varying different parameters on the performance of the antenna and the radiation pattern of the antenna are also discussed.

Chapter 5: Investigations on the effect of superstrate on the performance characteristics of antennas

For enhancing the radiation characteristics of antennas, a superstrate printed with periodic pattern is used. Unit cell analysis of the pattern is performed and the values of effective permeability and effective permittivity are extracted. The effects of superstrate on the performance characteristics of antennas are investigated.

Chapter 6: Summary and future prospects

A brief summary of main topics described in the previous chapters is presented here. Whether any promising paths are present for further improving the techniques presented in the thesis is also considered here.

References

- [1] Z. Chen and M. Chia, *Broadband Planar Antennas: Design and Applications*. Wiley, 2006.
- [2] K. Wong, *Planar Antennas for Wireless Communications*. Wiley Series in Microwave and Optical Engineering, Wiley, 2003.
- [3] R. Garg, P. Bhartia, I. Bahl, and A. Ittipiboon, *Microstrip Antenna Design Handbook*. Antennas and Propagation Library, Artech House, 2001.
- [4] I. Bahl and P. Bhartia, *Microstrip Antennas*. The Artech House Microwave Library, Artech House, Incorporated, 1980.
- [5] P. C. Bybi, G. Augustin, B. Jitha, C. K. Aanandan, K. Vasudevan, and P. Mohanan, “A quasi-omnidirectional antenna for modern wireless communication gadgets,” *IEEE Antennas and Wireless Propagation Letters*, vol. 7, pp. 505–508, 2008.
- [6] Chien-Jen Wang, Jin-Jei Lee, and Rey-Bin Huang, “Experimental studies of a miniaturized cpw-fed slot antenna with the dual-frequency operation,” *IEEE Antennas and Wireless Propagation Letters*, vol. 2, pp. 151–154, 2003.
- [7] N. Alexopoulos and D. Jackson, “Fundamental superstrate (cover) effects on printed circuit antennas,” *IEEE Transactions on Antennas and Propagation*, vol. 32, pp. 807–816, August 1984.
- [8] R. Mittra, Y. Li, and K. Yoo, “A comparative study of directivity enhancement of microstrip patch antennas with using three different superstrates,” *Microwave and Optical Technology Letters*, vol. 52, no. 2, pp. 327–331, 2010.
- [9] R. M. Hashmi, B. A. Zeb, and K. P. Esselle, “Wideband high-gain ebg resonator antennas with small footprints and all-dielectric superstructures,” *IEEE Transactions on Antennas and Propagation*, vol. 62, pp. 2970–2977, June 2014.

- [10] W. H. Syed and A. Neto, “Front-to-back ratio enhancement of planar printed antennas by means of artificial dielectric layers,” *IEEE Transactions on Antennas and Propagation*, vol. 61, pp. 5408–5416, Nov 2013.

Chapter 2

Literature review

Contents

2.1 Planar antennas	14
2.2 Superstrate loading of antennas	15
2.3 Parameter extraction	16
References	18

This chapter gives a review of developments that has taken place in the design of planar antennas. For enhancing gain and other radiation parameters, superstrates can be used. A review of developments that has taken place in the design of superstrates is done. When we use artificially engineered materials, extraction of their material parameters is important. Recent developments in the area of parameter extraction techniques is also discussed.

2.1 Planar antennas

The term planar antenna is used to denote a wide variety of antennas including microstrip antennas, slot antennas, monopole antennas, planar inverted F antennas, printed monopole antennas, and CPW fed antennas. The technology used in printed circuit board can be used for printing antennas onto a substrate. A review of literature in the area of planar antennas is discussed in this section.

Gain enhancement in microstrip antennas is discussed in [1–10].

In [1] a power amplifier is used as an active component in enhancing the gain of a patch antenna. The gain enhancement achieved is 13.65 dB

In [4] split ring resonators are used to generate a magnetic response and to get a negative value of permeability.

For enhancing gain and bandwidth a slot is loaded to a patch antenna in [6]. The antenna gain is enhanced from 4.24 dBi to 6.12 dBi.

Gain enhancement in CPW-fed antennas is discussed in [11–18]. In [11] artificial magnetic conductor structure, which is insensitive to polarization is designed. It is used as a reflector for a CPW-fed monopole antenna.

In [12] a hexagonal ring shaped defected ground structure is used for the gain and bandwidth enhancement of a cpw-fed monopole antenna.

A CPW-fed circularly polarized antenna is considered in [13]. Frequency selective surface is used to enhance the gain of the antenna.

Various design techniques for Planar inverted F antennas are discussed in [19–27]. A planar inverted F antenna for multiband mobile communications is presented in [20]. In order to obtain triple band operation, two parasitic elements are placed under the main radiating patch.

A planar inverted F antenna for ISM, HIPERLAN, UNII bands are presented in [22].

A triple band planar inverted F antenna is presented in [25]. To implement the antenna, radiating conductors are printed on both sides of an FR-4 substrate.

2.2 Superstrate loading of antennas

Early days a superstrate layer was used to protect printed circuit antennas from environmental threats. People thought keeping a material very near to an antenna which was not a part of the design of the antenna will adversely affect its performance. But N. G. Alexopoulos et al. proved that by the proper selection of superstrates, it is possible to enhance the radiation characteristics of an antenna.

Enhancing the gain of an antenna using super strates is discussed in [28–46]

In [40] authors demonstrate that by the proper selection of substrate and superstrate thickness resonance conditions can be generated which will greatly improve antenna gain, radiation resistance and efficiency.

When a printed antenna is loaded with a superstrate, transmission line analogy can be used to analyze the radiation from the antenna structure [41]. In this paper David R. Jackson et al. demonstrates how resonance condition can be used to generate large antenna gain

In [42] authors propose a metasurface based superstrate for improving gain and radiation efficiency of a multifrequency dipole antenna array. In the metasurface the resonating unit cells are formed by capacitively loaded strips and split ring resonators.

A comparative study of various types of superstrates in enhancing the directivity of a microstrip patch antenna is done in [43]. A frequency selective surface, a plain dielectric slab and double negative slab are used as superstrates. The authors demonstrate that level of directivity enhancement using a double negative superstrate is not as high as enhancement achieved using a plain dielectric slab or a frequency selective surface.

In [44] an artificial magnetic superstrate is designed with a modified split ring resonator. This engineered magnetic superstrate is used to enhance the gain and efficiency of a microstrip antenna. The authors claim an improvement in gain by 3.4 dB and efficiency by 17%

Properly designed metamaterial reflective surface can be used as a superstrate to enhance the gain, bandwidth and axial-ratio bandwidth of a circularly polarized patch antenna [45]. The metamaterial reflective surface is designed with a high value of epsilon and mu near zero.

Enhancing the gain of an aperture coupled microstrip antenna by loading the antenna with a dielectric superstrate is explained in [46]. The authors have analyzed how radiation properties of the antenna is affected with variation in superstrate size, thickness and spacing height.

2.3 Parameter extraction

When materials which consists of small elements are operated in the long wavelength region, their response will be that of a continuous media. Therefore their behaviour can be characterized effective permeability and effective permittivity. The material behaviour is similar to a homogenous material. The role of small elements will be that of atoms or molecules in a homogenous material. The material with small elements can be considered as an artificially engineered material whose behaviour will depend upon the values of effective permeability and effective permittivity.

From the previous paragraph it is clear that when we have an artificially engineered material, the extraction of effective permeability and permittivity

are very important. A review of literature dealing with parameter extraction techniques is discussed below

In [47] David R. Smith et al. performs a fullwave electromagnetic simulation to get local field. These fields are averaged to get macroscopic fields. Field averaging is used to retrieve effective parameters.

In [48] J M Lerat et al. uses field summation method to determine the effective permeability and effective permittivity of metamaterial structures. One of the limitation that the author report is if the metamaterial is thick, close to resonance frequency we cannot consider it as a homogenous material.

3D field simulation data is used for extracting effective permeability and effective permittivity in [49]. A homogenous slab is used for the equivalent representation of the metamaterial.

In [50], transfer matrix simulation of electromagnetic waves are performed to determine reflection and transmission coefficients. These are used to determine effective permeability and effective permittivity. Structures used for analysis include periodic arrangements of wires and split ring resonators.

The main drawbacks of Nicholson-Ross-Weir retrieval procedure is discussed in [51]. the authors prove that when the transmission coefficient is near to unity, the presence of a small noise or perturbation can cause instability.

Peter Markos et al. analyzes transmission properties of metamaterials with both permeability and permittivity negative([52]). Effective permeability and effective permittivity are extracted from transmission coefficients.

Xudong Chen et al. describes how to determine effective permeability and permittivity of a slab material from scattering parameters([53]). Method to select proper sign of effective impedance is also provided.

Issues associated with homogenization is discussed in [54].The process of extracting refractive index and impedance is presented. Physical significance of extracted values are also described.

In order to determine effective parameters of magnetic materials, a non resonant method is described in [55]. One of the advantages with this method is the absence of ripples in the evaluated material parameters.

When we retrieve material parameters which are complex quantities, ambiguity may result in branching. Determining the major branch with the help of Fourier Transform is explained in [56].

Homogenization method to extract effective parameters are presented in [57]. The authors make an effort to rectify the limitations of standard homogenization techniques.

W. B. Weir et al. describes a new method for determining permittivity and permeability [58]. In order to determine the parameters the material sample is inserted in a waveguide reflection and transmission coefficients are determined.

In order to retrieve effective parameters scattering parameters can be used. If the medium that we are considering is dispersive measurement of exact phase change will be difficult. When we solve for the wavenumber, a number of solutions will result since it is a complex quantity. Causality of the medium is considered in determining the predominant branch in [59].

In order to determine the effective parameters using scattering parameters, one of the requirement was normal incidence of electromagnetic waves into the sample. A more generalized approach is provided in [60].

References

- [1] F. Y. Zulkifli, M. Fahmi, Basari, and E. T. Rahardjo, "Active integrated microstrip mimo antenna for gain enhancement," in *2013 IEEE International Conference on Communication, Networks and Satellite (COMNETSAT)*, pp. 37–40, Dec 2013.
- [2] D. Guha, S. Chattopadhyaya, and J. Y. Siddiqu, "Estimation of gain enhancement replacing ptfе by air substrate in a microstrip patch antenna [antenna designer's notebook]," *IEEE Antennas and Propagation Magazine*, vol. 52, pp. 92–95, June 2010.
- [3] H. Wang, S. Liu, L. Chen, W. Li, and X. Shi, "Gain enhancement for broadband vertical planar printed antenna with h-shaped resonator structures," *IEEE Transactions on Antennas and Propagation*, vol. 62, pp. 4411–4415, Aug 2014.
- [4] Z. Liu, P. Wang, and Z. Zeng, "Enhancement of the gain for microstrip antennas using negative permeability metamaterial on low temperature co-fired ceramic (ltcc) substrate," *IEEE Antennas and Wireless Propagation Letters*, vol. 12, pp. 429–432, 2013.

-
- [5] A. J. Abdulqader and Y. Ahmed Ali, "Microstrip array antenna design with directivity enhancement using reflector surface," in *2018 International Conference on Advanced Science and Engineering (ICOASE)*, pp. 194–199, Oct 2018.
- [6] R. K. Prasad, D. K. Srivastava, and J. P. Saini, "Gain and bandwidth enhancement of rectangular microstrip antenna by loading slot," in *2016 International Conference on Innovation and Challenges in Cyber Security (ICICCS-INBUSH)*, pp. 304–307, Feb 2016.
- [7] C. N. Ineneji and M. Kusaf, "Gain enhancement in microstrip patch antenna using the multiple substrate layer method," in *2015 23rd Signal Processing and Communications Applications Conference (SIU)*, pp. 560–560, May 2015.
- [8] A. Rivera-Albino and C. A. Balanis, "Gain enhancement in microstrip patch antennas using hybrid substrates," *IEEE Antennas and Wireless Propagation Letters*, vol. 12, pp. 476–479, 2013.
- [9] H. Satow, E. Nishiyama, and I. Toyoda, "Gain enhancement of a dual feed microstrip array antenna using parasitic elements," in *2015 International Symposium on Antennas and Propagation (ISAP)*, pp. 1–4, Nov 2015.
- [10] V. P. Sarin and K. Vasudevan, "Compact high gain stacked offset broadband microstrip antennas as an alternative to normal stacked and array configurations," in *Proceedings of the 2012 IEEE International Symposium on Antennas and Propagation*, pp. 1–2, July 2012.
- [11] P. Prakash, M. P. Abegaonkar, A. Basu, and S. K. Koul, "Gain enhancement of a cpw-fed monopole antenna using polarization-insensitive amc structure," *IEEE Antennas and Wireless Propagation Letters*, vol. 12, pp. 1315–1318, 2013.
- [12] A. Saxena, S. Joshi, A. Gupta, S. Saxena, and D. Kumar, "Gain and bandwidth enhancement of cpw-fed patch antenna for wideband applications," in *2016 IEEE International Conference on Recent Trends in Electronics, Information Communication Technology (RTEICT)*, pp. 1622–1625, May 2016.

- [13] N. Kushwaha and R. Kumar, “On the gain enhancement of a wideband cpw-fed circularly polarized antenna using fss,” in *2015 IEEE MTT-S International Microwave and RF Conference (IMaRC)*, pp. 378–380, Dec 2015.
- [14] S. N. Islam, G. Sen, A. Banerjee, M. Kumar, and S. Das, “Design and gain enhancement of a cpw-fed dual band slot antenna using a metamaterial inspired superstrate,” in *2016 International Conference on Advances in Computing, Communications and Informatics (ICACCI)*, pp. 2539–2541, Sep. 2016.
- [15] A. Naghar, A. V. Alejos, M. Garcia Sanchez, O. Aghzout, and F. Falcone, “Stacked cpw-fed antenna for satellite applications with gain enhancement,” in *2015 IEEE International Symposium on Antennas and Propagation USNC/URSI National Radio Science Meeting*, pp. 2421–2422, July 2015.
- [16] S. R. Emadian, C. Ghobadi, J. Nourinia, M. H. Mirmozafari, and J. Pourahmadazar, “Bandwidth enhancement of cpw-fed circle-like slot antenna with dual band-notched characteristic,” *IEEE Antennas and Wireless Propagation Letters*, vol. 11, pp. 543–546, 2012.
- [17] N. A. Jan, M. Lashab, C. Zebiri, D. Linda, R. A. Abd-Alhameed, and F. Benabdelaziz, “Compact cpw antenna loaded with crlh-tl and ebg for multi-band and gain enhancement,” in *2016 Loughborough Antennas Propagation Conference (LAPC)*, pp. 1–4, Nov 2016.
- [18] F. Habib, M. Zafrullah, and M. K. Islam, “Gain and bandwidth enhancement of patch antenna fed by coplanar waveguide at 10ghz,” in *2009 Second International Conference on Computer and Electrical Engineering*, vol. 2, pp. 507–510, Dec 2009.
- [19] H. T. Chattha, M. Nasir, Q. H. Abbasi, Y. Huang, and S. S. AlJa’afreh, “Compact low-profile dual-port single wideband planar inverted-f mimo antenna,” *IEEE Antennas and Wireless Propagation Letters*, vol. 12, pp. 1673–1675, 2013.

- [20] F. N. M. Redzwan, M. T. Ali, M. N. M. Tan, and N. Miswadi, “Design of tri-band planar inverted f antenna (pifa) with parasitic elements for umts2100, lte and wimax mobile applications,” in *2015 International Conference on Computer, Communications, and Control Technology (I4CT)*, pp. 550–554, April 2015.
- [21] Z. Shao and Y. P. Zhang, “Miniaturization of differentially-driven microstrip planar inverted f antenna,” *IEEE Transactions on Antennas and Propagation*, vol. 67, pp. 1280–1283, Feb 2019.
- [22] H. Liu, Y. Chen, C. Wu, and P. Chiu, “Dual-band planar inverted-f antenna for application in ism, hiperlan, and unii,” in *The 8th European Conference on Antennas and Propagation (EuCAP 2014)*, pp. 2372–2374, April 2014.
- [23] Hoon Park, Kyungho Chung, and Jaehoon Choi, “Design of a planar inverted-f antenna with very wide impedance bandwidth,” *IEEE Microwave and Wireless Components Letters*, vol. 16, pp. 113–115, March 2006.
- [24] Zhu Qi, Fu Kan, and Liang Tie-zhu, “Analysis of planar inverted-f antenna using equivalent models,” in *2005 IEEE Antennas and Propagation Society International Symposium*, vol. 3A, pp. 142–145 vol. 3A, July 2005.
- [25] W. . Kwak, S. . Park, and J. . Kim, “A folded planar inverted-f antenna for gsm/dcs/bluetooth triple-band application,” *IEEE Antennas and Wireless Propagation Letters*, vol. 5, pp. 18–21, 2006.
- [26] M. I. Hossain, M. R. I. Faruque, and M. T. Islam, “Low sar planar inverted-f antenna for mobile phone,” in *2016 International Conference on Advances in Electrical, Electronic and Systems Engineering (ICAEES)*, pp. 572–576, Nov 2016.
- [27] S. Pflaum, R. Staraj, and G. Kossiavas, “Planar inverted f antenna circularly polarized for rfid applications,” in *Proceedings of the 2012 IEEE International Symposium on Antennas and Propagation*, pp. 1–2, July 2012.

-
- [28] A. Kumar and R. Mittra, “Gain and side lobe level enhancement of array antennas using metasurface superstrates,” in *2018 IEEE International Symposium on Antennas and Propagation USNC/URSI National Radio Science Meeting*, pp. 1503–1504, July 2018.
- [29] H. Vettikalladi, O. Lafond, and M. Himdi, “High-efficient and high-gain superstrate antenna for 60-ghz indoor communication,” *IEEE Antennas and Wireless Propagation Letters*, vol. 8, pp. 1422–1425, 2009.
- [30] J. H. Kim, C. Ahn, and J. Bang, “Antenna gain enhancement using a holey superstrate,” *IEEE Transactions on Antennas and Propagation*, vol. 64, pp. 1164–1167, March 2016.
- [31] L. Martin, E. Motta Cruz, B. Froppier, and T. Razban, “New heterogeneous superstrate high gain antenna,” in *2015 9th European Conference on Antennas and Propagation (EuCAP)*, pp. 1–5, April 2015.
- [32] A. K. Singh, M. P. Abegaonkar, and S. K. Koul, “High-gain and high-aperture-efficiency cavity resonator antenna using metamaterial superstrate,” *IEEE Antennas and Wireless Propagation Letters*, vol. 16, pp. 2388–2391, 2017.
- [33] M. Warad, A. Sharma, C. S. Prasad, and A. Biswas, “A high gain aperture coupled cylindrical dielectric resonator antenna with metamaterial superstrate,” in *2016 IEEE International Symposium on Antennas and Propagation (APSURSI)*, pp. 133–134, June 2016.
- [34] R. Singha and D. Vakula, “Compact ultra-wideband fractal monopole antenna with high gain using single layer superstrate,” *Microwave and Optical Technology Letters*, vol. 59, no. 2, pp. 482–488, 2017.
- [35] J. Ju, D. Kim, W. J. Lee, and J. I. Choi, “Wideband high-gain antenna using metamaterial superstrate with the zero refractive index,” *Microwave and Optical Technology Letters*, vol. 51, no. 8, pp. 1973–1976, 2009.
- [36] M. Sharifian Mazraeh Mollaei, E. Zanganeh, and M. Feshki Farahani, “Enhancement of patch antenna gain using cylindrical shell-shaped superstrate,” *IEEE Antennas and Wireless Propagation Letters*, vol. 16, pp. 2570–2573, 2017.

-
- [37] D. Bhattacharjee, T. Shaw, T. Das, and D. Mitra, "Gain enhancement of a slot antenna with a metamaterial superstrate structure," in *2015 IEEE Applied Electromagnetics Conference (AEMC)*, pp. 1–2, Dec 2015.
- [38] S. Chiu and S. Chen, "High-gain circularly polarized resonant cavity antenna using fss superstrate," in *2011 IEEE International Symposium on Antennas and Propagation (APSURSI)*, pp. 2242–2245, July 2011.
- [39] R. M. Hashmi, B. A. Zeb, and K. P. Esselle, "Wideband high-gain ebg resonator antenna employing an unprinted composite superstrate," in *2013 IEEE Antennas and Propagation Society International Symposium (APSURSI)*, pp. 278–279, July 2013.
- [40] N. Alexopoulos and D. Jackson, "Fundamental superstrate (cover) effects on printed circuit antennas," *IEEE Transactions on Antennas and Propagation*, vol. 32, pp. 807–816, August 1984.
- [41] D. Jackson and N. Alexopoulos, "Gain enhancement methods for printed circuit antennas," *IEEE Transactions on Antennas and Propagation*, vol. 33, pp. 976–987, Sep. 1985.
- [42] E. Senz, R. Gonzalo, I. Ederra, J. C. Vardaxoglou, and P. de Maagt, "Resonant meta-surface superstrate for single and multifrequency dipole antenna arrays," *IEEE Transactions on Antennas and Propagation*, vol. 56, pp. 951–960, April 2008.
- [43] R. Mittra, Y. Li, and K. Yoo, "A comparative study of directivity enhancement of microstrip patch antennas with using three different superstrates," *Microwave and Optical Technology Letters*, vol. 52, no. 2, pp. 327–331, 2010.
- [44] H. Attia, L. Yousefi, M. M. Bait-Suwailam, M. S. Boybay, and O. M. Ramahi, "Enhanced-gain microstrip antenna using engineered magnetic superstrates," *IEEE Antennas and Wireless Propagation Letters*, vol. 8, pp. 1198–1201, 2009.
- [45] K. L. C. S. Chaimool and P. Akkaraekthalin, "Simultaneous gain and bandwidths enhancement of a single-feed circularly polarized microstrip patch antenna using a metamaterial reflective surface," *Progress In Electromagnetics Research B*, vol. 22, pp. 23–37, 2010.

- [46] C. J. Meagher and S. K. Sharma, “A wideband aperture-coupled microstrip patch antenna employing spaced dielectric cover for enhanced gain performance,” *IEEE Transactions on Antennas and Propagation*, vol. 58, pp. 2802–2810, Sep. 2010.
- [47] D. R. Smith and J. B. Pendry, “Homogenization of metamaterials by field averaging (invited paper),” *J. Opt. Soc. Am. B*, vol. 23, pp. 391–403, Mar 2006.
- [48] J.-M. Lerat, N. Malljac, and O. Acher, “Determination of the effective parameters of a metamaterial by field summation method,” *Journal of Applied Physics*, vol. 100, no. 8, p. 084908, 2006.
- [49] G. Lubkowski, R. Schuhmann, and T. Weiland, “Extraction of effective metamaterial parameters by parameter fitting of dispersive models,” *Microwave and Optical Technology Letters*, vol. 49, no. 2, pp. 285–288, 2007.
- [50] D. R. Smith, S. Schultz, P. Markoš, and C. M. Soukoulis, “Determination of effective permittivity and permeability of metamaterials from reflection and transmission coefficients,” *Phys. Rev. B*, vol. 65, p. 195104, Apr 2002.
- [51] J. J. Barroso and A. L. de Paula, “Retrieval of permittivity and permeability of homogeneous materials from scattering parameters,” *Journal of Electromagnetic Waves and Applications*, vol. 24, no. 11-12, pp. 1563–1574, 2010.
- [52] P. Markoš and C. M. Soukoulis, “Transmission properties and effective electromagnetic parameters of double negative metamaterials,” *Opt. Express*, vol. 11, pp. 649–661, Apr 2003.
- [53] X. Chen, T. M. Grzegorzczak, B.-I. Wu, J. Pacheco, and J. A. Kong, “Robust method to retrieve the constitutive effective parameters of metamaterials,” *Phys. Rev. E*, vol. 70, p. 016608, Jul 2004.
- [54] C. R. Simovski, “Material parameters of metamaterials (a review),” *Optics and Spectroscopy*, vol. 107, p. 726, Dec 2009.
- [55] U. C. Hasar, “A microwave method for accurate and stable retrieval of constitutive parameters of low- and medium-loss materials,” *IEEE*

- Microwave and Wireless Components Letters*, vol. 20, pp. 696–698, Dec 2010.
- [56] N. A. Mortensen, M. Yan, O. Sigmund, and O. Breinbjerg, “On the unambiguous determination of effective optical properties of periodic metamaterials: a one-dimensional case study,” *Journal of the European Optical Society - Rapid publications*, vol. 5, no. 0, 2010.
- [57] A. Alù, “First-principles homogenization theory for periodic metamaterials,” *Phys. Rev. B*, vol. 84, p. 075153, Aug 2011.
- [58] W. B. Weir, “Automatic measurement of complex dielectric constant and permeability at microwave frequencies,” *Proceedings of the IEEE*, vol. 62, pp. 33–36, Jan 1974.
- [59] V. V. Varadan and R. Ro, “Unique retrieval of complex permittivity and permeability of dispersive materials from reflection and transmitted fields by enforcing causality,” *IEEE Transactions on Microwave Theory and Techniques*, vol. 55, pp. 2224–2230, Oct 2007.
- [60] J. Qi, H. Kettunen, H. Wallen, and A. Sihvola, “Compensation of fabryprot resonances in homogenization of dielectric composites,” *IEEE Antennas and Wireless Propagation Letters*, vol. 9, pp. 1057–1060, 2010.

Chapter 3

Methodology

Contents

3.1	Antenna fabrication method	27
3.2	CST studio suite	27
3.3	Experimental setup for antenna measurement . .	28
3.3.1	E8362B Network analyzer	28
3.3.2	Anechoic chamber	29
3.3.3	Turn table assembly	29
3.4	Antenna parameter measurements	29
3.4.1	Return loss and bandwidth measurement	29
3.4.2	Radiation pattern measurement	30
3.4.3	Antenna gain measurement	31
3.4.4	Antenna efficiency measurement	31
	References	32

The software and experimental methodology used for design and analysis of the proposed antennas are discussed in this chapter. Topics covered include antenna fabrication technology, CST software simulation tool and facilities used for antenna measurements. The techniques used for the measurement of various antenna parameters are also discussed.

3.1 Antenna fabrication method

One of the advantages associated with printed antennas is that they can be manufactured by the same technology used for printed circuit board. For antenna fabrication photolithographic technique can be used. With this technique high accuracy can be obtained for etched patterns. The various steps involved in the fabrication of the antenna using photolithographic technique is explained below. The geometry of the antenna to be printed is designed using computer. Negative mask of the geometry is printed on a butter paper. A copper clad lamination of suitable size is cleaned using suitable solvents to get rid of any chemical impurities present. A very thin layer of negative photo resist material is applied on the copper substrate. The mask prepared is properly placed over the copper clad and it is exposed to ultra violet light. The portion of the photo resist material getting exposed to UV light will be hardened. The clad is now immersed in a developer solution for few minutes to remove the photo resist material from the unexposed portions. The unwanted portion of the copper from the substrate can be removed by rinsing it using ferric chloride solution to get the required antenna geometry. The laminate is then washed with water and then cleaned using acetone to remove the hardened photo resist.

3.2 CST studio suite

CST studio suite is a software package which can be used for designing, analyzing and optimizing electromagnetics related systems. Different types of solvers are available with CST. Accurate results can be obtained for high frequency applications involving connectors, transmission lines, and antennas with the use of time domain solver. Frequency domain solver will be preferred for applications like simulation of dispersive materials, radar cross section calculations, unit cell analysis of infinite arrays and for electromagnetic field distributions at different frequencies. When we have highly resonant structures, different modes can be calculated efficiently using eigen mode solver. Before simulation depending up on our problem we have to specify different boundaries. For high frequency applications different types of boundaries include electric, magnetic, open, periodic and unit cell. When we use CST for

antenna analysis, almost all parameters of the antenna including 3D and 2D radiation pattern, antenna gain, efficiency, scattering parameters and surface currents can be simulated using CST. Using simulation software, optimization can be done before physically manufacturing the antenna.

3.3 Experimental setup for antenna measurement

The antenna characteristics to be measured are return loss, radiation pattern, gain and efficiency. Components that are a part of the experimental set up are discussed in this section.

3.3.1 E8362B Network analyzer

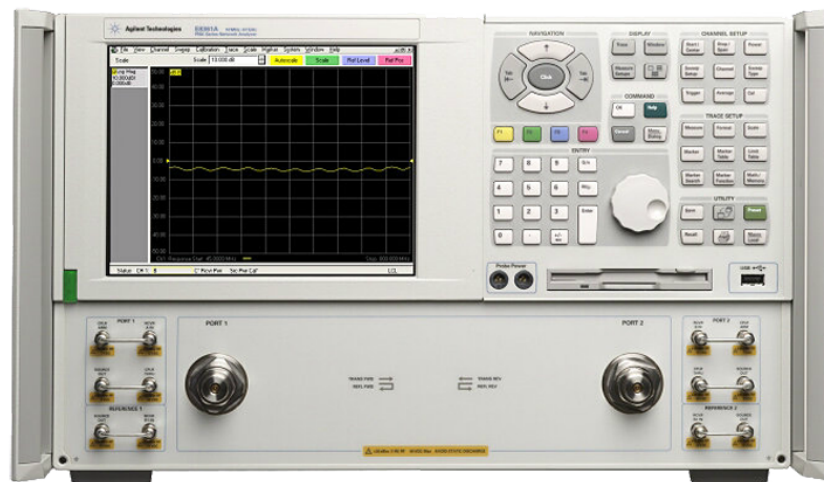


Figure 3.1: E8362B Network analyzer

Network analyzer can be used for measuring network parameters. It can be used for determining scattering parameters, verifying design simulations, checking component specifications etc. A vector network analyzer measures amplitude as well as phase. E8362B network analyzer is from Agilent Technologies which can be operated from 10 MHz to 20 GHz. Network analyzer

can be employed for the measurement of antenna parameters including return loss characteristics, radiation pattern, gain, and efficiency.

3.3.2 Anechoic chamber

If the testing of an antenna is carried out at outdoors, the measurements will be affected by electromagnetic interference. In order to minimize these interferences indoor anechoic chambers are used. In an anechoic chamber all the side walls, roof and the floor are covered with RF absorbing materials. The materials used are having a reflection coefficient of around -40 dB in the MHz frequency region. At microwave frequencies their performance will be much better. The RF absorbers used are of tapered shape to achieve good impedance matching with the microwave power falls into it. In order to prevent electromagnetic interferences from outside anechoic chamber is usually built into a screened room designed using continuous covering of highly conductive material. A photograph of anechoic chamber used for antenna measurements is shown in Fig.3.2.

3.3.3 Turn table assembly

For taking radiation pattern measurements the antenna under test is paced on a turn table. A stepper motor is attached to the turn table and the rotation is controlled using software. For radiation pattern measurement a standard wideband horn is used to receive signals from the antenna under test.

3.4 Antenna parameter measurements

3.4.1 Return loss and bandwidth measurement

The return loss characteristics of the antenna can be obtained from network analyzer. Before connecting the antenna under test the corresponding port cable is calibrated for frequency range of interest. Then the antenna is connected and scattering parameter corresponding to reflection characteristics (S_{11}) is measured. The range of frequencies over where return loss characteristics is



Figure 3.2: Anechoic chamber

within -10 dB is termed as bandwidth. The frequency at which return loss value is minimum is considered as the resonance frequency.

3.4.2 Radiation pattern measurement

In order to avoid external interferences, radiation pattern measurement is carried out in an anechoic chamber. The antenna under test is placed on a turn table whose rotation can be controlled by software. A standard wide

range horn is used as the receiving antenna. After connecting the antennas calibration is performed. Now the turn table is rotated and the measured results displayed in the network analyzer can be stored into a computer.

3.4.3 Antenna gain measurement

Antenna gain measurement is performed using a gain transfer method. The gain of the antenna under test is measured relative to another antenna whose gain is known. First we will mount 2 antennas on tripod with far field separation between antennas. One of the antennas is considered as reference antenna whose gain is accurately known. These antennas will be aligned in the direction of maximum intensity. In the network analyser frequency range of interest is selected and normalization is done. Now we will have response at 0 dB for the frequency range of interest. The next step is to replace the reference antenna with antenna under test. The value of scattering parameter S_{21} is recorded. This value represents the gain of the antenna relative to reference antenna. The gain of the antenna under test is obtained by adding gain of the antenna under test relative to the reference antenna with the gain of the reference antenna at every frequency point.

3.4.4 Antenna efficiency measurement

Wheeler cap method can be used to measure the efficiency of an antenna. In this technique two impedance measurements are performed. The first impedance measurement is performed with a cylindrical box completely enclosing the antenna and in the second case the impedance is measured without the cylindrical box. The conductive sphere is used to reflect all of the antenna radiation without much disturbance to near field. The test antenna behaves like a series resonant RLC circuit and the efficiency can be calculated using the following expression

$$\text{Efficiency} = \frac{R_{nocap} - R_{cap}}{R_{nocap}}$$

Where R_{nocap} represents the input impedance without the cap and R_{cap} represents the input impedance with cap.

References

- [1] H. A. Wheeler, "The Radiansphere around a Small Antenna," *Proceedings of the IRE*, vol. 47, no. 8, pp. 1325-1331, Aug. 1959.
- [2] Huang Y. (2016) Radiation Efficiency Measurements of Small Antennas. In: Chen Z., Liu D., Nakano H., Qing X., Zwick T. (eds) Handbook of Antenna Technologies. Springer, Singapore
- [3] M. A. Moharram and A. A. Kishk, "Modified Wheeler cap method for measurement of antenna efficiency," *2014 XXXIth URSI General Assembly and Scientific Symposium (URSI GASS), Beijing*, 2014, pp. 1-4.
- [4] Constantine A. Balanis, Antenna Theory: Analysis and Design, 4th Edition, *John Wiley and sons Inc.*, 2016
- [5] John D. Kraus and Ronald J. Marhefka, Antennas, 3rd Edition, *McGraw-Hill Education*, 3rd edition December 1, 2001

Chapter 4

Design and analysis of CPW-fed planar antennas for wireless applications

Contents

4.1	Introduction	34
4.2	Open ended CPW transmission line	34
4.3	Transformation of a CPW transmission line into a radiating structure	35
4.4	Analysis of the position of the short on reflection characteristics.	36
4.5	Antenna design	39
4.5.1	Antenna geometry	40
4.5.2	Antenna reflection characteristics	40
4.5.3	Radiation characteristics of the antenna.	43
4.5.4	Gain and efficiency	43
4.6	CPW fed dual-band antenna	47
4.6.1	Antenna Geometry	47
4.6.2	Antenna evolution	47
4.6.3	Parametric analysis	48
4.6.4	Reflection characteristics	50
4.6.5	Radiation pattern	51

4.6.6 Gain and efficiency	52
4.7 Conclusion	57
References	57

4.1 Introduction

Coplanar waveguide(CPW) transmission line consists of a centre conductor and two semi-infinite ground planes on either side. As a transmission line it has certain advantages such as it simplifies fabrication, it eliminates the need for via holes, it reduces radiation loss and cross talk effects between adjacent lines are very weak. A non-radiating CPW transmission line can be converted into an efficient radiator of electromagnetic waves by a few modifications. This chapter discusses these modifications to develop two antennas. The impedance bandwidth of the first antenna is from 2.47 GHz to 2.71 GHz. The second antenna is a dual band antenna with its lower frequency band from 2.31 GHz to 2.9 GHz and the upper frequency band from 4.65 GHz to 7.74 GHz. These antennas meet the specifications of many wireless standards including IEEE 802.11a, IEEE 802.11b, Hiperlan/2 and HiSWaNa

4.2 Open ended CPW transmission line

Consider a coplanar waveguide(CPW) transmission line. If there is any radiation from this transmission line, it will adversely affect its performance because we prefer minimum losses from a transmission line. Let us feed the transmission line from one end of the centre conductor and keep the other end open. When we consider the reflection characteristics with one end open, it can be seen that extending up to several gigahertz the signal is fully reflected, i.e., the radiation is minimum.

The scattering parameter corresponding to reflection, S_{11} , in Fig.4.2 is very close to 0 dB indicating that majority of the signal gets reflected. Therefore the radiation losses from this transmission line is minimum. Now let us take up the issue of converting this transmission line into an efficient radiating structure.

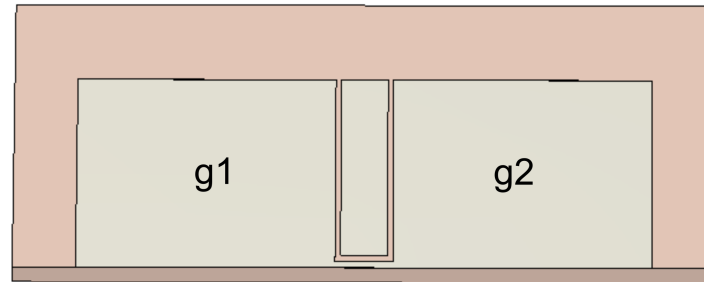


Figure 4.1: An open ended CPW transmission line.

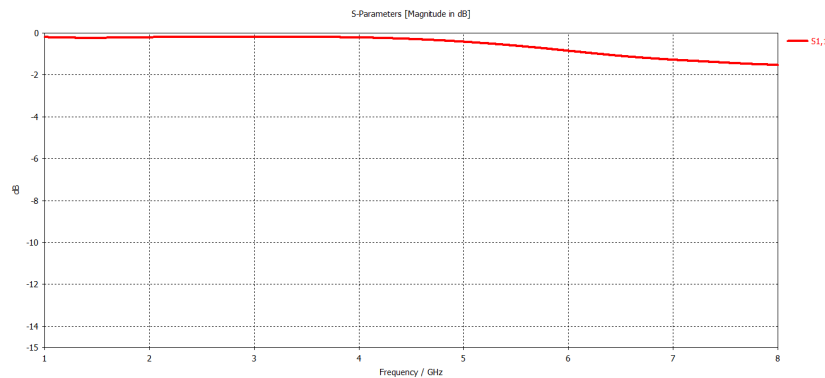


Figure 4.2: Reflection characteristics of an open ended CPW transmission line.

4.3 Transformation of a CPW transmission line into a radiating structure

When a structure radiates electromagnetic waves, we will call it an antenna. We can very easily transform the non-radiating CPW transmission line into a radiating structure by shorting one of the grounds to the centre conductor. The reflection characteristics of an open ended CPW transmission line is shown in Fig.4.2. From the figure it is clear that up to 8 GHz almost whole signal is reflected. Let us consider a particular frequency, say 3.1 GHz. The surface current distribution of the open ended transmission line at this frequency is shown in Fig.4.3.

Consider the gap between centre conductor and ground g1 on the left hand side of the centre conductor. The surface current flowing through the edges of

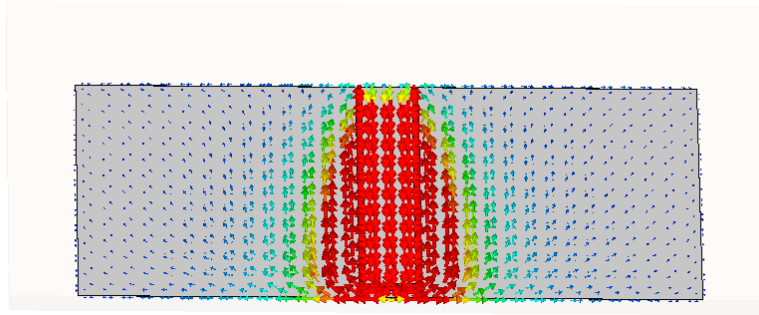


Figure 4.3: Surface current distribution of an open ended transmission line.

ground g_1 and the centre conductor near this gap are in opposite directions. Therefore the corresponding electric fields will also be in opposite directions. These opposing fields will cancel each other and no resultant field will be existing in the far field. Now consider the gap between centre conductor and ground g_2 . Similar explanation holds for surface current flowing through the edges on either side of this gap. Hence we can say that no radiation field exists for this structure in the farfield. If the current flow in the opposite directions at the edges near the gap is somehow disturbed, there will be a resulting electric field component in the far field. This is exactly what happens when we short one of the grounds to the centre conductor [1].

4.4 Analysis of the position of the short on reflection characteristics.

Our aim is to convert a non-radiating CPW transmission line into an efficient radiator. Hence at the required frequency of operation proper impedance matching is also important. In this section we are analysing the effect of position of the short between one of the grounds and centre conductor on reflection characteristics of the structure.

Let us first consider the case where the position of the short is 11.5 mm away from the bottom. The resulting structure is shown in Fig.4.4 and the corresponding simulated reflection characteristics is shown in Fig.4.5. A resonance is observed at 3.1 GHz. The scattering parameter for reflection, S_{11} has a value which is less than -10 dB at this resonance frequency.

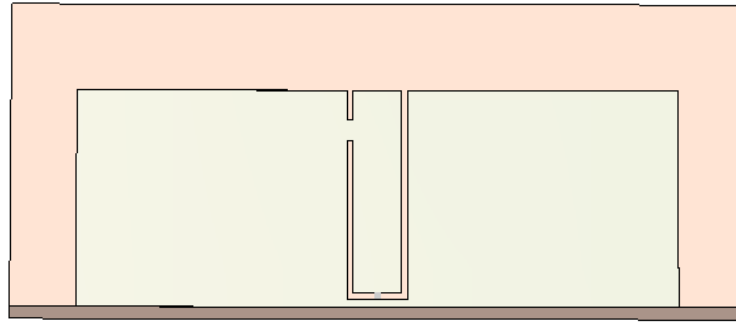


Figure 4.4: Open ended CPW transmission line with a short at 11.5 mm away from the bottom.

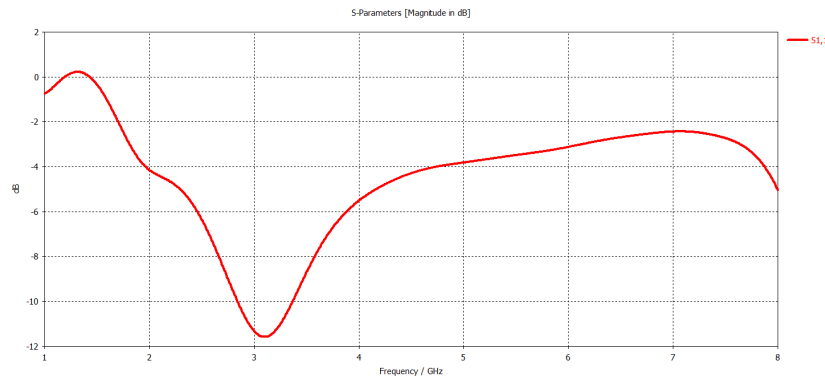


Figure 4.5: Reflection characteristics of an open ended CPW transmission line with a short at 11.5 mm away from the bottom.

Now consider the case where the position of the short is 7.5 mm away from the bottom. The resulting structure is shown in Fig.4.6 and the corresponding reflection characteristics is shown in Fig.4.7. In this case three resonances are observed, the first one at 1.22 GHz, the second one at 1.96 GHz and the third one at 3.1 GHz. The scattering parameter S_{11} of the all the three resonances are above -7 dB.

Now let us consider the case where the position of the short is 3.5 mm away from the bottom. The resulting structure is shown in Fig.4.8 and the corresponding reflection characteristics is plotted in Fig.4.9. Four resonances are observed at frequencies 1.14 GHz, 1.5 GHz, 1.99 GHz and 3.1 GHz. But

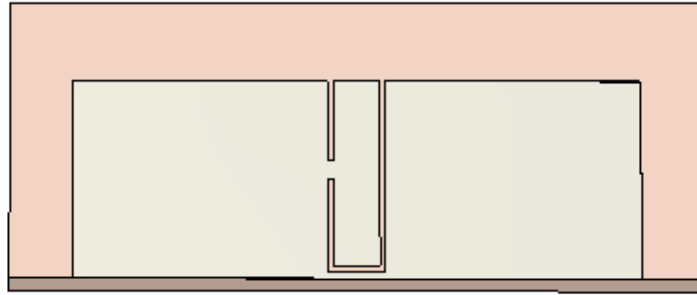


Figure 4.6: Open ended CPW transmission line with a short at 7.5 mm away from the bottom.

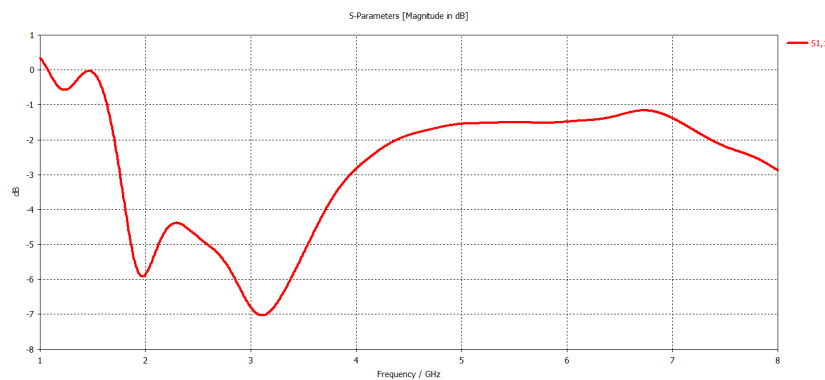


Figure 4.7: Reflection characteristics of an open ended CPW transmission line with a short at 7.5 mm away from the bottom.

only the resonance at 1.99 GHz has a value of S_{11} which is less than -10 dB.

In this section we have considered the effect of position of the short on reflection characteristics of the structure. The scattering parameter S_{11} has a value which is less than -10 dB for two cases, namely when the position of the short is 11.5 mm and 3.5 mm away from the bottom. The bandwidth obtained when the position of the short is 11.5 mm away from the bottom is 525 MHz. A bandwidth of 140 MHz is obtained when the position of the short is 3.5 mm away from the bottom.

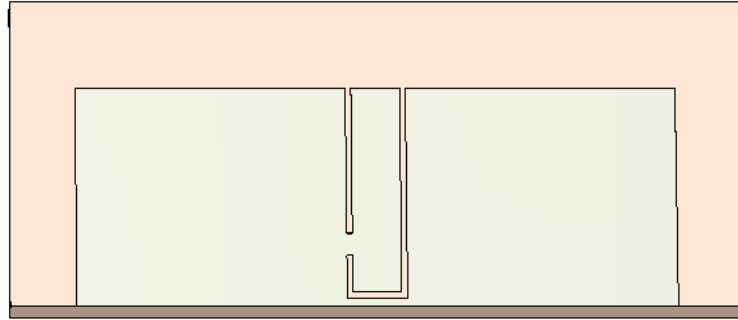


Figure 4.8: Open ended CPW transmission line with a short at 3.5mm away from the bottom.

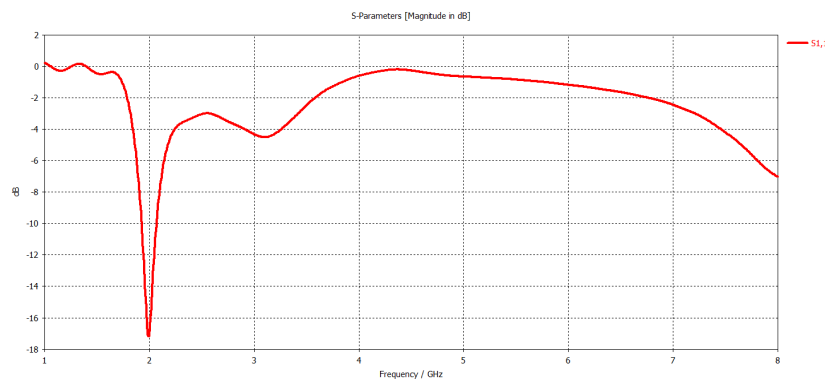


Figure 4.9: Reflection characteristics of an open ended CPW transmission line with a short at 3.5 mm away from the bottom.

4.5 Antenna design

In the previous section we discussed the effect of position of the short on reflection characteristics. For the antenna to be developed, let us choose the position of the short to be at 11.5 mm away from the bottom since it is having better bandwidth. The corresponding resonance observed is at 3.1 GHz. This can be brought to a lower frequency region by carving out a slot of length L_s in ground g1. The resulting antenna structure is shown in Fig.4.10.

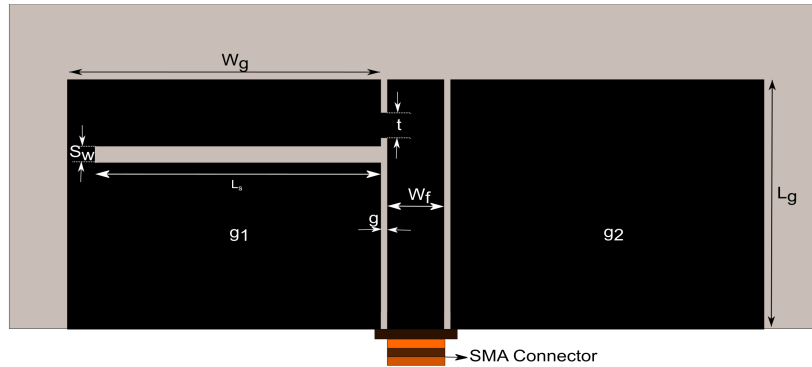


Figure 4.10: Antenna structure formed by carving out a slot and adding a short on an open ended CPW line. $W_f = 3$, $W_g = 16.6$, $g = 0.35$, $L_s = 13$, $S_w = 1$, $L_g = 15$ and $t = 1.5$ (All units are in mm)

4.5.1 Antenna geometry

Fig.4.10 depicts the geometry of the antenna. The antenna is fabricated on an FR-4 material of thickness 1.6 mm and relative permittivity 4.3. The widths W_g of two ground planes g1 and g2, width of the signal strip W_f , the gap between the signal strip and the two finite ground planes g are selected so that the impedance of the transmission line will be 50Ω . L_g is used to denote the length of the ground planes. L_s and S_w are used to denote the length and width of the slot carved out in ground g1. The width of the metal strip used to short feed line to ground g1 is denoted using t . With the introduction of the slot, the antenna resonant frequency is brought down to 2.58 GHz.

4.5.2 Antenna reflection characteristics

The simulated reflection characteristics of the antenna is shown in Fig.4.11. The -10 dB bandwidth of the antenna is 240 MHz from 2.47 GHz to 2.71 GHz. The measured reflection characteristics of the antenna is shown in Fig.4.12. From the plot the resonance frequency is observed at 2.62 GHz. The -10dB impedance bandwidth obtained varies from 2.484 GHz to 2.84 GHz with a bandwidth of 356 MHz. The impedance curve of the structure is shown in Fig.4.13. The marker denotes the impedance corresponding to the resonance frequency.

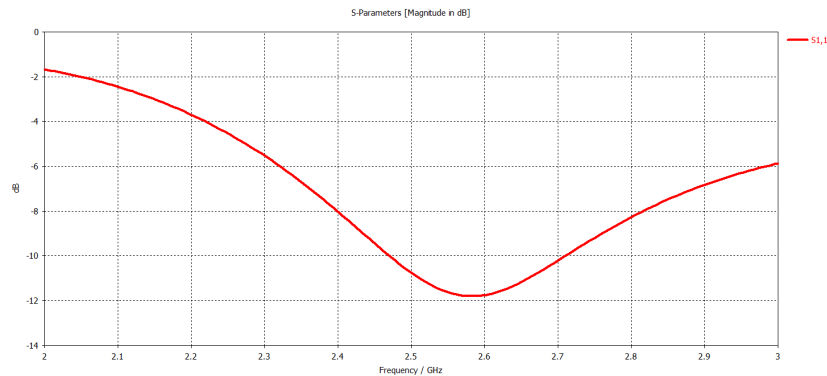


Figure 4.11: Simulated reflection characteristics of the antenna structure formed by carving out a slot and adding a short on an open ended CPW line.

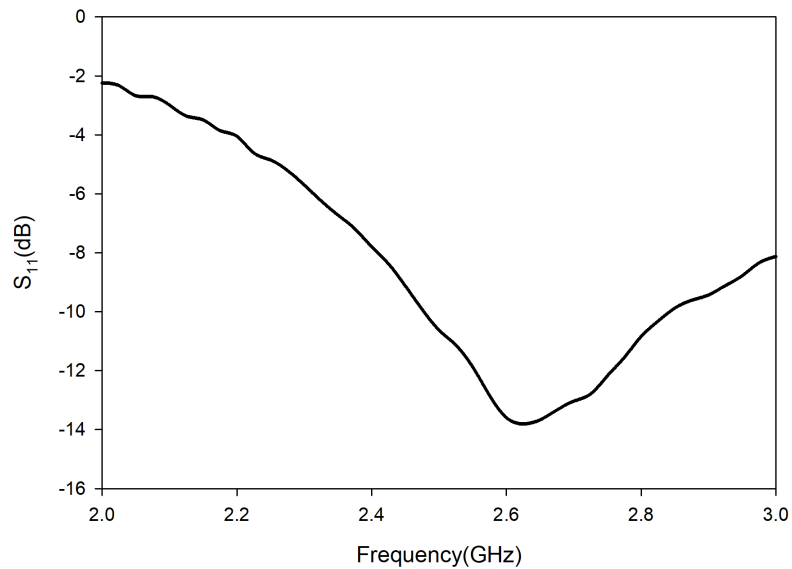


Figure 4.12: Measured reflection characteristics of the proposed antenna.

The antenna surface current distribution in the structure at resonance frequency is shown in Fig.4.14. It is clear from the figure that the current distribution in the centre conductor is not balanced by the current distribution in the ground g1 due to the presence of short and slot. This unbalanced current distribution is the cause of radiation.

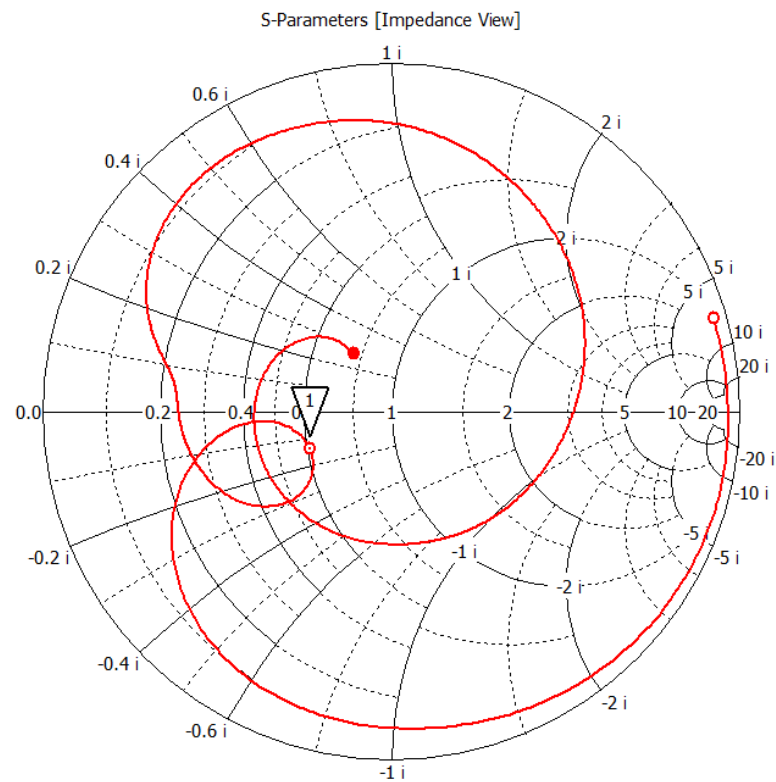


Figure 4.13: Impedance plot of the antenna structure formed by carving out a slot and adding a short on a CPW line.

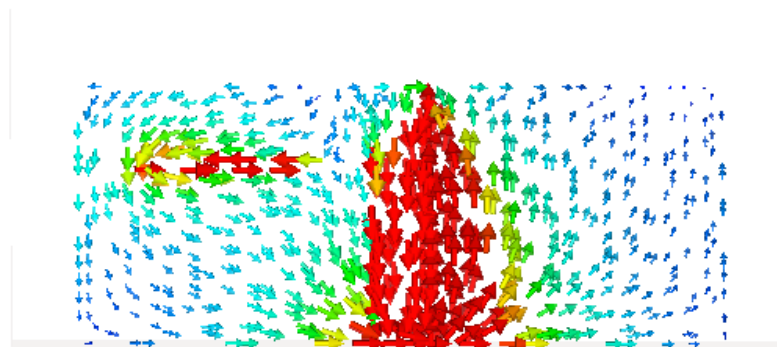


Figure 4.14: Surface current at resonance frequency of the proposed antenna structure .

4.5.3 Radiation characteristics of the antenna.

The software simulated 3D radiation pattern of the antenna is shown in Fig.4.15. The unbalanced current flow along the structure results in far field radiation with radiated fields exists in the YZ plane for a wide range of elevation angle theta.

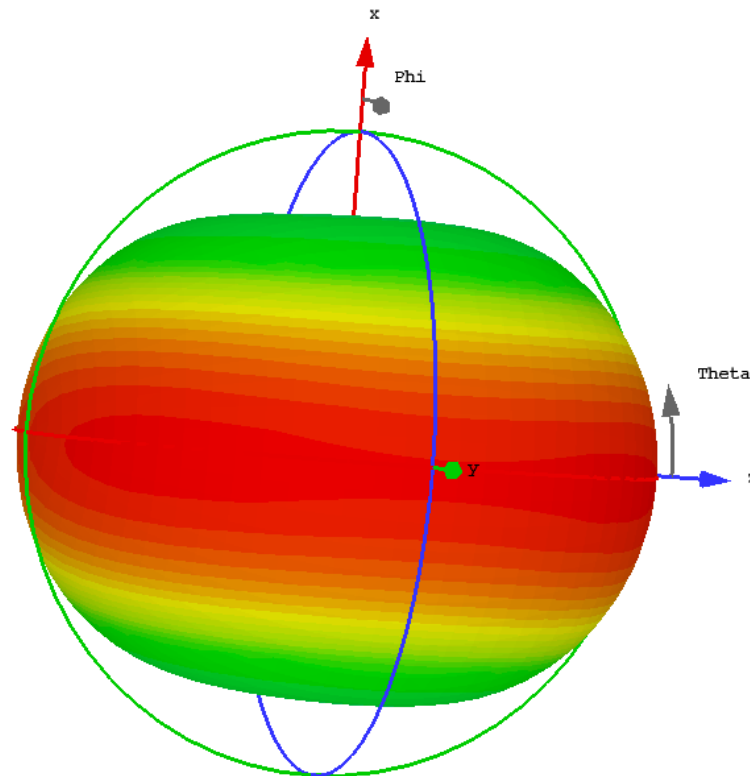


Figure 4.15: Simulated 3D radiation pattern of the proposed antenna.

The measured radiation pattern of the antenna at resonant frequency in XZ and YZ plane are shown in Fig.4.16 and Fig.4.17. In both planes cross polar isolation of more than 10 dB is observed along the bore-sight.

4.5.4 Gain and efficiency

The simulated gain obtained for the antenna at resonance frequency is 1.96 dB. The measured gain against frequency is plotted in Fig.4.18. At the resonance

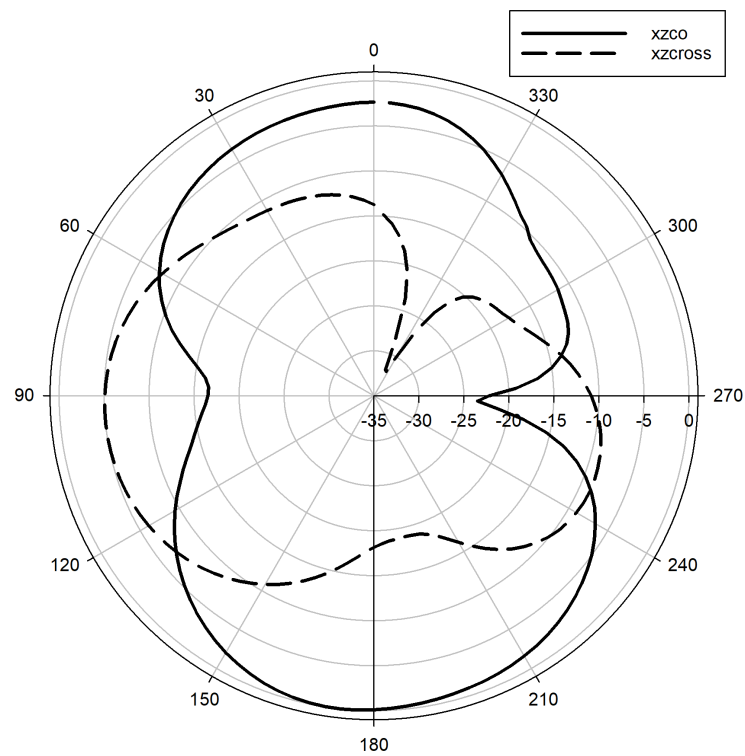


Figure 4.16: Measured 2D radiation pattern of the proposed antenna in the XZ plane.

frequency the measured gain obtained is 1.72 dB. The simulated radiation efficiency of the antenna is 92.13%

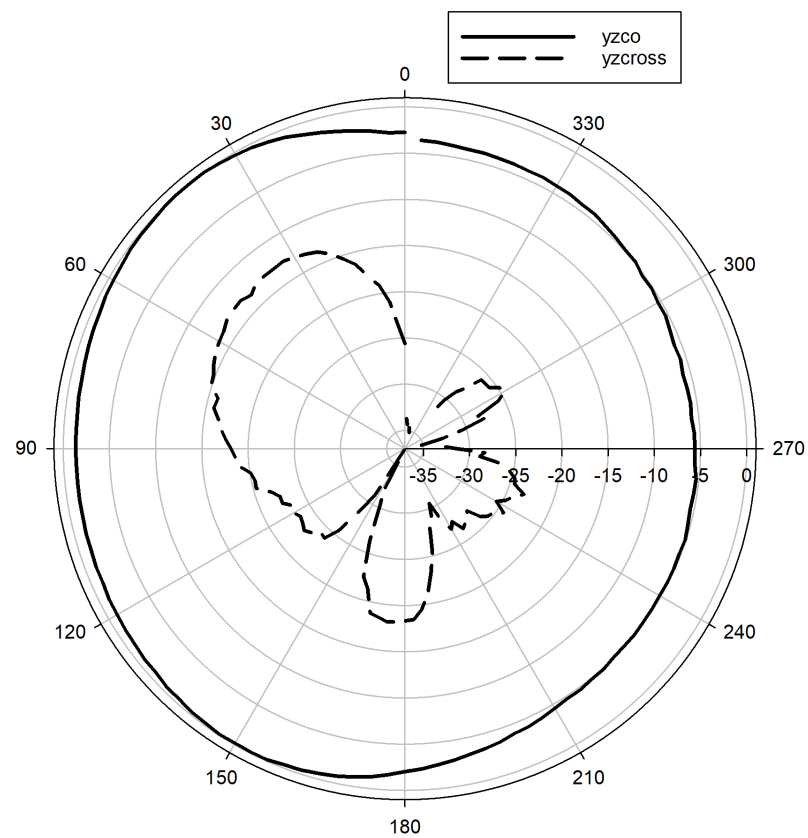


Figure 4.17: Measured 2D radiation pattern of the proposed antenna in the YZ plane.

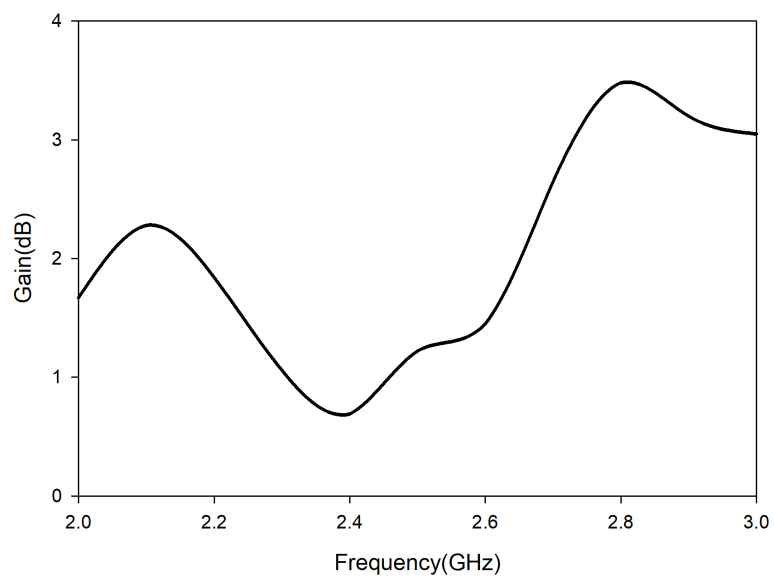


Figure 4.18: Measured gain of the proposed antenna.

4.6 CPW fed dual-band antenna

The antenna developed in the previous section had resonances with scattering parameter S_{11} less than -10 dB at 2.58 GHz and the next higher resonance is beyond 8 GHz. Impedance matching with S_{11} less than -10 dB and resonance frequency below 8 GHz which satisfies WLAN standard frequency bands can be obtained by suitable modifications. The modified antenna and its radiation characteristics are discussed in the following sections.

4.6.1 Antenna Geometry

Fig.4.19 shows the geometry of the proposed dual band antenna. The antenna is printed on an FR4 substrate of thickness 1.6 mm and relative permittivity 4.3. The size of the antenna is $36.9 \times 18 \times 1.6$ mm³. In order to feed the antenna, a 50 Ω transmission line consisting of a signal strip of width W_f and a gap distance of g between signal strip and ground plane is used. The two finite ground planes on either side of the CPW feed line are labelled g1 and g2. The length of each ground plane is denoted by L_g and its width is denoted by W_g . There is a slot of length L_s and width S_w on g1. The feed line is shorted to ground g1 using a metal strip of width t . An asymmetric T shaped strip is connected to ground g2. The horizontal portion of the T shaped strip has the dimensions of length $L_{t1} + b + L_{t2}$ and width h_t . The vertical portion of the asymmetric T has the dimensions of height a and width b . The vertical portion of T shaped strip is at a distance d from left end of ground g2.

4.6.2 Antenna evolution

The evolution of the antenna is shown in Fig.4.20. When the strip line is shorted to ground plane g1, a resonance is observed around 3.1 GHz. Addition of a slot to this structure shifts the resonance towards lower frequency region. An additional resonance is also observed at higher frequency. Finally when an asymmetric T shaped metal strip is added, two more resonances generated are merged with the already existing resonance to give a wider bandwidth in the upper frequency band.

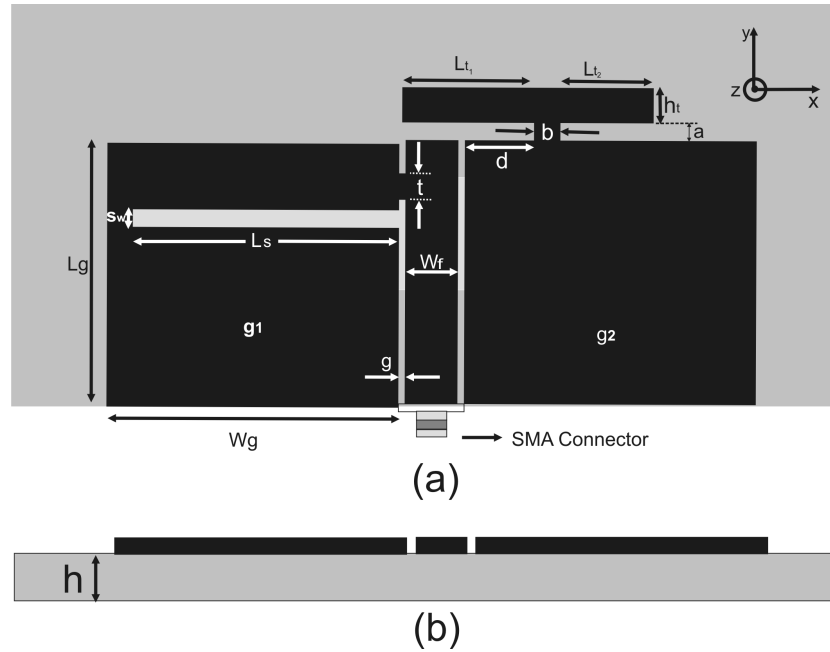


Figure 4.19: The configuration of the proposed dual band antenna. (a) Top view and (b) Side view. $L_g = 15$, $W_g = 16.6$, $S_w = 1$, $g = 0.35$, $t = 1.5$, $d = 3.95$, $W_f = 3$, $b = 1.5$, $L_{t1} = 7.5$, $L_{t2} = 5.3$, $h_t = 2$, $h = 1.6$, and $L_s = 15.15$ (Units in mm)

4.6.3 Parametric analysis

The radiation performance of an antenna depends upon a lot of parameters. In order to design an antenna with optimum features, parametric analysis can be performed. Software simulation is used for the analysis. In parametric analysis we will consider major parameters affecting the performance of the antenna. These parameters are varied and the results are analyzed to select the optimum value.

4.6.3.1 Effect of variation of length of slot on reflection characteristics

The effect of variation of length of the slot on the reflection characteristics of the antenna is studied. The results are illustrated in Fig.4.21. It is observed that the lower resonance at 2.5 GHz is not much affected by variation of the length of the slot. The higher resonances are shifted towards the lower side as

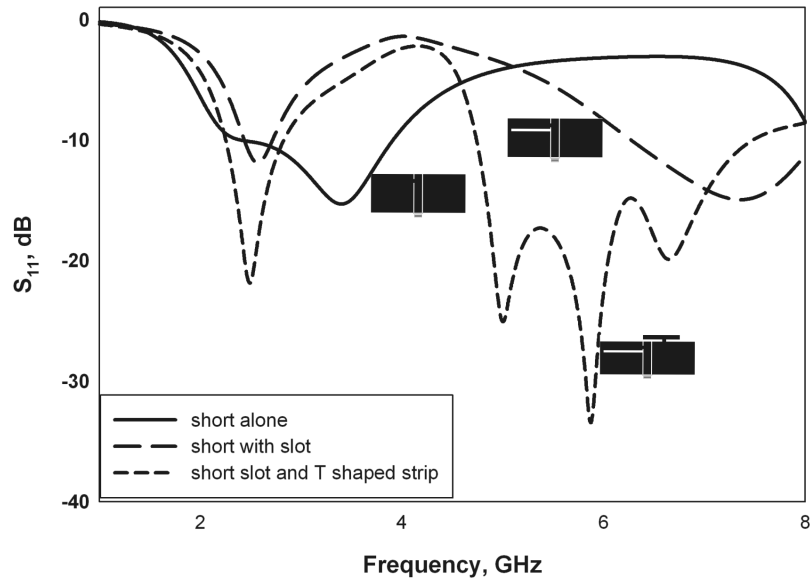


Figure 4.20: Evolution of the antenna.

the slot length is reduced. For both lower and upper resonances impedance matching becomes poorer with reduction in slot length.

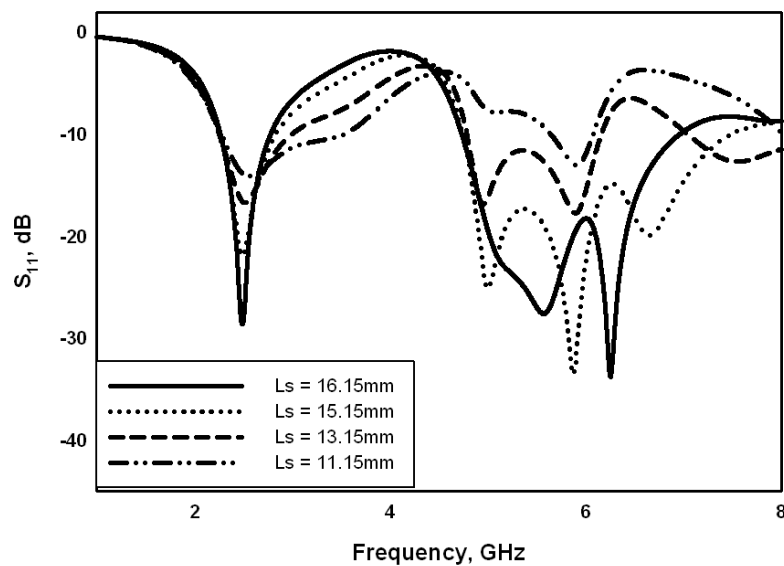


Figure 4.21: Variation in S_{11} with L_s variation.

4.6.3.2 Effect of variation of length of horizontal position of the T shaped strip

The variation of reflection characteristics with the length of horizontal portion of the T shaped strip is analyzed. Fig.4.22 illustrates the variation of S_{11} with L_{t1} . Resonance frequency in the lower band is not affected by change in L_{t1} , but matching is affected. In the upper band though the second and third resonances are not much affected by change in length, the first resonance is shifted towards lower frequency region with increase in length. Neither the impedance matching nor the resonant frequency of the lower resonance and the third resonance in the upper band are affected as a result of change in L_{t2} as illustrated in Fig.4.23. For the first and second resonances impedance matching becomes poorer with increase in L_{t2} .

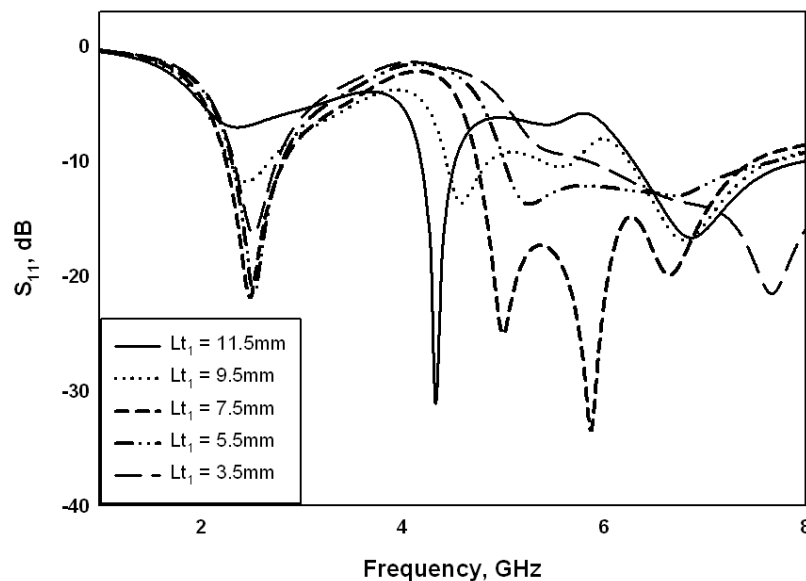


Figure 4.22: Variation in S_{11} with L_{t1} variation.

4.6.4 Reflection characteristics

Comparison of measured and simulated reflection characteristics is shown in Fig.4.24. It is observed that simulated and measured results are in good agreement. From the measured results it can be seen that the lower frequency

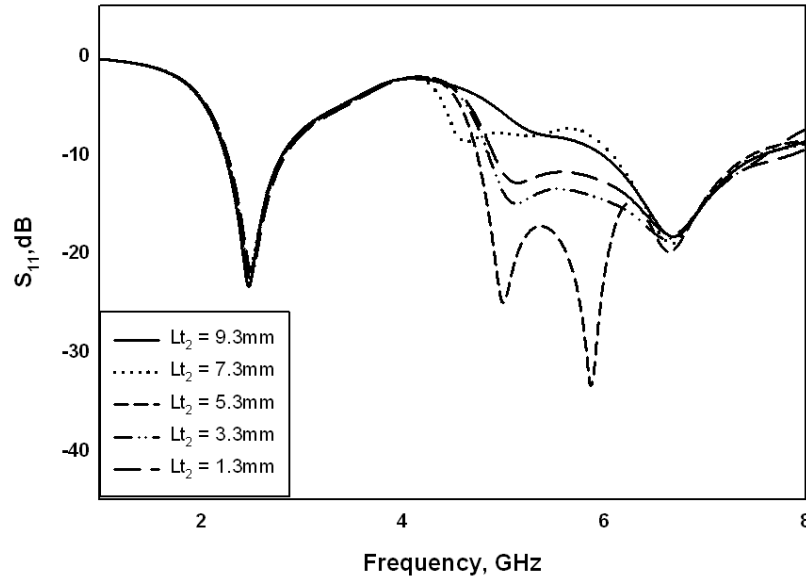


Figure 4.23: Variation in S_{11} with L_{t2} variation.

band has -10dB impedance bandwidth of 590 MHz (2.31 to 2.90 GHz) which satisfies the IEEE 802.11b WLAN standards. For the upper frequency band much wider band width is obtained. For it the -10dB impedance bandwidth is about 3.09 GHz (4.65 to 7.74 GHz) which satisfies the IEEE 802.11a WLAN standards as well as the Hiperlan/2 standard.

4.6.5 Radiation pattern

Simulated 3D radiation pattern at 2.5 GHz and 5.21 GHz are shown in Fig.4.25 and Fig.4.26 respectively. For the lower frequency band, in the far field, major radiation exists along YZ plane for a wide range of elevation angle theta. In the upper frequency region the major radiation of the antenna is not along a plane, but it spreads out. The measured 2D radiation pattern for both lower and upper frequency bands are plotted in Fig.4.27. The copolar and crosspolar radiation pattern in the XZ and YZ plane for the lower frequency band is illustrated in Fig.4.27(a) It can be seen from the figure that in the case of lower frequency band cross polar isolation of more than 10 dB is observed along the bore sight for both XZ and YZ planes. The copolar and crosspolar

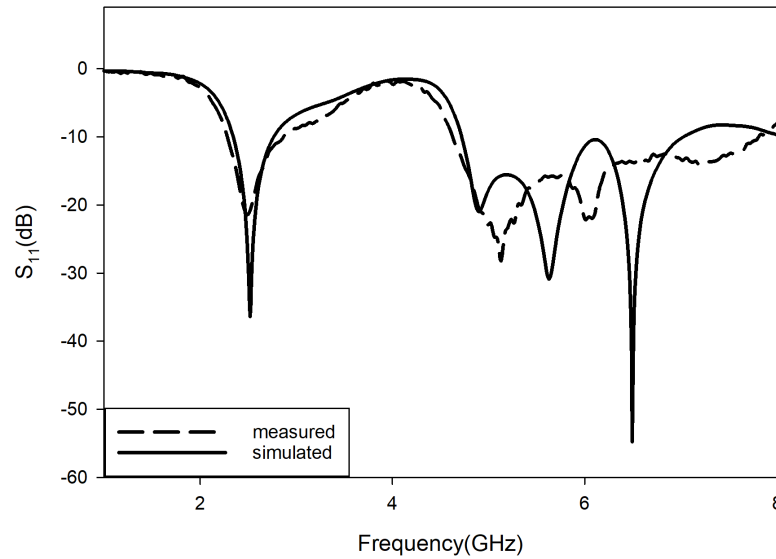


Figure 4.24: Measured and simulated reflection characteristics.

radiation pattern in the XZ and YZ plane for the upper frequency band is illustrated in Fig.4.27(b) Compared with lower frequency band the cross polar isolation observed for the upper frequency band is less.

4.6.6 Gain and efficiency

The simulated as well as measured antenna gain are analyzed. At resonance a gain of 1.96 dB is obtained for the lower frequency band and the corresponding value at the upper frequency band is 3.28 dB. The measured gain of the antenna versus frequency for the lower band is plotted in Fig.4.28 and for the upper band is plotted in Fig.4.29. The measured gain plotted for the upper band is not the maximum gain since there is a tilt for the major lobe in the upper frequency band. The simulated efficiency of the antenna at the resonance frequency for the lower frequency band is 92.51 % and that for the upper frequency band is 86.24 %

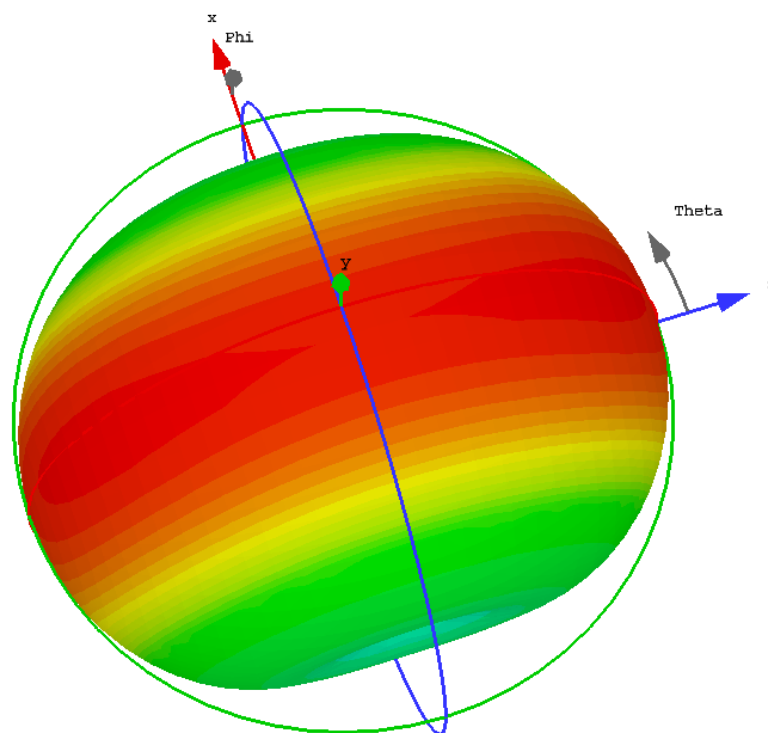


Figure 4.25: 3D radiation pattern at 2.5 GHz.

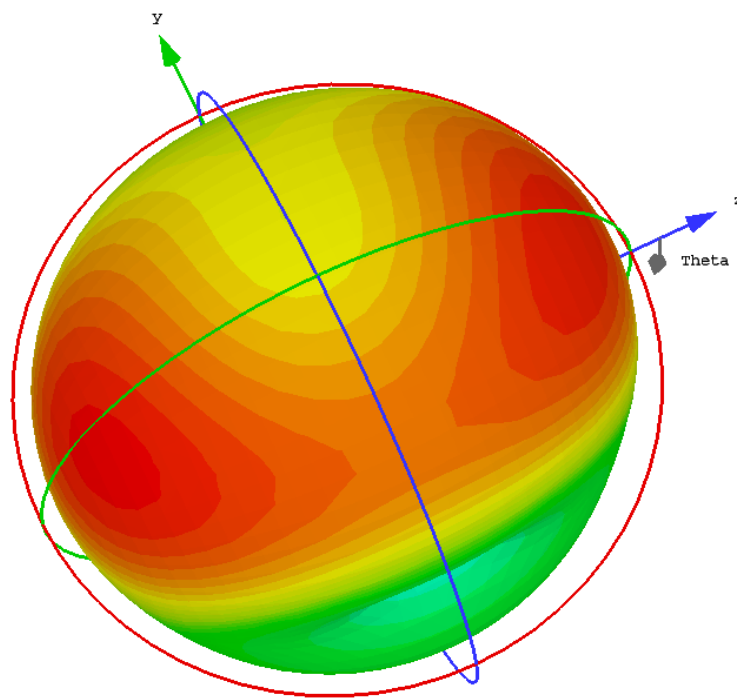


Figure 4.26: 3D radiation pattern at 5.21 GHz.

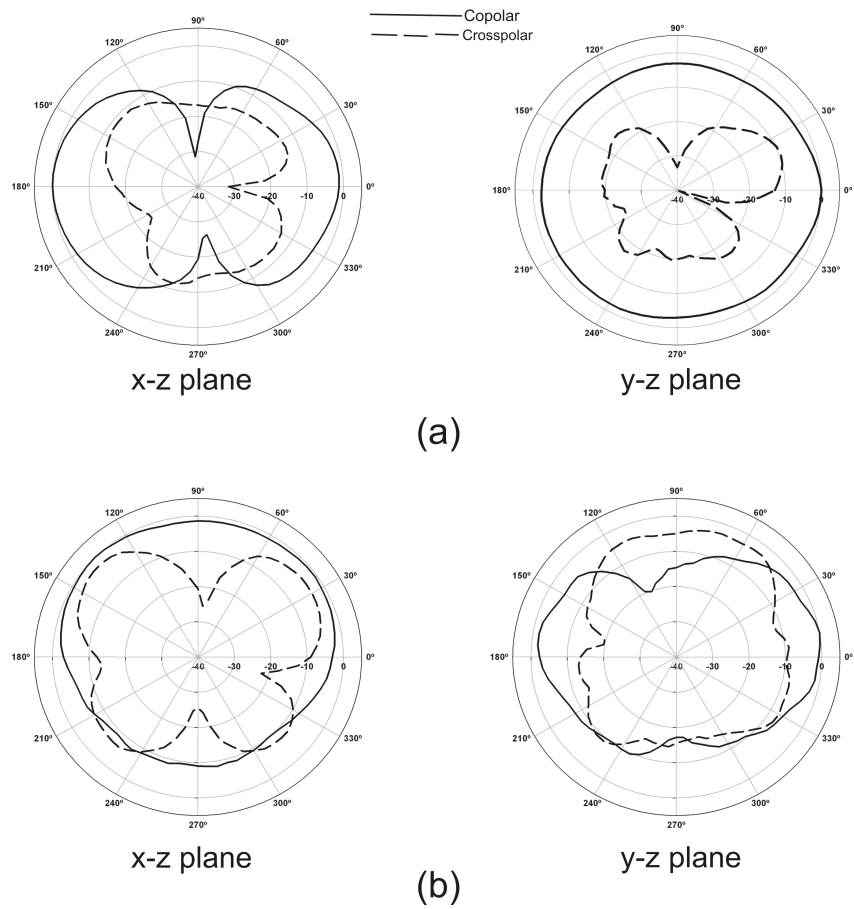


Figure 4.27: Measured 2D radiation pattern (a) at 2.5 GHz and (b) at 5.21 GHz.

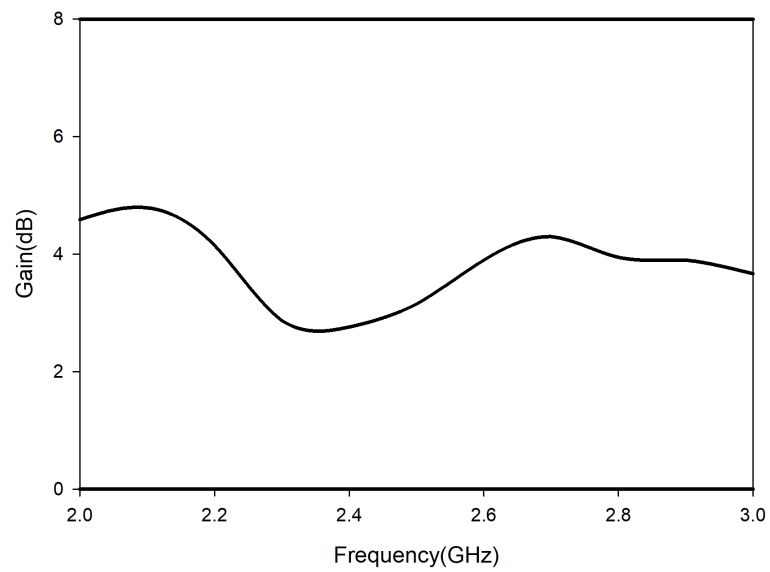


Figure 4.28: Measured gain of the antenna for the lower frequency band.

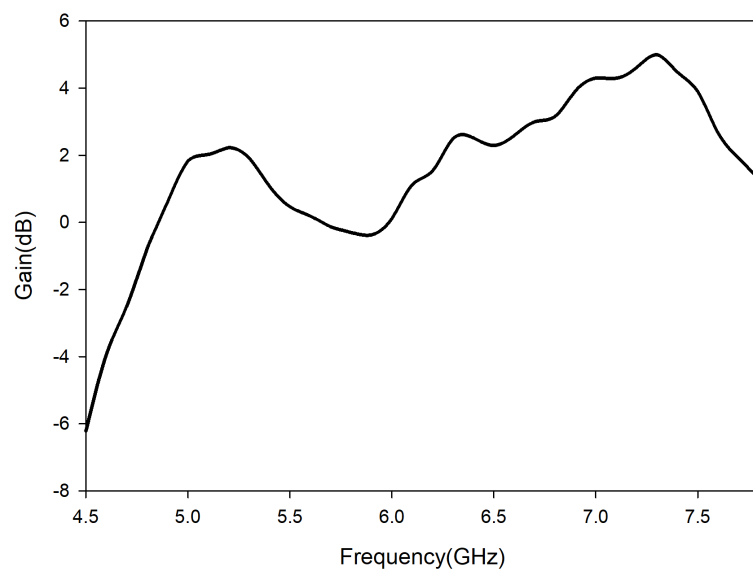


Figure 4.29: Measured gain of the antenna for the upper frequency band.

4.7 Conclusion

Conversion of CPW transmission line into an efficient radiator was discussed in this chapter. Two antennas were designed and their performance characteristics were analyzed. These antennas can be used for WLAN devices since it provides sufficient bandwidth for 2.4 and 5.2/5.8 GHz WLAN/HIPERLAN2/HiSWaNa standards.

References

- [1] P. C. Bybi, G. Augustin, B. Jitha, C. K. Aanandan, K. Vasudevan, and P. Mohanan, "A quasi-omnidirectional antenna for modern wireless communication gadgets," *IEEE Antennas and Wireless Propagation Letters*, vol. 7, pp. 505–508, 2008.
- [2] J. Wu, "2.4/5ghz dualband triangular slot antenna with compact operation," *Microwave and Optical Technology Letters*, vol. 45, pp. 81 – 84, 04 2005.
- [3] Chien-Jen Wang, Jin-Jei Lee, and Rey-Bin Huang, "Experimental studies of a miniaturized cpw-fed slot antenna with the dual-frequency operation," *IEEE Antennas and Wireless Propagation Letters*, vol. 2, pp. 151–154, 2003.
- [4] C. . Wu, "Dual-band cpw-fed cross-slot monopole antenna for wlan operation," *IET Microwaves, Antennas Propagation*, vol. 1, pp. 542–546, April 2007.
- [5] C.-Y. Huang, H.-C. Lin, and J.-S. Kuo, "Dual-band monopole antenna excited by a capacitive coupling feed for wlan applications," *Microwave and Optical Technology Letters*, vol. 49, no. 5, pp. 1135–1138, 2007.

Chapter 5

Investigations on the Effect of Superstrate on the Performance Characteristics of Antennas

Contents

5.1	Introduction	59
5.2	Formation of unit cell	61
5.3	Antenna array size selection	72
5.3.1	Analysis with 3×3 unit cell periodic array pattern	72
5.3.2	Analysis with 3×4 unit cell periodic array pattern	73
5.3.3	Analysis with 4×4 unit cell periodic array pattern	76
5.4	Gain variation with spacing between antenna and superstrate	78
5.5	Unit cell periodicity selection	78
5.6	Analysis of antenna loaded with periodic pattern printed superstrate	86
5.6.1	Antenna loaded with superstrate	87
5.6.2	Gain	87
5.6.3	Radiation Pattern	89
5.7	Two layer superstrate	95
5.7.1	The effect of spacing variations on bandwidth . . .	95

5.7.2	The effect of spacing variations on resonance frequency	96
5.7.3	The effect of spacing variations on gain	97
5.8	Conclusion	101
	References	101

5.1 Introduction

The performance of printed circuit antennas used for outdoor applications were affected by environmental hazards, severe weather conditions etc. A superstrate layer, also called a cover layer was introduced to protect antenna from these threats. Initially it was assumed that when we use a cover layer, it will adversely affect the performance of the antenna. Alexopoulos et al. showed that by the proper selection of superstrate layer it is possible to enhance the radiation parameters of printed antenna[1]. Jackson et al. used transmission line analogy to explain radiation from antenna structure. There the authors established two dual resonance conditions for substrate-superstrate printed antenna geometry by which better gain can be obtained for a high value of permittivity or permeability of the superstrate. Researchers started showing greater interest in developing new methods by which antenna parameters can be improved by manipulating material parameters of superstrates. They successfully implemented superstrates in beam steering, enhancing gain and improving bandwidth. Some authors proposed EBG structures as superstrates for improving antenna parameters. But the thickness of the antenna was the main barrier for these structures. Raj Mittra et al.[3] have done a comparative study of three superstrates, namely double negative slab, frequency selective surface and plain dielectric in improving directivity of microstrip antenna. The authors came to the conclusion that the physical mechanism behind directivity enhancement is not the focussing effect of superstrate alone. They attributed the directivity enhancement to the resonance resulting from Fabry-Perot resonant cavity formed by the superstrate and metallic ground plane. Jae Hee Kim et al. Proposed a holey dielectric superstrate for enhancing the gain of a microstrip patch antenna[8]. The effective permittivity was

controlled by changing the radius of holes in the superstrate so as to generate an in-phase electric field which resulted in improved gain.

In this chapter a technique for improving the radiation parameters of a CPW-fed planar antenna using a non-resonant superstrate is discussed. It is based on a novel engineered artificial dielectric with high value of effective permittivity. The effect of artificial dielectric on antenna reflection characteristics, gain and radiation pattern are investigated.

Propagation of electromagnetic magnetic waves through a media is affected by the material parameters of the media. Therefore we can control the propagation of EM waves through a media by properly setting the material parameters. The major parameters on which electromagnetic wave propagation depends are conductivity, permittivity and permeability. Artificially engineered materials are formed by the periodic repetition of elements. The term unit cell is used to describe one such element. The size of the unit cell is very small compared to operating wavelength. The materials derive their properties based on the design and orientation of the unit cells. From the analysis of unit cell, we can predict the behaviour of electromagnetic wave through a structure formed by the periodic repetition of the unit cell. Hence unit cell analysis is very important.

As mentioned earlier, in order to determine the nature of propagation of electromagnetic wave through a media, effective material parameters of the media are required. It is possible to extract material parameters from reflection characteristics(S_{11})[14].

When we are working with planar periodic structures, Floquet port will be very useful in the analysis. In the ideal case we will assume that the planar periodic structure extends upto infinity in its plane. In the analysis we will have to compute the electromagnetic fields at every location in the infinitely extending structure. Due to the limitations of the machine and storage capabilities, it is not practically realizable. As a solution to this problem, we will perform unit cell analysis. Unit cell is the basic building block of the periodic structure. By analysing this basic building block, it is possible to predict how the infinitely extending periodic structure responds to electromagnetic waves incident on it. In order to perform unit cell analysis using simulation software, we will apply unit cell boundary condition along X and Y directions. This implies that the modelled structure repeats periodically upto infinity along X and Y directions. Along the Z directions we will assign two Floquet ports. The

structure to be analysed is placed between these two ports. These ports can be used to excite electromagnetic waves. One port can be used for receiving both transmitted signals from the other port as well as reflected signal from the structure. Once we excite the ports with proper signals, it is possible to determine scattering parameters (S parameters). From S parameters refractive index (n) and impedance (z) can be calculated. We will use the values of n and z to extract effective permeability (μ_{eff}) and effective permittivity (ϵ_{eff}).

5.2 Formation of unit cell

The geometry of the unit cell is formed in the following manner. Consider two cylinders of same radii 2 mm and another one of radius 6 mm. All the cylinders are of negligible thickness and made up of highly conductive material. They are placed at the centre of an FR-4 substrate of size $14 \times 14 \times 1.6 \text{ mm}^3$ and relative permittivity 4.3. The thickness of the metallization etched on the substrate is $35 \mu\text{m}$. The two cylinders of radius 2 mm are shifted by 4.2 mm in opposite directions along a straight line which makes an angle 45° with Y axis (Fig. 5.1).

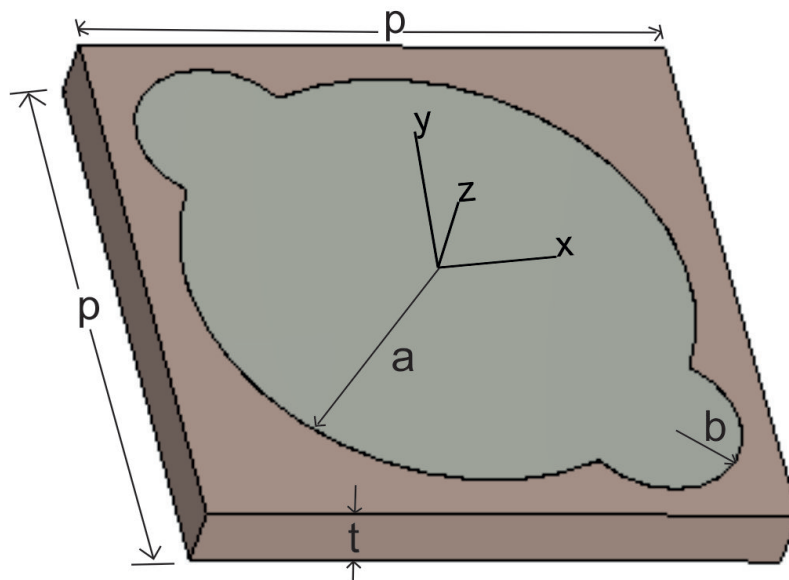


Figure 5.1: Geometry of the unitcell. $p=14$, $a=6$ and $b=2$ (units in mm.)

In Fig.5.2 the unit cell is placed between the two Floquet ports Z_{\max} and Z_{\min} . The substrate is made up of FR-4 with relative permeability 1 and relative permittivity 4.3. We are assuming that the metallization is of perfectly conducting material.

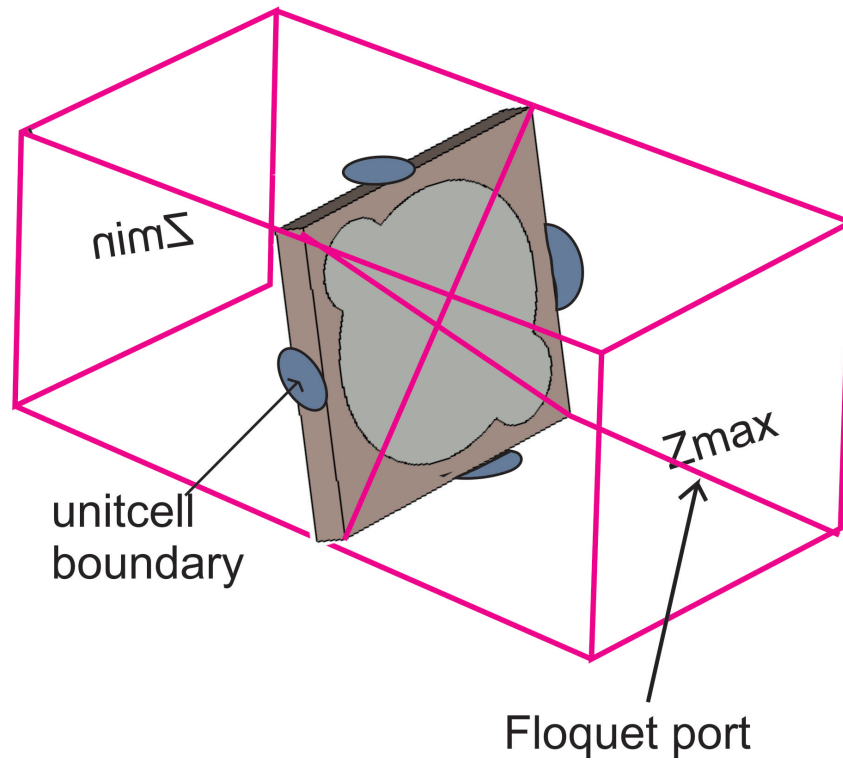


Figure 5.2: Unitcell between two Floquet ports.

For characterising artificially engineered materials, retrieval of effective permittivity and effective permeability are required. The usual method is to use S parameters calculated from the incident wave to first obtain effective refractive index n and impedance z . The effective permittivity and permeability can then be calculated directly from the expressions $\mu = nz$ and $\epsilon = n/z$.

The refractive index n and impedance z of a slab of material can be obtained from the following expressions [14],

$$z = \pm \sqrt{\frac{(1 + S_{11})^2 - S_{21}^2}{(1 - S_{11})^2 - S_{21}^2}} \quad (5.1)$$

$$e^{ink_0d} = X \pm i\sqrt{1 - X^2} \quad (5.2)$$

where $X = 1/2S_{21} (1 - S_{11}^2 + S_{21}^2)$. k_0 denotes the wave number of the incident wave in free space and d is the thickness of the slab. For a passive medium, the signs of the above equations are determined by the requirement

$$z' \geq 0 \quad (5.3)$$

$$n'' \geq 0 \quad (5.4)$$

where $(.)'$ and $(.)''$ denote the real part and imaginary part operators, respectively. Since equation 5.2 is a complex exponential, inverting it will result in a multi-valued logarithmic function. Solving for refractive index we get

$$n = \frac{1}{k_0 d} \left\{ \left[\ln (e^{ink_0 d}) \right]'' + 2m\pi \right] - i \left[\ln (e^{ink_0 d}) \right]' \right\} \quad (5.5)$$

where m is the branch number of n' .

Before extracting material parameters of newly designed unit cell array structure, we apply parameter extraction process to few simple structures whose material parameters are known. These simple structures can be obtained from the unit cell structure by appropriately assigning material properties to the composites of unit cell structure. For example, let us consider the case where we want to extract the material properties of vacuum. We will start with the unit cell. Along X and Y directions unit cell boundary conditions are applied. Let us assume that the periodicity of the unit cell structure is $p = 14$ mm. As mentioned earlier, the unit cell is placed between Floquet ports Zmax and Zmin. The wave propagation through vacuum can be simulated by simply assigning material properties of vacuum to both the substrate and metallization of the unit cell. Now we excite one of the ports with electromagnetic waves. The graphs of reflection and transmission characteristics, refractive index, effective permeability and effective permittivity are plotted.

In Fig.5.3, for the entire frequency range S11 has a magnitude of zero indicating that there is no reflection in vacuum.

Transmission scattering parameter S21 In Fig.5.4 has a magnitude of 1 which implies full transmission.

The graph obtained in Fig.5.5 is in agreement with permeability of vacuum which is very close to 1.

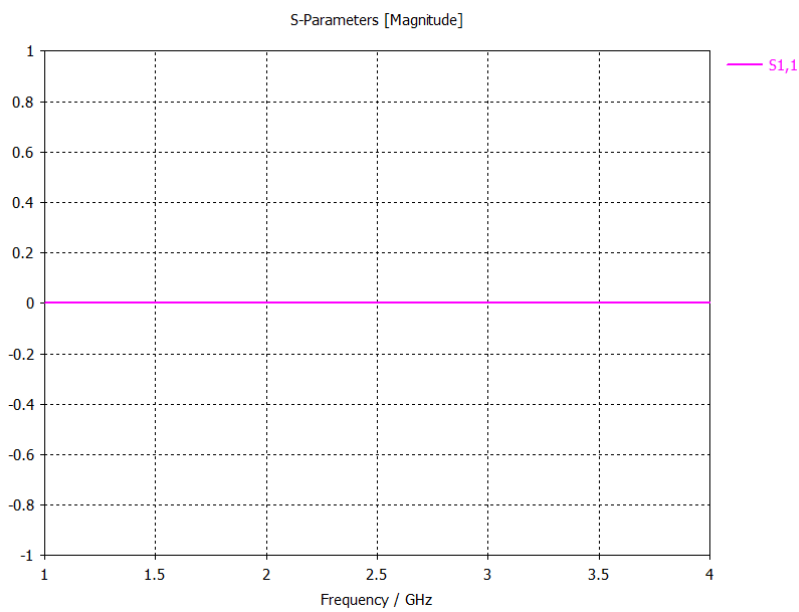


Figure 5.3: Reflection characteristics when properties of vacuum is assigned to unitcell.

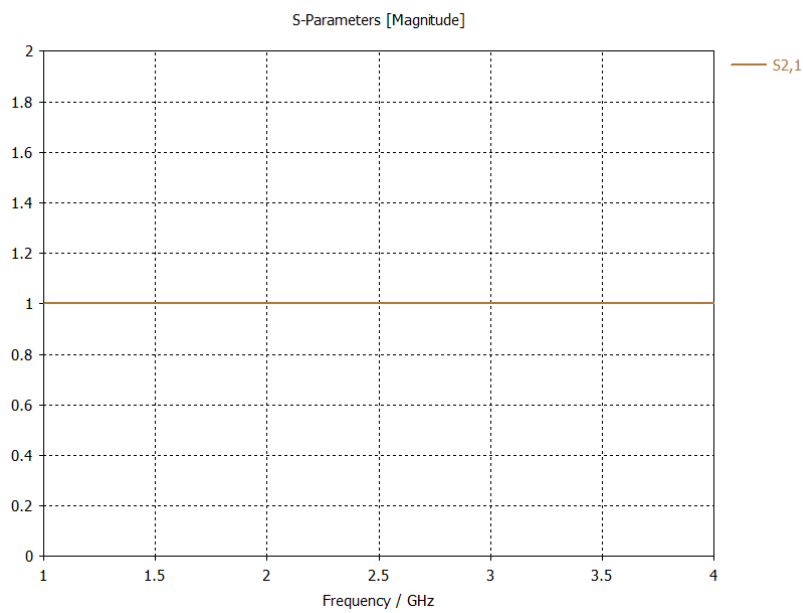


Figure 5.4: Transmission characteristics when properties of vacuum is assigned to unitcell.

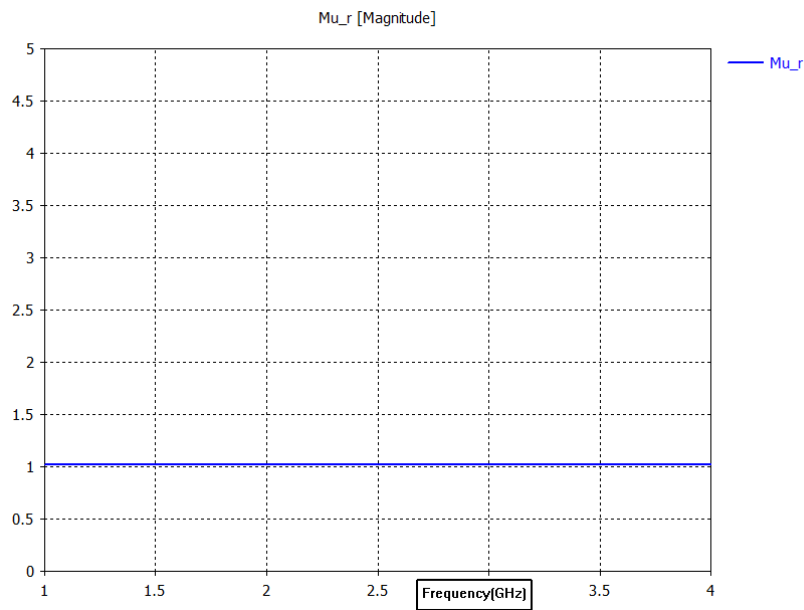


Figure 5.5: Effective permeability when properties of vacuum is assigned to unitcell.

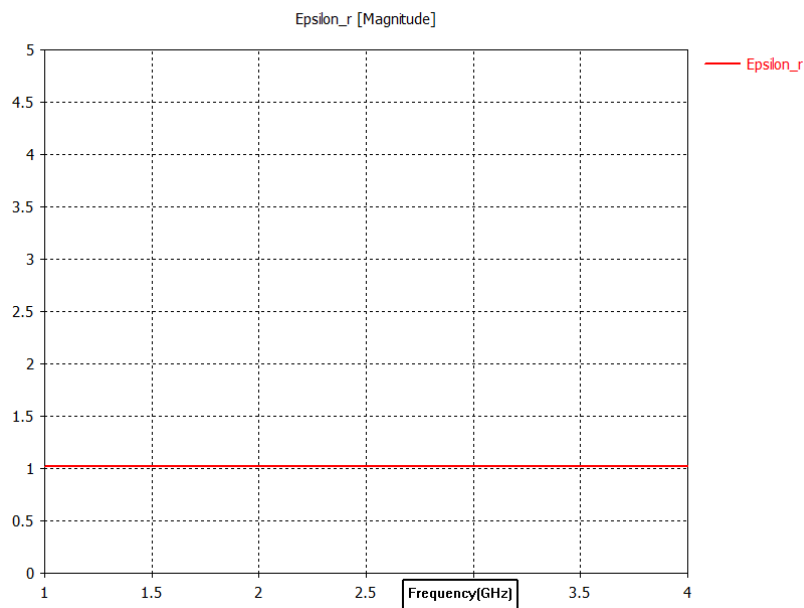


Figure 5.6: Effective permittivity when properties of vacuum is assigned to unitcell.

Effective permittivity has a magnitude very close to unity, which is same as permittivity of vacuum.

Extracted value of refractive index has a value 1 which is same as refractive

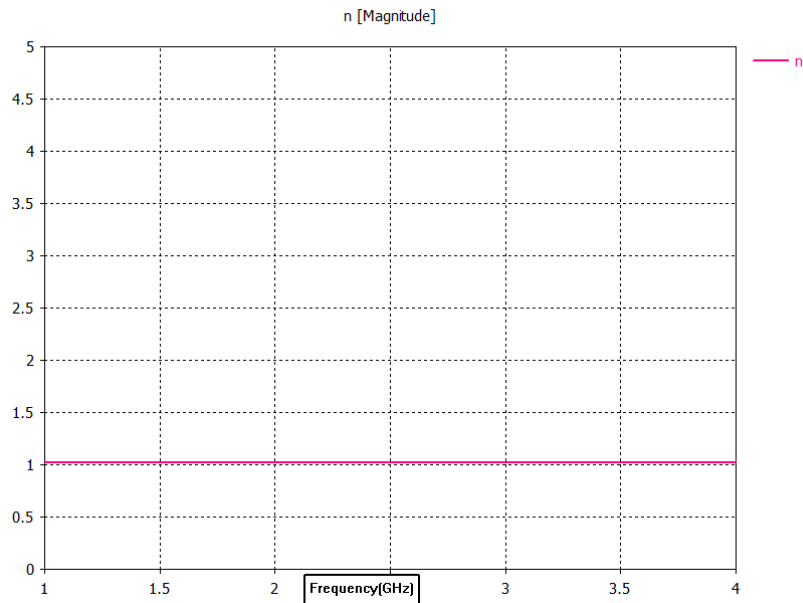


Figure 5.7: Refractive index when properties of vacuum is assigned to unitcell.

index of vacuum. Since we have assigned material property of vacuum to substrate and metallization, in effect, the electromagnetic wave excited from Floquet port Zmax is propagating through free space before reaching Floquet port Zmin. Hence the electromagnetic wave will be transmitted without any reflection. The value of refractive index, effective permeability and effective permittivity will be that of free space.

Let us consider another case where we assign vacuum to metallization and material properties of FR-4 to substrate. Let us simulate the values of reflection and transmission characteristics, effective permeability, effective permittivity and refractive index

With FR-4 material a small amount of reflection is there and the reflection increases with frequency. From the plot5.9 it can be seen that almost whole signal passes through FR-4 material. The simulated value of refractive index for FR-4 attains a value slightly above 2. The value of effective permeability is very close to unity which is same as that of vacuum. For simulation we are assigning a value of 4.3 as permittivity of FR-4. The extracted value of permittivity is also 4.3.

In the present case since we have assigned vacuum to metallization, the electromagnetic wave will be propagating through FR-4 material of the sub-

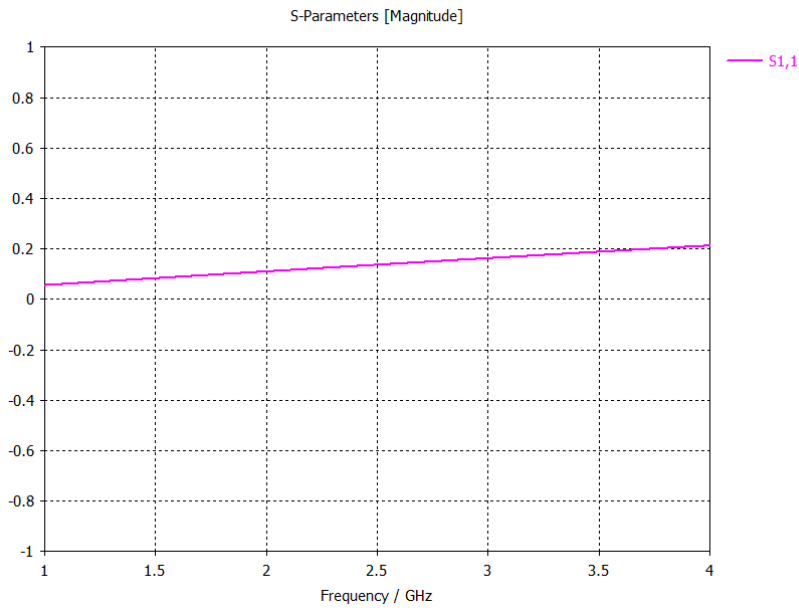


Figure 5.8: Reflection characteristics for FR-4 equivalent of unitcell.

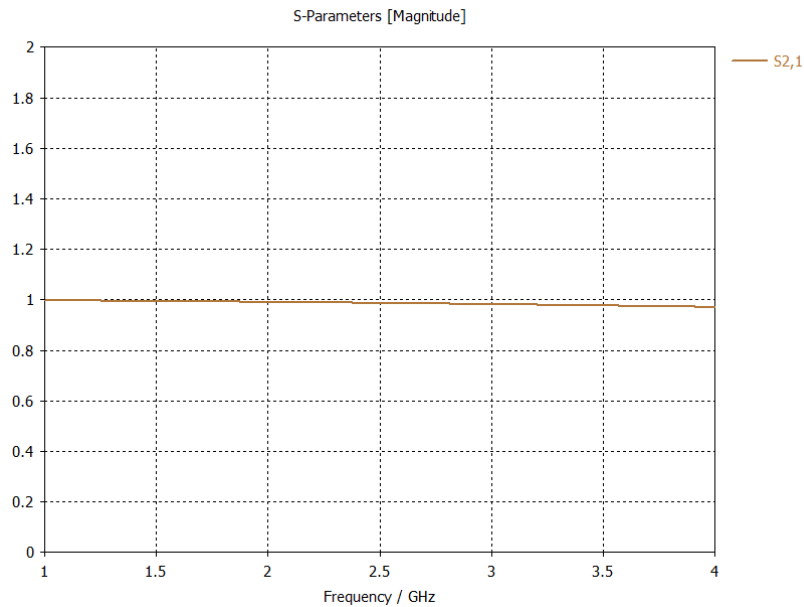


Figure 5.9: Transmission characteristics for FR-4 equivalent of unitcell.

strate. The results are as expected. From the plot is is clear that the extracted values of effective permeability and effective permittivity are same as that of FR-4 material.

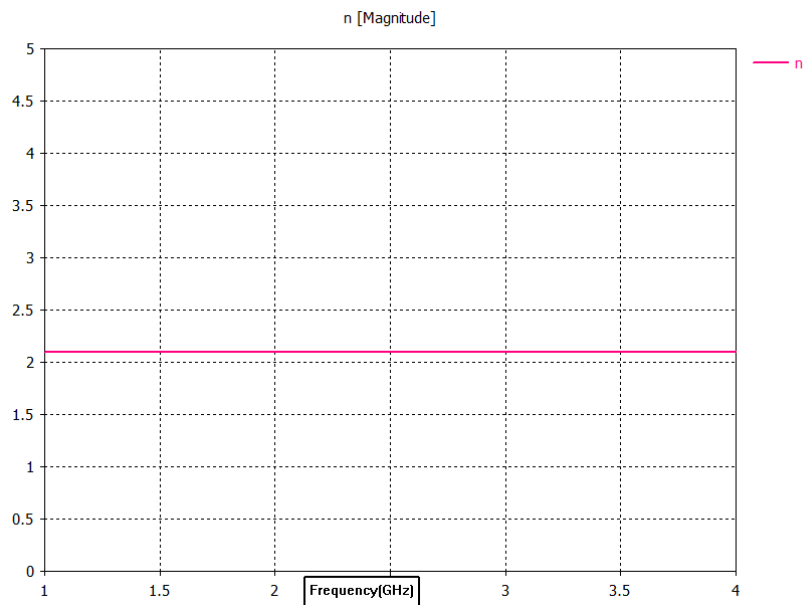


Figure 5.10: Refractive index for FR-4 equivalent of unitcell.

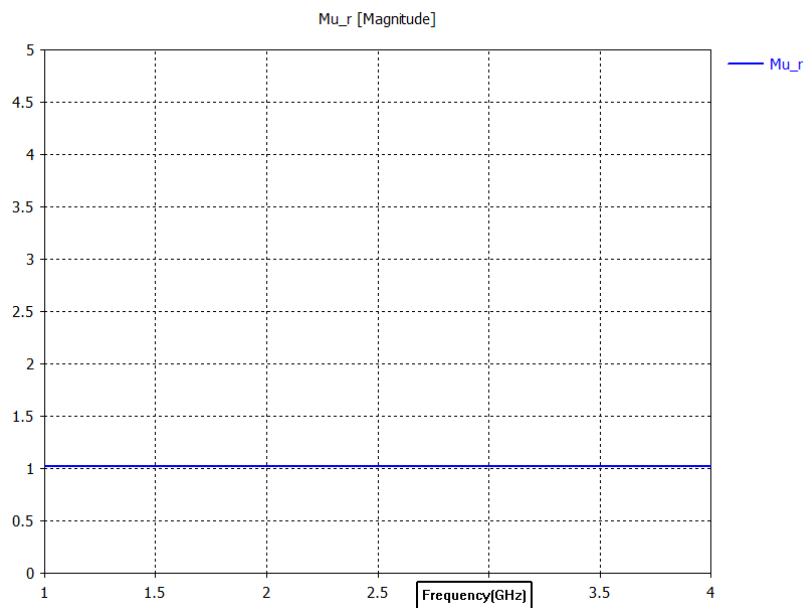


Figure 5.11: Effective permeability for FR-4 equivalent of unitcell.

Now we are considering the case where we assign material properties of FR-4 to substrate and a perfectly conducting material to metallization etched on the surface of substrate. The transmission and reflection characteristics for

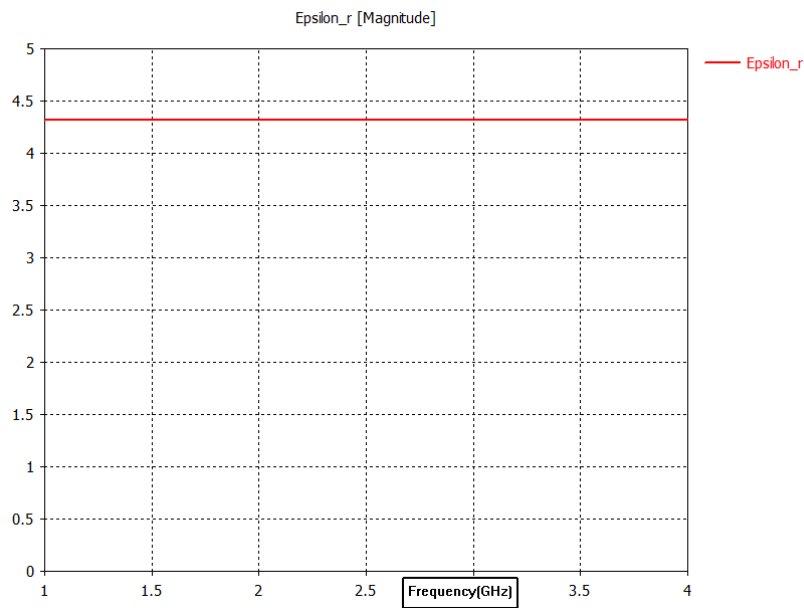


Figure 5.12: Effective permittivity for FR-4 equivalent of unitcell.

this case is shown in Fig.5.13.

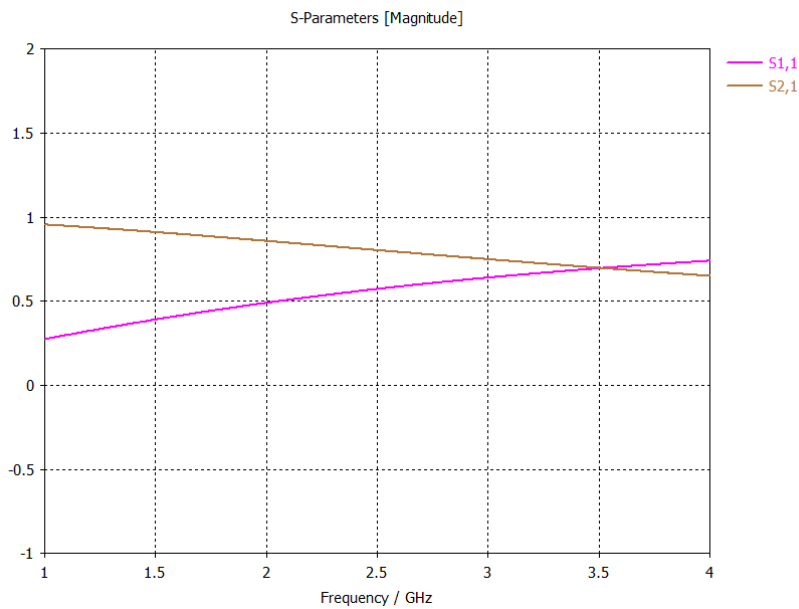


Figure 5.13: Reflection and transmission characteristics of FR-4 with periodic pattern.

From the Fig.5.13 it is clear that reflection and transmission characteristics is a function of frequency. At frequencies below 3.5 GHz, there is more transmission than reflection. For frequencies above 3.5 GHz, there is more reflection than transmission.

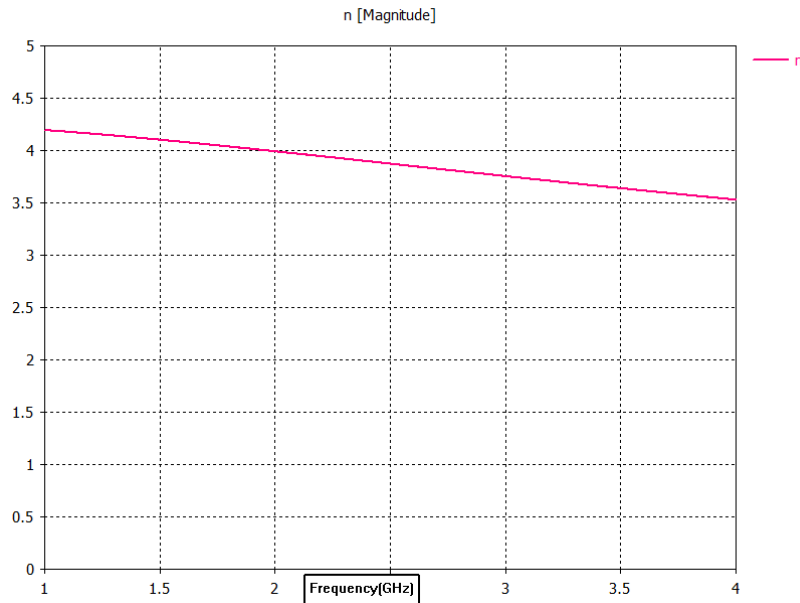


Figure 5.14: Refractive index of FR-4 with periodic pattern.

The refractive index evaluated from the S parameters is shown in Fig.5.14. From the figure it is clear that the refractive index is a function of frequency. At low frequencies the refractive index attains a value greater than 4. With increase in frequency a decrease in refractive index is observed. From the figure it is clear that when we etch the periodic pattern on the substrate refractive index attains a higher value than that of FR-4 substrate.

At low frequencies effective permeability is very close to unity. With increase in frequency a slight decrease in the value of permeability is observed. From the graph in Fig.5.15, it is clear that the magnetic nature of this structure is very feeble as the effective permeability is very small.

The extracted value of effective permittivity is shown in Fig.5.16. The effective permittivity of the structure attains a high value which is greater than 18. Therefore if we periodically repeat this pattern, the resulting structure can be considered as an artificially engineered material. If we load an antenna

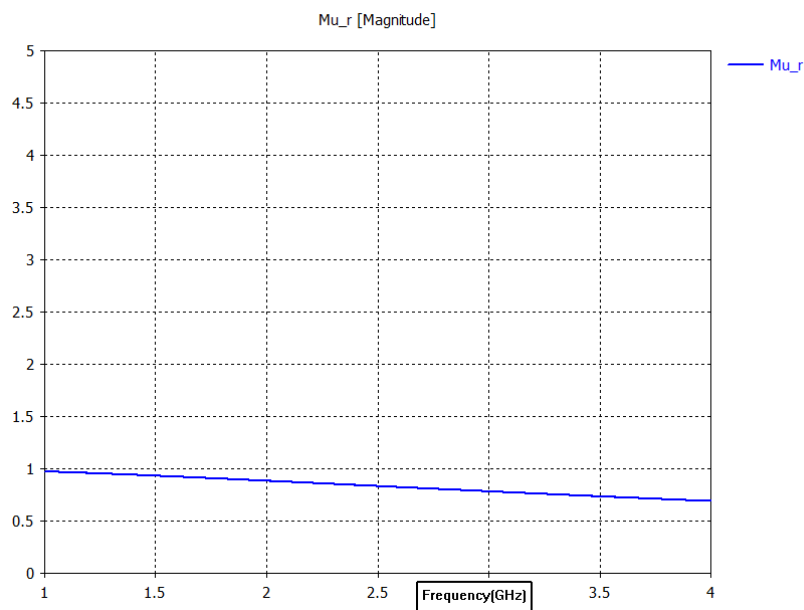


Figure 5.15: Effective permeability of FR-4 with periodic pattern.

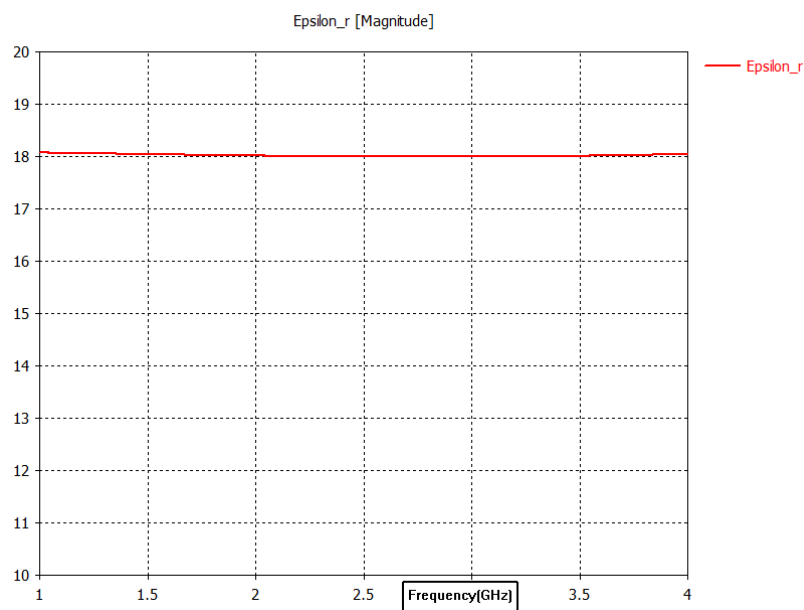


Figure 5.16: Effective permittivity of FR-4 with periodic pattern.

with a periodically repeating pattern of this unit cell printed on a superstrate, it is possible to modify the radiation properties of the antenna.

5.3 Antenna array size selection

Based on the unit cell analysed in the previous section, let us form a periodic array which can be used as a superstrate for a planar antenna. The radiation properties of the antenna will be a function of unit cell array size. In order to select the appropriate array size, simulation analysis is performed. Unit cell array of sizes 3×3 , 3×4 and 4×4 are used for the analysis.

5.3.1 Analysis with 3×3 unit cell periodic array pattern

For analysis let us consider the antenna developed in section 4.5. The resonance frequency of the antenna was 2.58 GHz. and had a bandwidth of 240 MHz. We are using 3×3 unit cell periodic array pattern printed on FR-4 substrate with size $46.46 \times 42.48 \times 1.6 \text{ mm}^3$ as superstrate. Let us load the antenna with this superstrate.

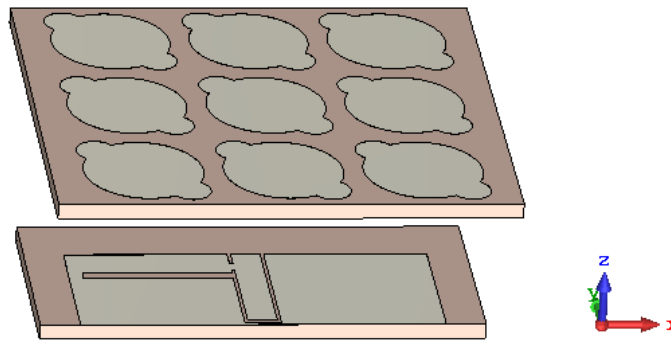


Figure 5.17: Reference antenna loaded with 3×3 array periodic pattern.

The reflection characteristics of reference antenna loaded with 3×3 array periodic pattern is plotted in Fig.5.18. From the plot the resonance frequency is 2.56 GHz and bandwidth is 214 MHz

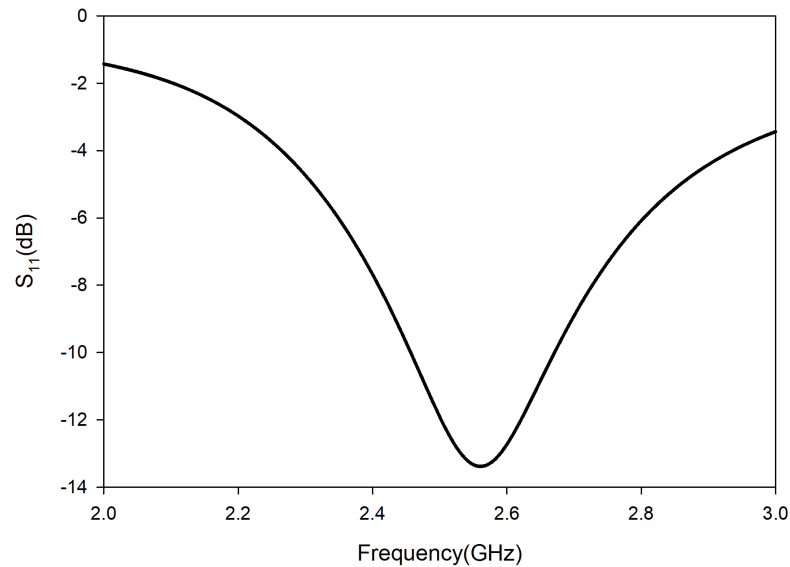


Figure 5.18: Reflection characteristics of reference antenna loaded with 3×3 array periodic pattern.

The 3D radiation pattern of the antenna loaded with 3×3 array superstrate is shown in Fig.5.19. Compared with the radiation pattern of the antenna alone, the beam is more focussed. The gain obtained is 3.86 dB.

5.3.2 Analysis with 3×4 unit cell periodic array pattern

For printing 3×4 unit cell periodic array pattern, we are using FR-4 substrate with size $46.68 \times 42.48 \times 1.6$ mm³.

When the antenna is loaded with 3×4 array superstrate, the reflection characteristics obtained is plotted in Fig.5.18.

The resonance frequency is 2.58 GHz and bandwidth is 188 MHz. Compared to 3×3 array, the resonance frequency shifts by 20 MHz and bandwidth decreases by 26 MHz. The 3D radiation pattern is shown in Fig.5.22.

The radiation pattern appears almost same as that of 3×3 array of unit cell. The gain of the antenna shows an improvement. With 3×4 periodic array pattern the simulated gain is 4.46 dB.

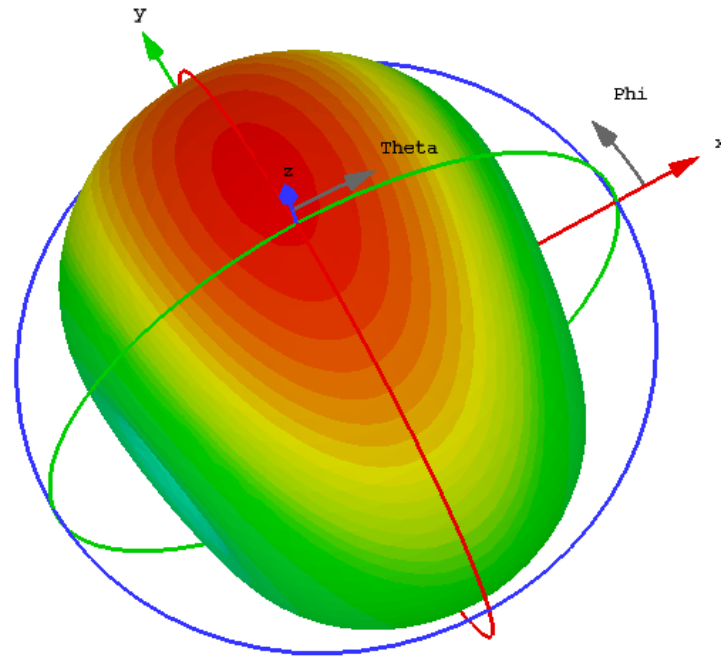


Figure 5.19: 3D radiation pattern of the reference antenna loaded with 3×3 array periodic pattern.

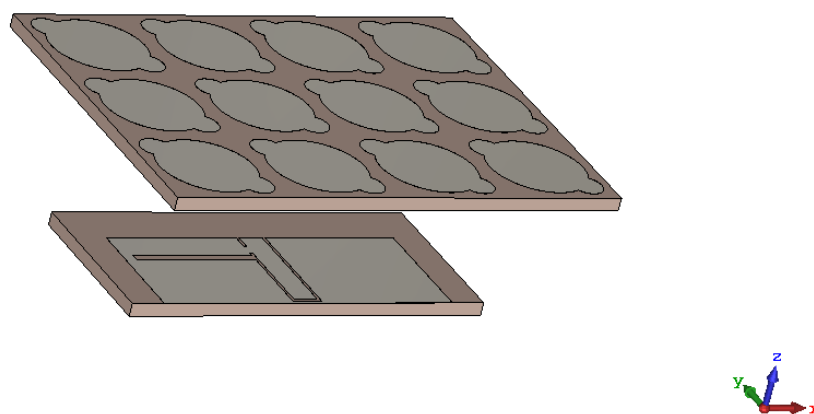


Figure 5.20: Reference antenna loaded with 3×4 array periodic pattern.

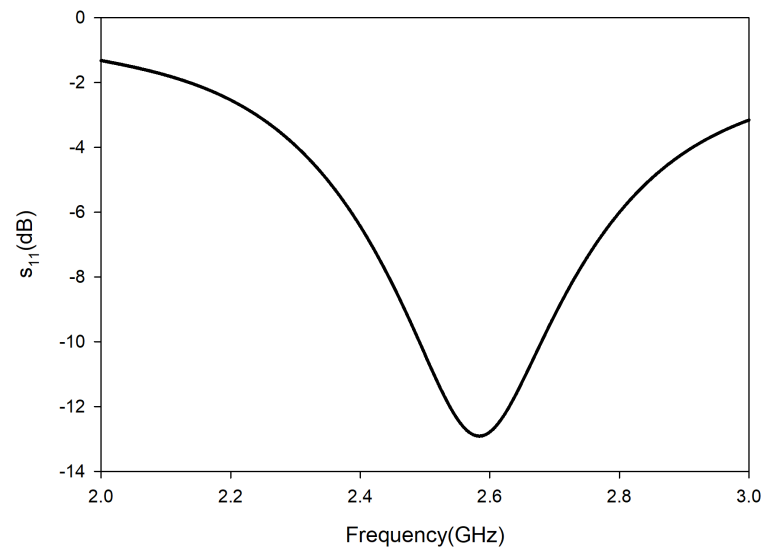


Figure 5.21: Reflection characteristics of reference antenna loaded with 3×4 array periodic pattern.

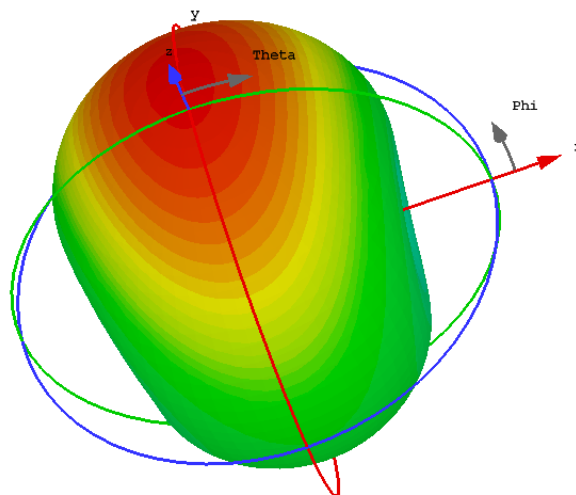


Figure 5.22: 3D radiation pattern of the reference antenna loaded with 3×4 array periodic pattern.

5.3.3 Analysis with 4×4 unit cell periodic array pattern

For the 4×4 unit cell periodic pattern the size of the FR-4 substrate is $56.46 \times 56.64 \times 1.6 \text{ mm}^3$.

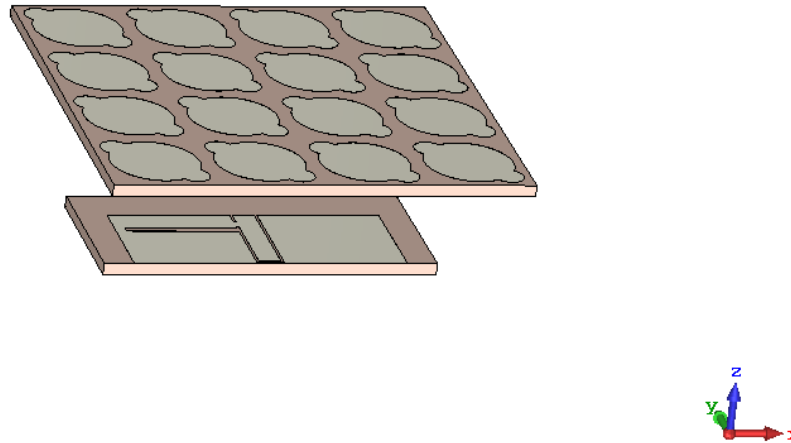


Figure 5.23: Reference antenna loaded with 4×4 array periodic pattern.

The reflection characteristics is plotted in Fig.5.24. The resonance frequency is 2.57 GHz and the bandwidth obtained is 203 MHz.

The 3D radiation pattern is shown in Fig.5.25. Just like the 3×3 and 3×4 array the beam from the antenna gets more focussed. The gain of the antenna in the present case is 4.65 dB.

A comparison of above three cases is done in Table 5.1.

From the above analysis it is clear that as we increase the size of the periodic array, there is an increase in gain. If we consider only gain, 4×4 array will be a better choice. The substrate on which the antenna etched is of size $56.46 \times 56.64 \times 1.6 \text{ mm}^3$. Hence if we use 4×4 array superstrate the antenna will become more bulkier. If we take compactness also into account, 3×4 array will be a better choice.

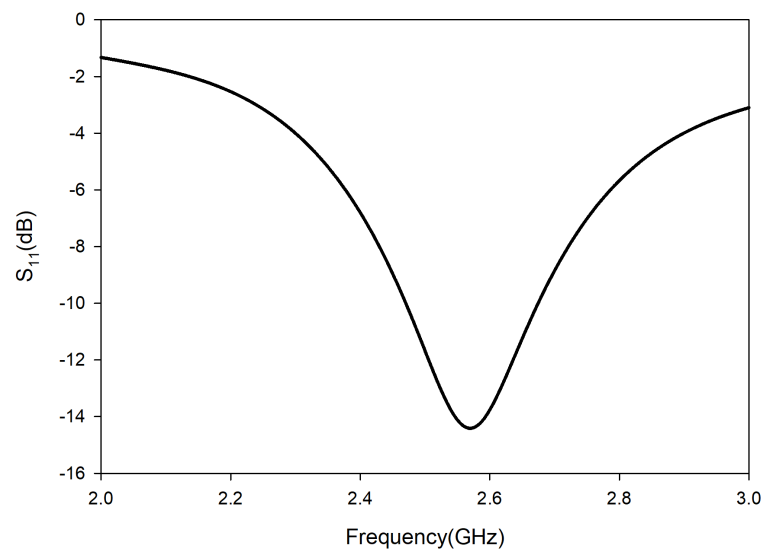


Figure 5.24: Reflection characteristics of reference antenna loaded with 4×4 array periodic pattern.

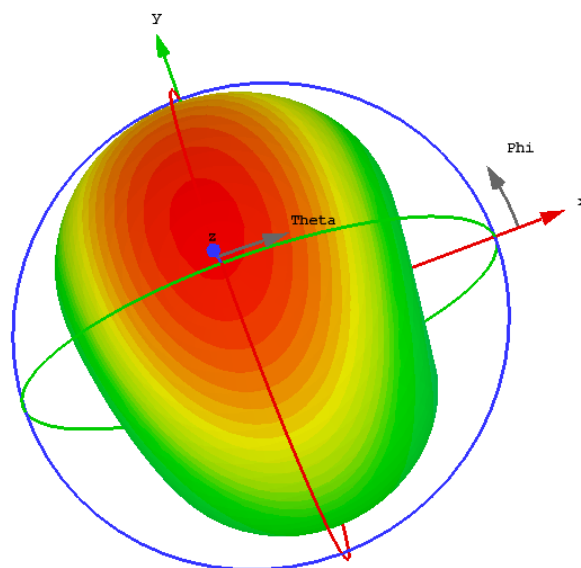


Figure 5.25: 3D radiation pattern of the reference antenna loaded with 4×4 array periodic pattern.

Table 5.1: Comparison of superstrate size, resonance frequency, bandwidth and gain for different array sizes.

Array size	Superstrate size(mm^3)	Resonance Frequency (GHz)	Bandwidth (MHz)	gain (dB)
3×3	45×21×1.6	2.56	214	3.86
3×4	56.45×42.48×1.6	2.58	188	4.46
4×4	56.45×56.64×1.6	2.57	203	4.65

5.4 Gain variation with spacing between antenna and superstrate

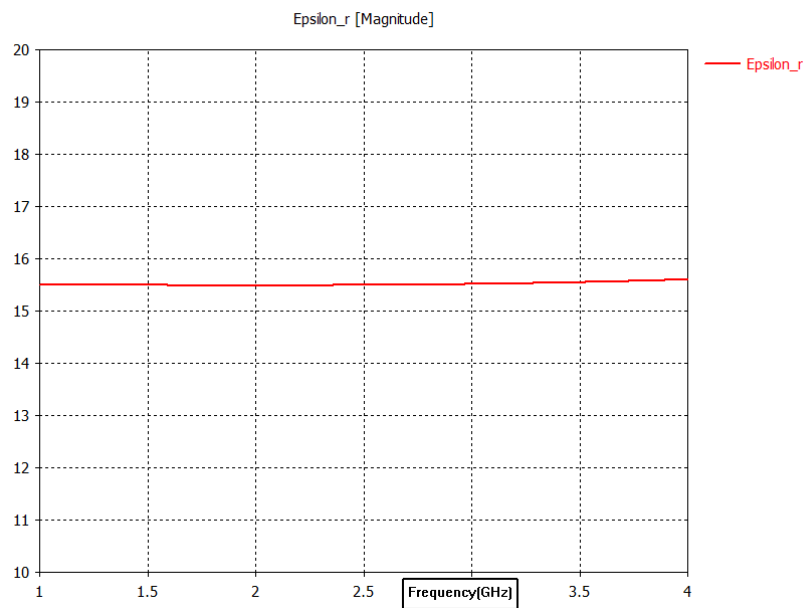
The gain is also a function of spacing between the antenna and the superstrate. The simulated results of variation in gain with respect to spacing is shown in Table 5.2. The optimum value of gain is obtained when the spacing is 20 mm.

5.5 Unit cell periodicity selection

When we print periodic pattern of unit cell discussed in section 5.2 on an FR-4 substrate, it acts as an artificial dielectric with high value of effective permittivity. The value of effective permittivity depends on inter-cell capacitance. Hence if we change the spacing between unit cell elements, the inter-cell capacitance will be changed, which in turn will change the values of effective parameters extracted. Unit cell analysis is carried out to study this variation. We have already done the unit cell analysis for the case where the periodicity $p = 14$ mm. Now let us consider the case where the periodicity $p = 15$ mm. The extracted value of effective permittivity is plotted in figure 5.26.

Table 5.2: Variation of gain with spacing between antenna and superstrate.

Spacing between antenna and superstrate(mm)	gain(dB)
15	3.94
18	4.08
20	4.13
22	4.07
25	4.00

Figure 5.26: Effective permittivity when periodicity $p = 15$ mm.

From the plot it is clear that there is not much variation for the value of effective permittivity with frequency.

The extracted value of effective permeability is shown in Fig.5.27. As frequency increases a slight decrease in effective permeability is observed.

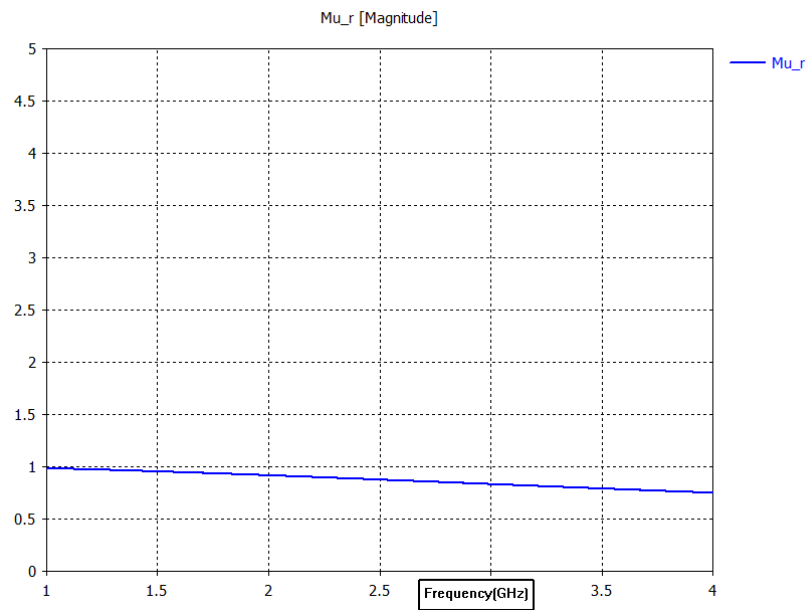


Figure 5.27: Effective permeability when periodicity $p = 15$ mm.

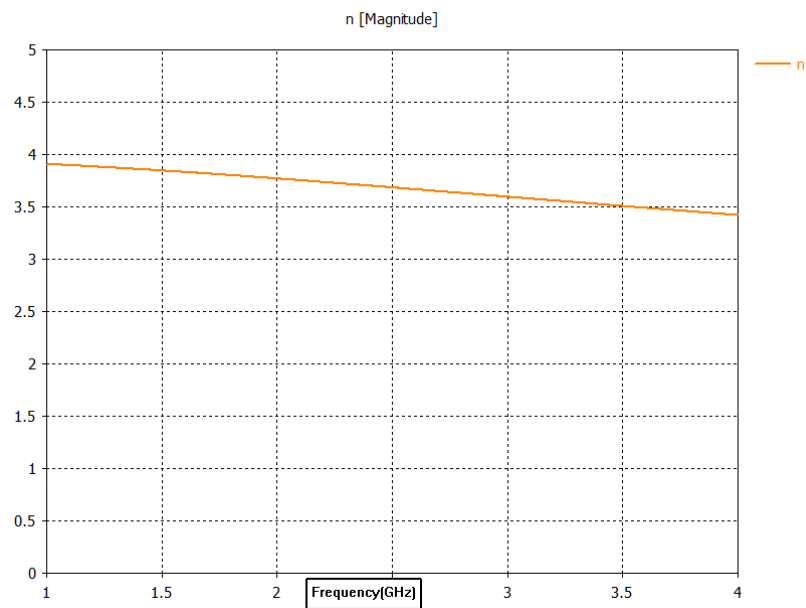


Figure 5.28: Refractive index when periodicity $p = 15$ mm.

The plot of refractive index versus frequency for periodicity $p = 15$ mm is shown in Fig.5.28. With increase in frequency a slight decrease in refractive index is observed.

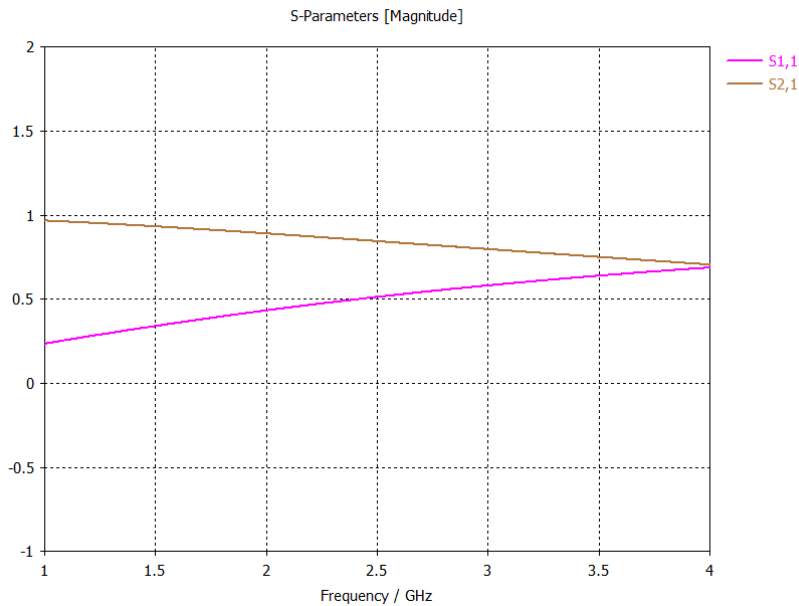


Figure 5.29: Reflection/transmission characteristics when periodicity $p = 15$ mm.

The reflection and transmission characteristics when periodicity is 15 mm is shown in Fig.5.29. The reflection coefficient increases while the transmission coefficient decreases with frequency. When we change the periodicity to $p = 16$ mm it can be seen that compared with periodicity $p = 15$ mm, effective permittivity decreases while the plot for the effective permeability is almost the same (Fig.5.30 and Fig. 5.31).

It can be seen from Fig.5.32 that the magnitude of refractive index decreases when periodicity is changed from $p = 15$ mm to $p = 16$ mm.

Similar to the plot of periodicity $p = 15$ mm, it can be seen that with increase in frequency the transmission decreases while there is an increase in reflection.

Now let us consider the case where we are reducing the periodicity to $p = 13$ mm. As shown in Fig.5.34, the effective permittivity attains a value which is greater than 23. The value of refractive index increases. For low values of frequency, its value is greater than 4.5. With increase in frequency a decrease in refractive index is observed.

The behaviour of reflection/transmission curves is similar to previous cases, i.e., transmission decreases while reflection increases with increase in frequency.

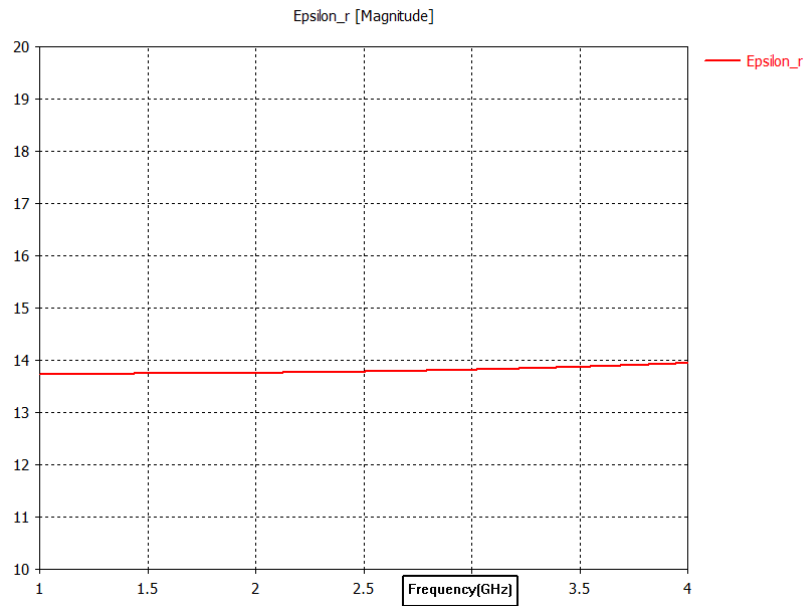


Figure 5.30: Effective permittivity when periodicity $p = 16$ mm.

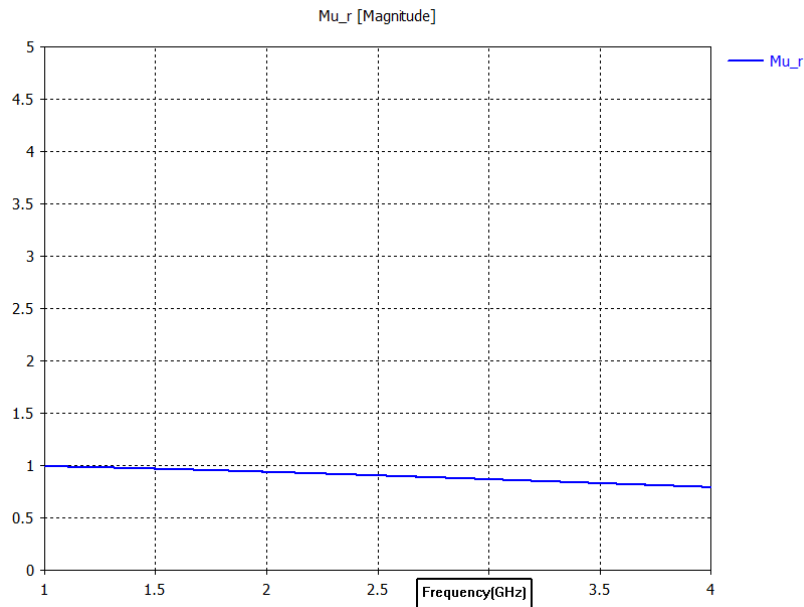


Figure 5.31: Effective permeability when periodicity $p = 16$ mm.

From the above analysis it can be seen that as we increase the periodicity, the value of effective permittivity decreases. The value of effective permeability is not much affected by change in periodicity indicating that it is not

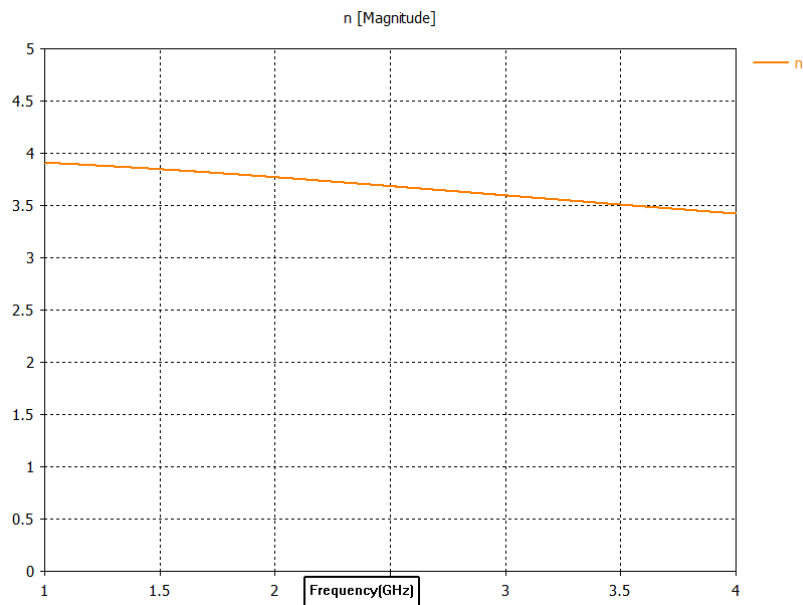


Figure 5.32: Refractive index when periodicity $p = 15$ mm.

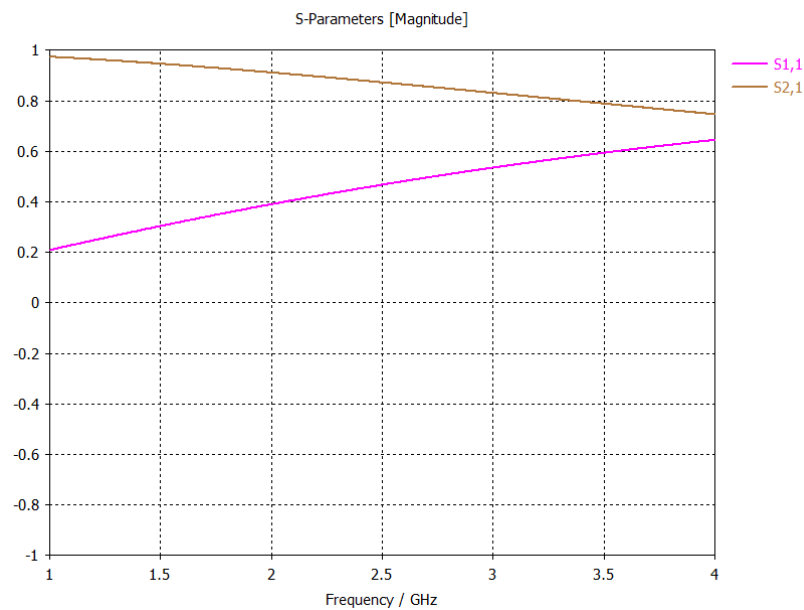


Figure 5.33: Reflection/transmission characteristics when periodicity $p = 16$ mm.

much magnetic in nature. The reflection /transmission characteristics is also affected by change in periodicity. When we increase the frequency, the transmission decreases and reflection increases. Since the curves of reflection and

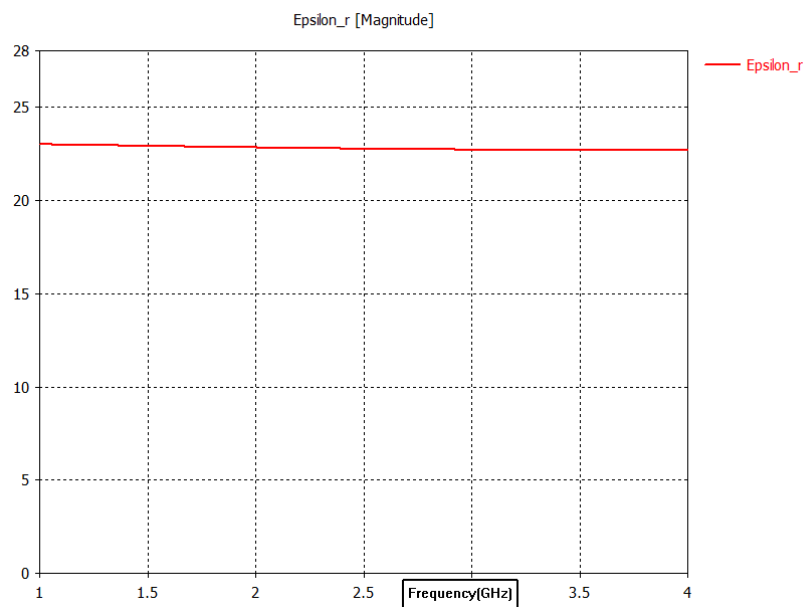


Figure 5.34: Effective permittivity when periodicity $p = 13\text{mm}$.

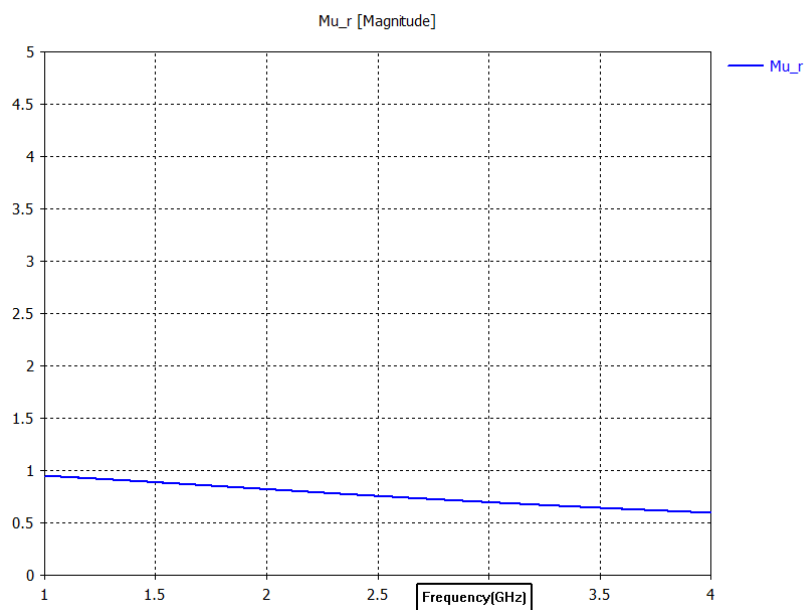


Figure 5.35: Effective permeability when periodicity $p = 13\text{ mm}$.

transmission are moving in opposite directions, with increase in frequency they will meet at a particular value of frequency. From the above cases, it is clear that if we decrease periodicity this meeting point will occur for a smaller

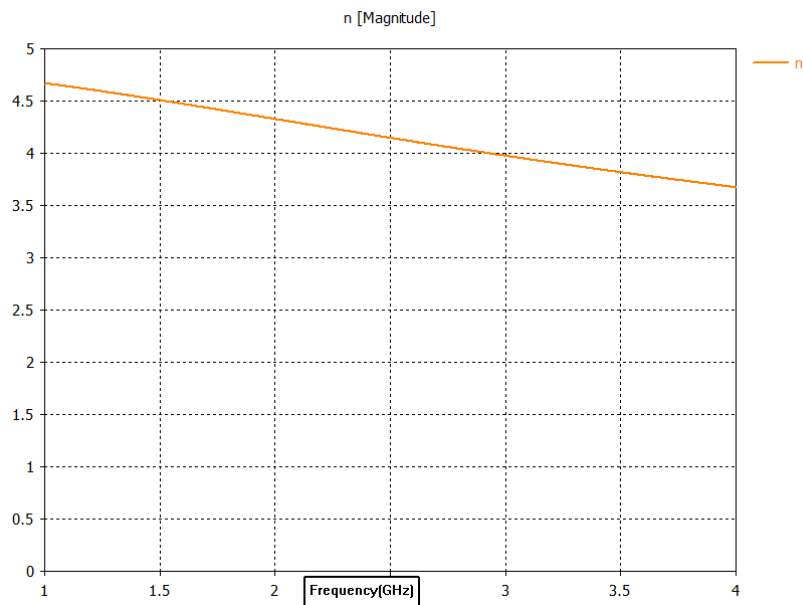


Figure 5.36: Refractive index when periodicity $p = 13$ mm.

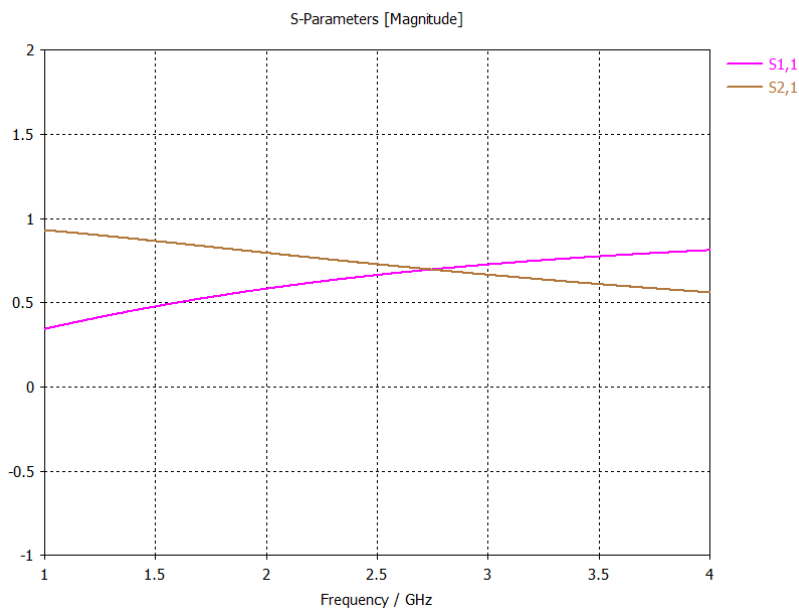


Figure 5.37: Reflection/transmission characteristics when periodicity $p = 13$ mm.

value of frequency. It simply means that if we reduce the periodicity there will be more reflections than transmission for a lower value of frequency.

Fig.5.37 shows the reflection/transmission characteristics when the period-

icity is 13 mm. The reflection and transmission curves meet around 2.7 GHz. From the previous paragraph it is clear that for a frequency beyond 2.7 GHz there will be more reflection than transmission. Therefore if we use this unit cell periodic pattern as a superstrate for an antenna whose passband includes 2.7 GHz it will have an adverse effect on the performance of the antenna.

5.6 Analysis of antenna loaded with periodic pattern printed superstrate

Let us take the antenna developed in section 4.5 as our reference antenna. The periodic pattern is formed from 3×4 array of unit cells. A photograph of the periodic pattern printed on an FR-4 substrate of relative permittivity 4.3 is shown in Fig.5.38. This will be used as the superstrate for the antenna.

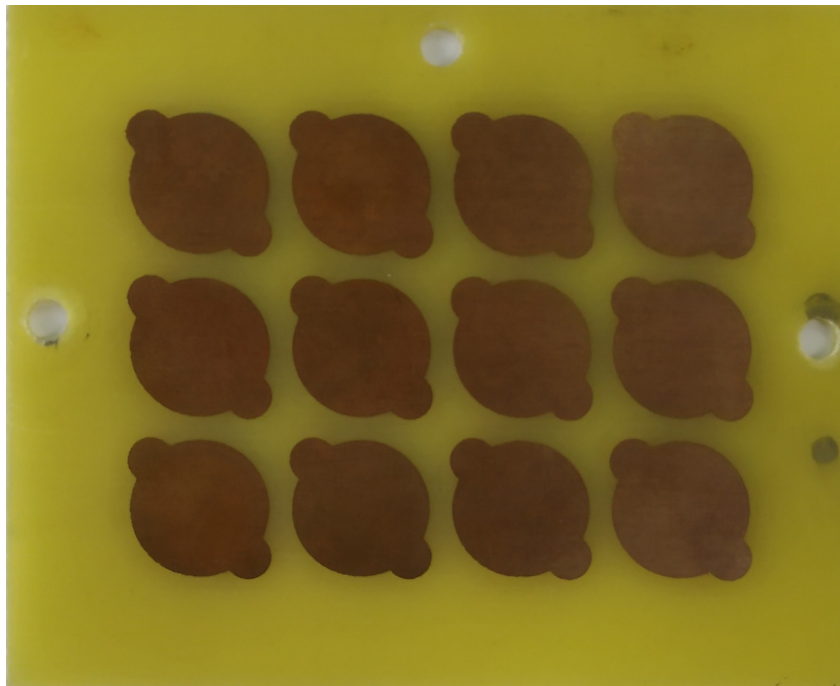


Figure 5.38: Photograph of periodic pattern

5.6.1 Antenna loaded with superstrate

The photograph of the reference antenna loaded with superstrate is shown in Fig.5.39. The spacing between antenna and superstrate is 20 mm.

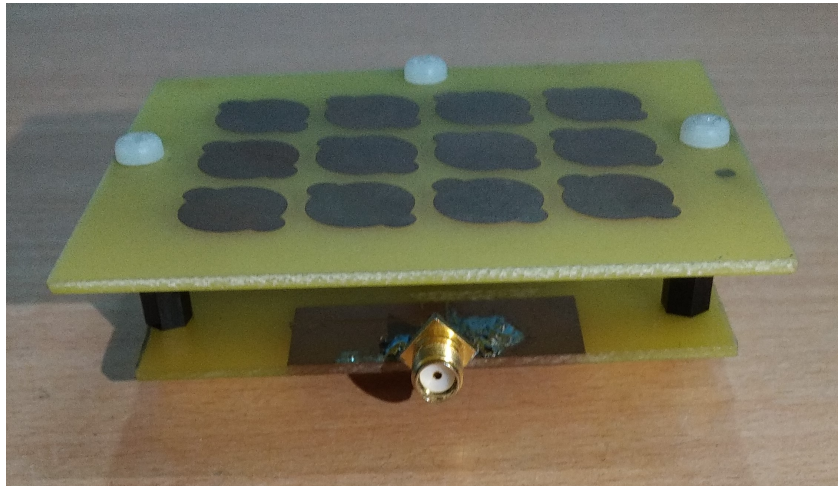


Figure 5.39: Antenna loaded with periodic pattern

The measured reflection characteristics of the antenna with and without superstrate is shown in Fig.5.40. It can be seen that when superstrate is added, the impedance matching is improved. When superstrate is added, the periodic pattern with substrate provides a parasitic loading which results in improved matching. Bandwidth is not much affected by the presence of the superstrate. The operating bandwidth is slightly shifted towards lower frequency region.

5.6.2 Gain

It is well known that the gain of printed antennas can be improved by the use of a superstrate with proper parameters. The gain can be further increased by printing appropriate periodic pattern on the superstrate. The simulation results show that the gain of the reference antenna is 1.96 dB at resonant frequency. The gain increases to 2.4 dB when a plain superstrate is used. When periodic pattern is printed on the superstrate, the gain further increases to 4.13 dB.

The measured gain of the reference antenna and the gain after adding the artificial dielectric superstrate are shown in Fig.5.41. For the reference

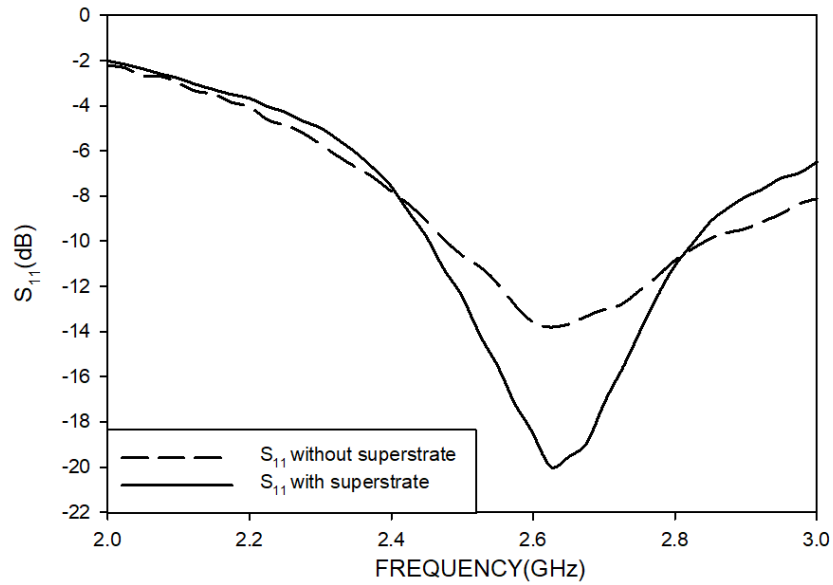


Figure 5.40: Reflection characteristics of the antenna with and without superstrate

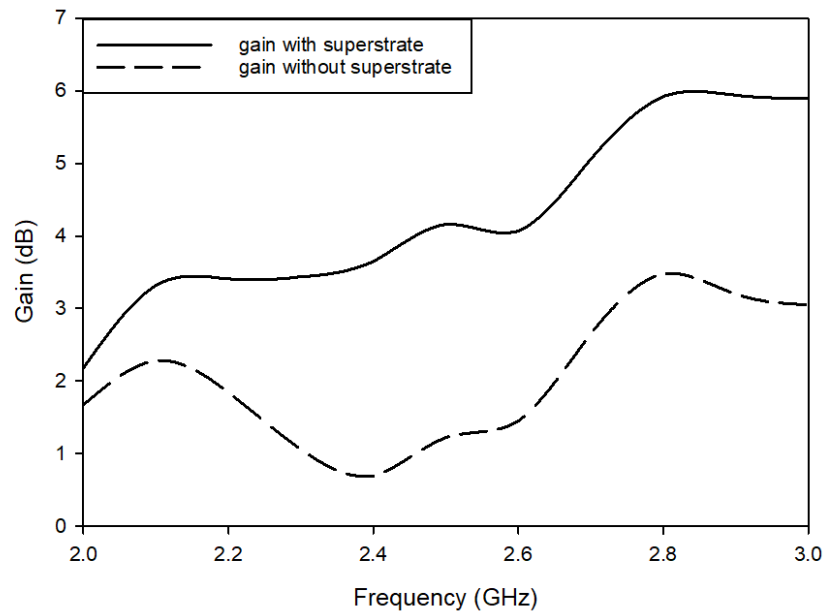


Figure 5.41: Measured gain of the reference antenna with and without superstrate

antenna at 2.65 GHz, a gain of 1.96 dB is observed. When the superstrate is added, the gain improves to 4.46 dB. At this frequency a high value of 18 is obtained for the effective permittivity of the artificial dielectric. Due to this

high value of effective permittivity, electric field confinement occurs which results in higher gain.

5.6.3 Radiation Pattern

Simulated results of radiation pattern is considered in this section. Here we are considering the radiation pattern of the reference antenna, reference antenna loaded with a plain superstrate and reference antenna loaded with periodic pattern printed on superstrate.

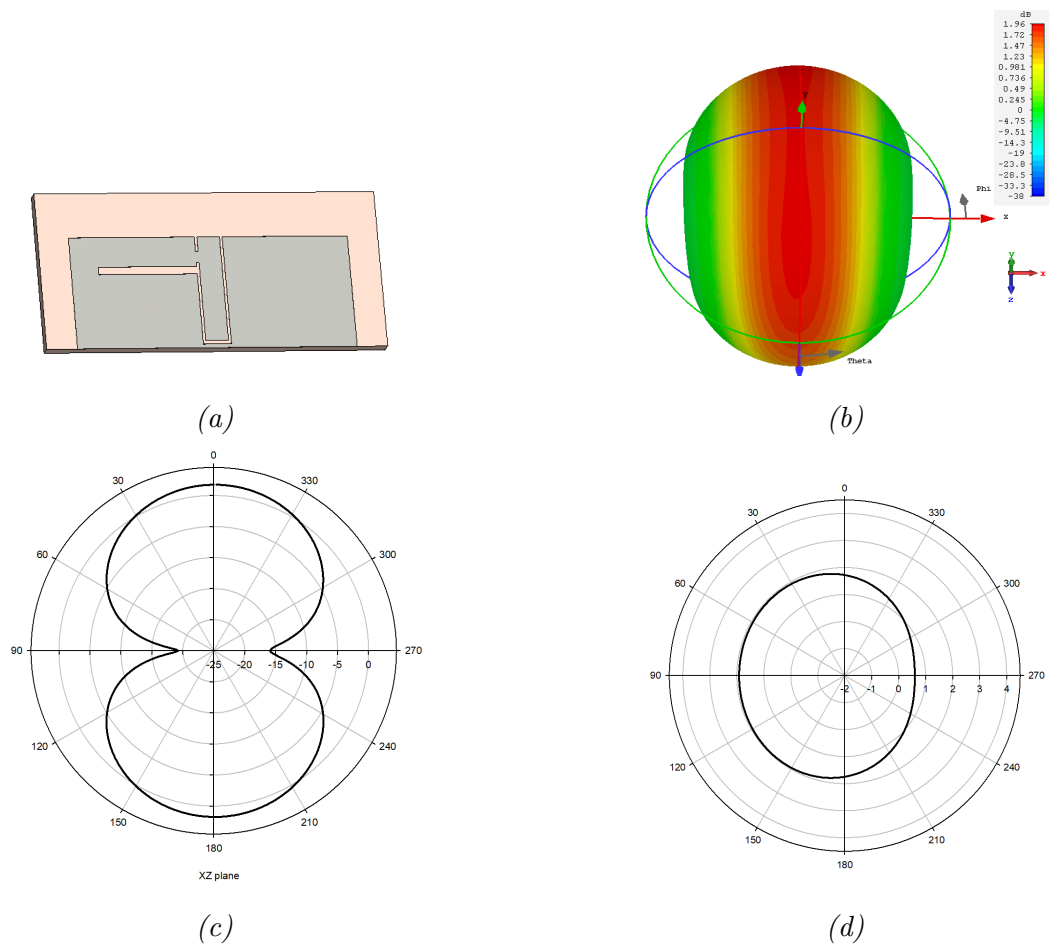


Figure 5.42: Structure(a), 3D pattern(b), 2D pattern in XZ plane(c) and 2D pattern in YZ plane(d) of the reference antenna

From Fig.5.42b it can be seen that for the reference antenna alone, in the plane YZ plane significant power exists for a wide range of elevation angle

theta. The simulated gain for this antenna is 1.96 dB.

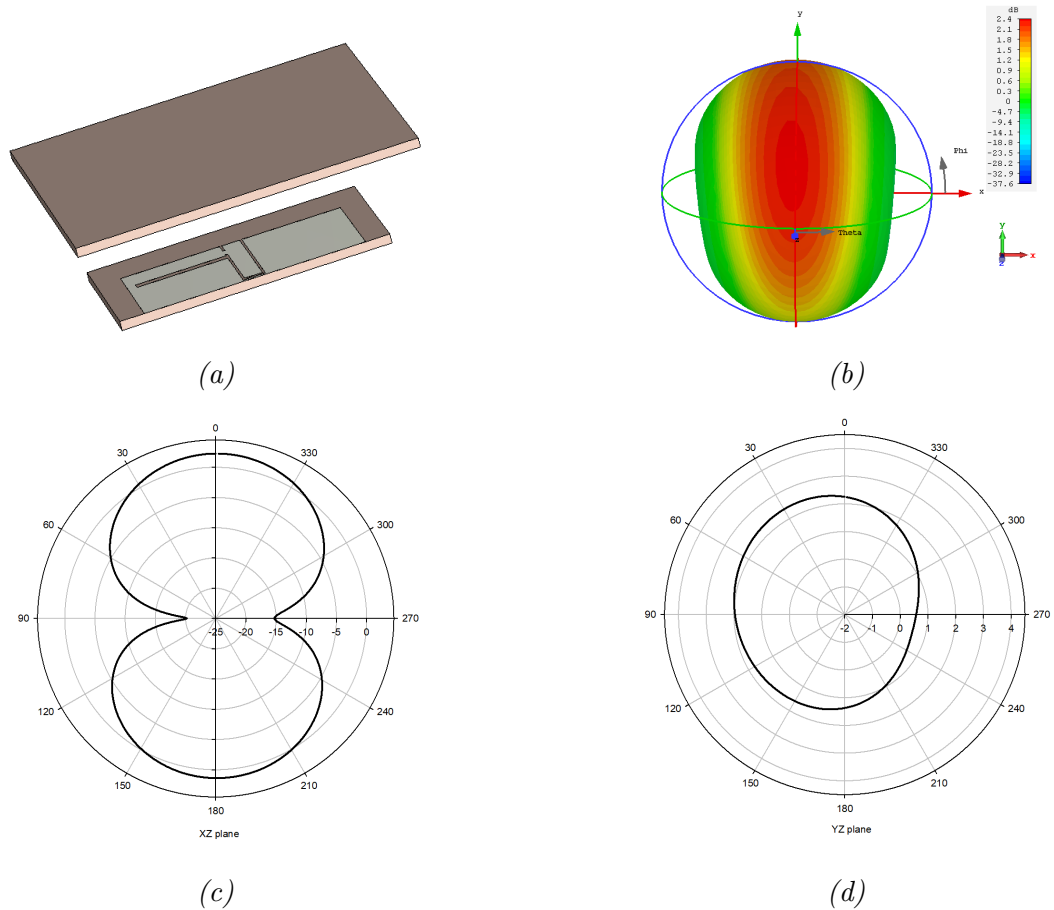


Figure 5.43: Structure(a), 3D pattern(b), 2D pattern in XZ plane(c) and 2D pattern in YZ plane(d) of the reference antenna loaded with plain superstrate

From Fig.5.43b it is clear that compared with reference antenna alone, when we load the antenna with plain superstrate the half power beam width is reduced. The gain improves to 2.4 dB.

When we load periodic pattern printed superstrate, the radiation pattern gets further focussed because of high value of effective permittivity. The main beam is steered towards boresight. The gain observed for this configuration is 4.13 dB.

The measured two-dimensional radiation pattern of the antenna with and without superstrate in XZ and YZ planes at 2.65 GHz for the co-polarization case is shown in Fig.5.45.

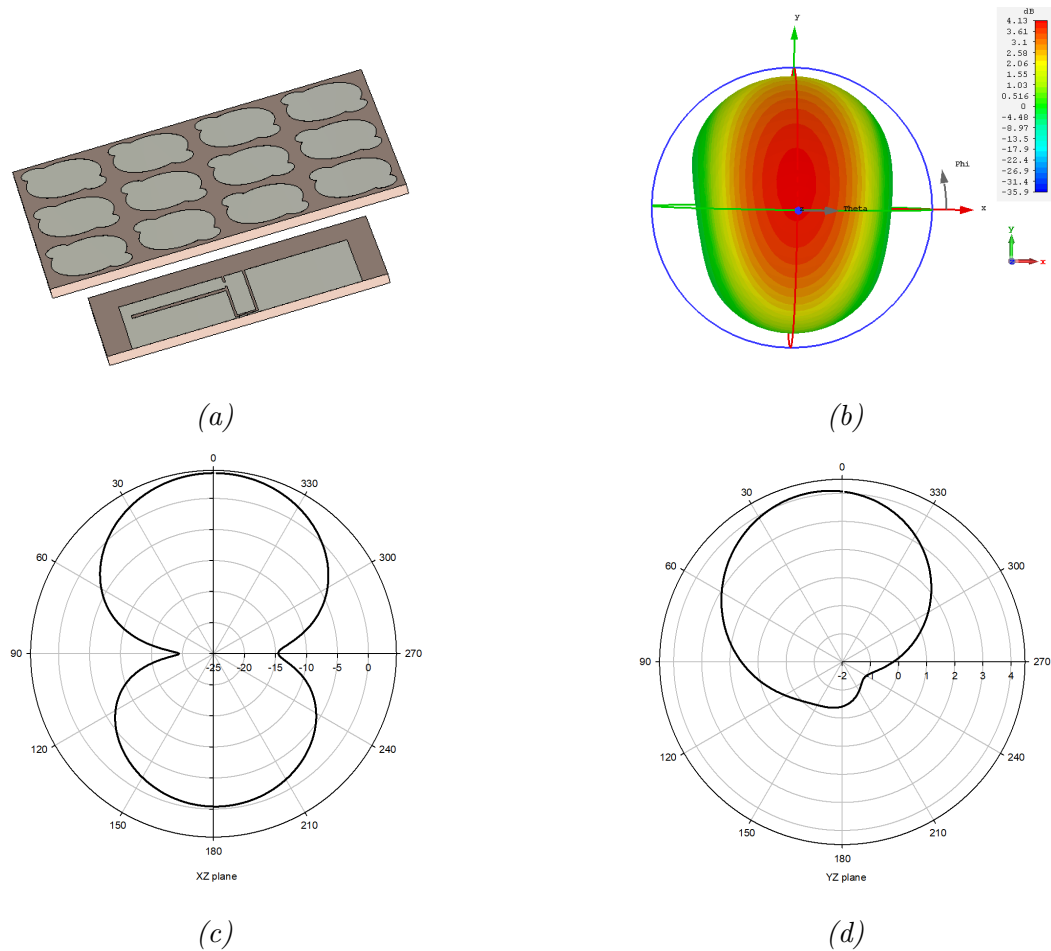


Figure 5.44: Structure(a), 3D pattern(b), 2D pattern in XZ plane(c) and 2D pattern in YZ plane(d) of the reference antenna loaded with periodic pattern printed superstrate

From the reflection/transmission characteristics of the superstrate in Fig.5.13, it is clear that the value of transmission co-efficient is more compared to reflection co-efficient up to 3.5 GHz. Above 3.5 GHz, there is more reflection from the superstrate than transmission. Therefore if we use this artificial dielectric as a superstrate for a dual band antenna with one of the resonances below 3.5 GHz and the other above 3.5 GHz, it will act as a transmitter for lower frequency band and as a reflector for the upper frequency band. This can be verified by loading the superstrate with the dual band antenna developed in section 4.6 Let us place the antenna in the XY plane. We are loading the

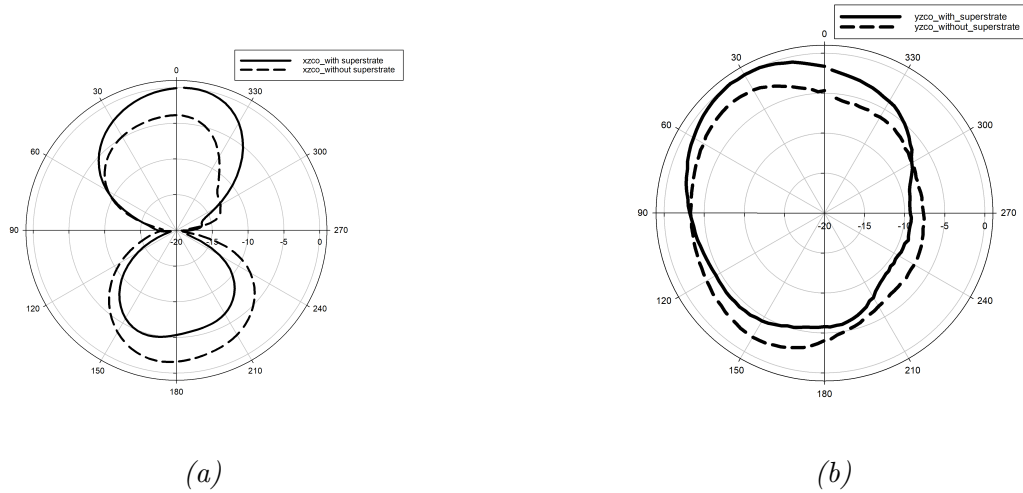


Figure 5.45: Measured two-dimensional co-polarization radiation pattern with and without superstrate for (a) XZ plane and (b) YZ plane

antenna with superstrate which is also placed in XY plane at a height of 10 mm above the antenna. For the antenna considered we had two transmission bands, one with a resonance frequency of 2.51 GHz and the other with a resonance frequency of 5.63 GHz. For the lower band the superstrate acts as a transmitter and we get the main lobe along positive Z direction 5.46(b). For the upper band since the superstrate is acting as a reflector, the main lobe will be directed along negative Z direction 5.46(b).

Consider a particular application where the main beam of the upper frequency band is required along positive Z direction. Since the superstrate acts as a reflector for the upper frequency band, it can be easily realized by loading the superstrate below the antenna. The resulting radiation pattern is shown in Fig. 5.49

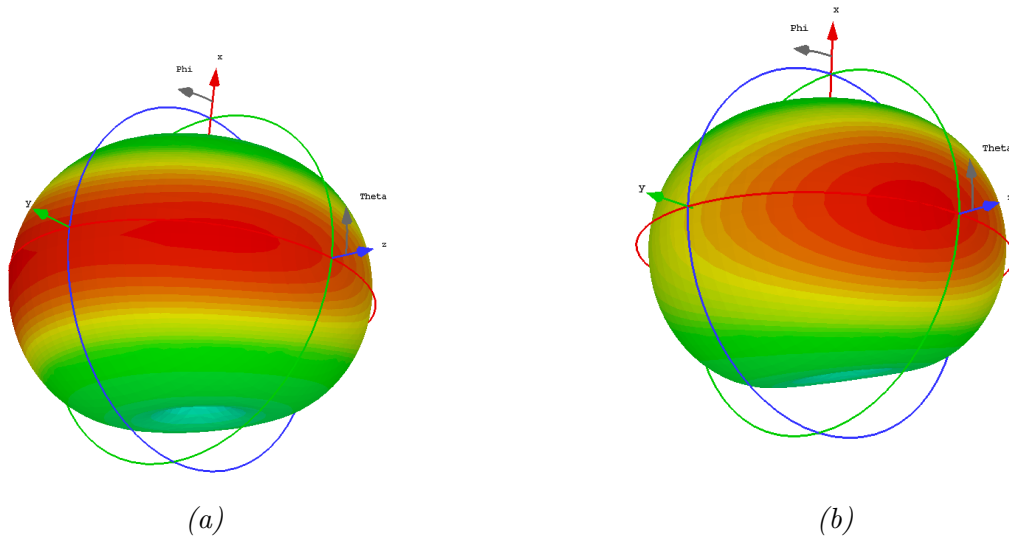


Figure 5.46: 3D radiation pattern of the antenna at 2.5 GHz (a) without superstrate and (b) with superstrate

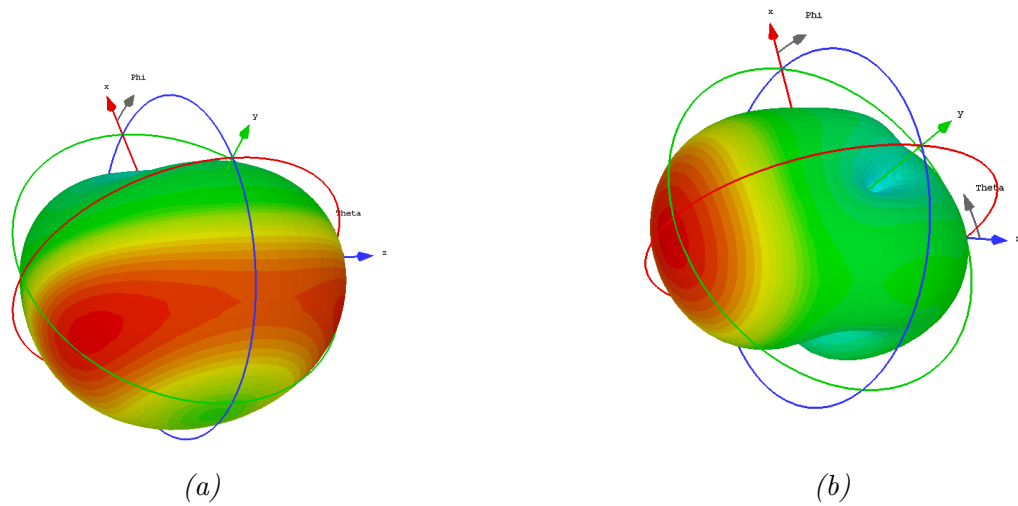


Figure 5.47: 3D radiation pattern of the antenna at 5.63 GHz (a) without superstrate and (b) with superstrate

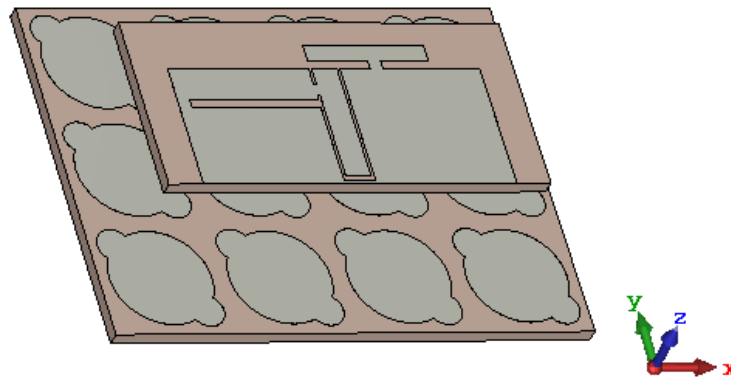


Figure 5.48: Antenna loaded with superstrate from bottom

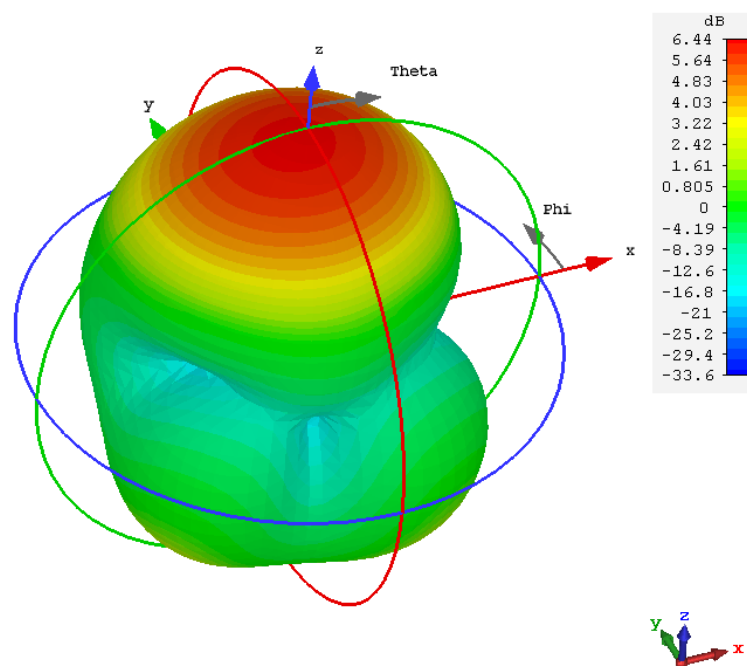


Figure 5.49: Radiation pattern at 5.6GHz when superstrate is loaded from bottom

5.7 Two layer superstrate

In the previous section we discussed how the radiation properties of the antenna can be improved by loading the antenna with a superstrate. In this section we will be analysing whether any further improvement of radiation properties of the antenna is possible by loading one more superstrate printed with the same periodic pattern. When only a single superstrate was used, the optimum spacing of superstrate from the antenna was 20 mm. When one more superstrate layer is added (Fig.5.50), we have to consider the effects of variation in spacing between the two superstrates as well as the spacing between antenna and the superstrate at the bottom. Let us analyse how the bandwidth, resonance frequency and gain is varied with spacing variations.

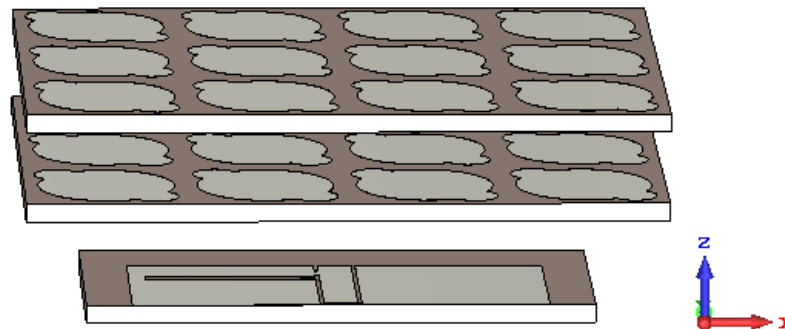


Figure 5.50: Antenna loaded with two layers of superstrate

5.7.1 The effect of spacing variations on bandwidth

The variation in bandwidth when we change the spacing between antenna and superstrate at the bottom as well as spacing between superstrates is studied. The corresponding results are shown in Table 5.3

It can be seen that when we reduce the spacing between antenna and superstrate at the bottom, there is an increase in bandwidth. If we keep the spacing between antenna and bottom superstrate fixed and vary the spacing between the two superstrates, it can be seen that the bandwidth is not much affected by the spacing variation.

h1	Bandwidth(MHz)				
	h2=20	h2=16	h2=6	h2=4	h2=1.6
12	248	250	248	247	243
15	229	235	233	232	230
16	214	225	226	225	221
18	212	222	223	223	221
20	205	216	220	222	219

Table 5.3: Bandwidth variation with antenna and superstrate spacings

$h1$ =spacing between antenna and bottom superstrate in mm

$h2$ =spacing between top surfaces of two superstrates in mm

5.7.2 The effect of spacing variations on resonance frequency

When we vary the spacing between the two superstrates or between the superstrate at the bottom and antenna, the resonance frequency is not much affected. The result of this analysis is shown in Table 5.4

For higher values of spacing between two superstrates, the resonance frequency is almost independent of spacing between antenna and the superstrate at the bottom. But for very small values of spacing between two superstrates, a small increase in resonance frequency is observed. Similarly for a fixed value of spacing between antenna and superstrate at the bottom, small increase in resonance frequency is observed when we reduce the spacing between superstrates.

h1	Resonance frequency(GHz)				
	h2=20	h2=16	h2=6	h2=4	h2=1.6
12	2.57	2.59	2.62	2.63	2.64
15	2.57	2.57	2.60	2.61	2.62
16	2.57	2.57	2.60	2.60	2.62
18	2.56	2.56	2.58	2.58	2.60
20	2.56	2.54	2.56	2.57	2.57

*Table 5.4: Resonance frequency variation with antenna and superstrate spacings
h1=spacing between antenna and bottom superstrate in mm
h2=spacing between top surfaces of two superstrates in mm*

5.7.3 The effect of spacing variations on gain

The result of analysis of gain variation when we change the spacing between superstrates and spacing between bottom superstrate and antenna is shown in Table 5.5

An increase in gain is observed when the spacing between the two superstrates is reduced. For a fixed value of spacing between superstrates, in general, as we increase the spacing between bottom superstrate and antenna, the gain decreases. But for smaller values of spacing between two superstrates, as we increase spacing between the bottom superstrate and antenna, there is an initial increase followed by a decrease for gain.

Based on the above analysis let us select the value of spacing between antenna and bottom superstrate as 15 mm and the spacing between top surfaces of the two superstrates as 1.61 mm. When we load the antenna with these two superstrates the simulated and measured reflection characteristics are illustrated in Fig.5.51. The two results are in good agreement. The measured 2D radiation pattern in XZ and YZ plane are shown in Fig.5.52

h1	Gain(dB)				
	h2=20	h2=16	h2=6	h2=4	h2=1.6
12	5.34	5.54	5.62	5.59	5.55
15	5.29	5.43	5.62	5.63	5.72
16	5.27	5.39	5.58	5.62	5.74
18	5.17	5.26	5.46	5.51	5.65
20	5.06	5.10	5.29	5.35	5.48

Table 5.5: Gain variation with antenna and superstrate spacings

h1=spacing between antenna and bottom superstrate in mm

h2=spacing between top surfaces of two superstrates in mm

The measured gain of the reference antenna loaded with two superstrates is shown in Fig.5.53 At 2.5 GHz, a gain of 5.34 dB is achieved.

When we used single layer superstrate, we obtained a gain of 4.46 dB and the overall height of the antenna was $\lambda_0/6$ where λ_0 is free space wavelength. With the usage of two layer superstrate, we were able to improve the gain to 5.34 dB. In this case the improvement in gain is achieved with the reduction in overall height of the antenna from $\lambda_0/6$ to $\lambda_0/7$.

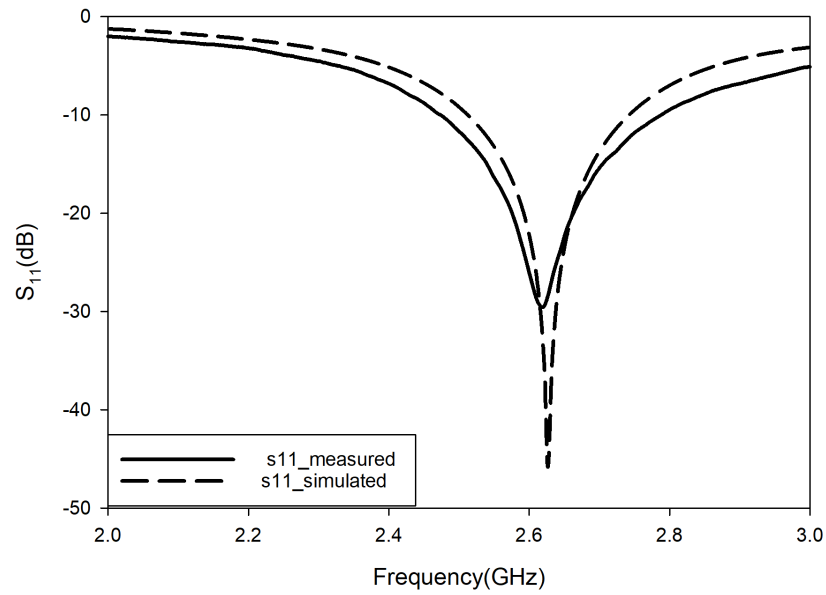


Figure 5.51: Simulated and measured reflection characteristics for antenna loaded with two layers of superstrates

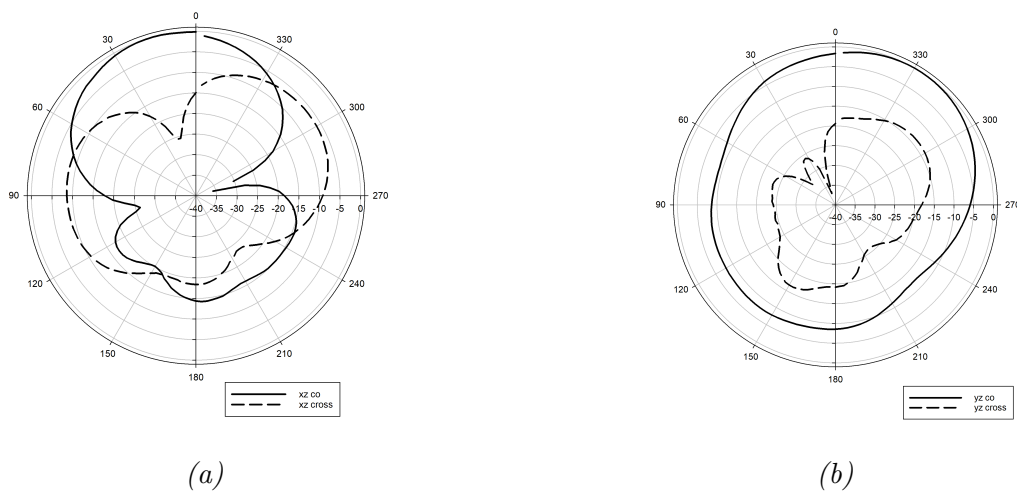


Figure 5.52: Measured 2D radiation pattern of reference antenna loaded with two layer superstrate at 2.5 GHz for (a) XZ plane and (b) YZ plane

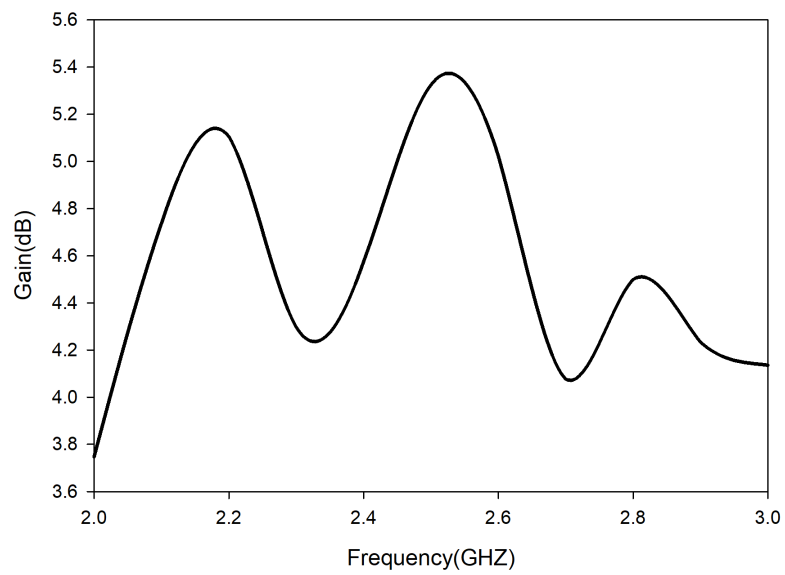


Figure 5.53: Measured gain of reference antenna loaded with two layer superstrate

5.8 Conclusion

Unit cell analysis of a novel design is carried out and the effective parameters are extracted. A high value of effective permittivity is observed for the material. A CPW fed antenna is loaded with a superstrate made up of periodic pattern of this unit cell and its characteristics are analyzed. With the use of superstrate an enhancement in gain is observed for the antenna. The variation in gain when we change the spacing between superstrate and antenna is also analyzed.

References

- [1] Alexopoulos N. and Jackson D., "Fundamental superstrate (cover) effects on printed circuit antennas", *IEEE Transactions on Antennas and Propagation*, Vol.32, No.8, 1984
- [2] Jackson D. and Alexopoulos N., "Gain enhancement methods for printed circuit antennas", *IEEE Transactions on Antennas and Propagation*, Vol. 33, No. 9, 976-987, 1985
- [3] Raj Mittra, Yanfie Li and Kyungho Yoo, "A comparative study of directivity enhancement of microstrip patch antennas with using three different superstrates", *Microwave and Optical Technology Letters*, Vol.52, No.2, 327-330, 2010
- [4] Ge Y., Esselle K. P. and Hao Y., "Design of Low-Profile High-Gain EBG Resonator Antennas Using a Genetic Algorithm", *IEEE Antennas and Wireless Propagation Letters*, Vol 6, 480-483, 2007
- [5] Young Ju Lee, Junho Yeo, R. Mittra R. and Wee Sang Park, "Application of electromagnetic bandgap (EBG) superstrates with controllable defects for a class of patch antennas as spatial angular filters", *IEEE Transactions on Antennas and Propagation*, Vol. 53, No. 1, 224-235, 2005
- [6] Chaimool S., Chung K. L. and Akkaraekthalin P. , Simultaneous gain and bandwidths enhancement of a single-feed circularly polarized microstrip

-
- patch antenna using a metamaterial reflective surface, *Progress in Electromagnetics research B*, Vol.22, 23-37, 2010
- [7] Tarakeswar Shaw, Deepanjan Bhattacharjee, and Debasis Mitra, "Gain enhancement of slot antenna using zero-index metamaterial superstrate", *International Journal of RF and Microwave Computer-Aided Engineering*, Vol. 27, e21078, 2016
- [8] Kim J. H., Ahn C. and Bang J., "Antenna Gain Enhancement Using a Holey Superstrate," *IEEE Transactions on Antennas and Propagation*, Vol. 64, No. 3, 1164-1167, 2016
- [9] Attia H., Yousefi L., Bait-Suwailam M. M., Boybay M. S. and Ramahi O. M., "Enhanced-Gain Microstrip Antenna Using Engineered Magnetic Superstrates," *IEEE Antennas and Wireless Propagation Letters*, Vol. 8, 1198-1201, 2009
- [10] Syed W. H. and Neto A., "Front-to-Back Ratio Enhancement of Planar Printed Antennas by Means of Artificial Dielectric Layers," *IEEE Transactions on Antennas and Propagation*, Vol. 61, No. 11, 5408-5416, 2013
- [11] Sarkhel, A. and Bhadra Chaudhuri S.R., "Enhanced-gain printed slot antenna using an electric metasurface superstrate", *Applied Physics A*, Vol.122, No. 10, 934, 2016
- [12] Hussein Attia, Omar Siddiqui, and Omar Ramahi, "Beam tilting of single microstrip antenna using high permittivity superstrate" *Microwave and Optical Technology Letters* Vol. 55, No.7, 1657-1661, 2013
- [13] Pirhadi A., Bahrami H. and Nasri J., "Wideband High Directive Aperture Coupled Microstrip Antenna Design by Using a FSS Superstrate Layer," *IEEE Transactions on Antennas and Propagation*, Vol. 60, No. 4, 2101-2106, 2012
- [14] Xudong Chen, Tomasz M. Grzegorzcyk, Bae-Ian Wu, Joe Pacheco, Jr. and Jin Au Kong "Robust method to retrieve the constitutive effective parameters of metamaterials", *Phys. Rev. E*, Vol. 70, No. 1, 016608, 2004

- [15] Buell K., Mosallaei H. and Sarabandi K., "A substrate for small patch antennas providing tunable miniaturization factors," *IEEE Transactions on Microwave Theory and Techniques*, Vol. 54, No. 1, 135-146, 2006
- [16] Rainee N. Simons R. N., *Coplanar Waveguide Cicuits, Components and Systems*, John Wiley and Sons, New York, 2001

Chapter 6

Summary and future prospects

A brief summary of experimental and numerical work done is presented in this chapter. The highlights of the CPW fed antenna and the use of superstrates is provided. The chapter concludes with suggestions which will further improve techniques presented in this thesis.

6.1 Thesis Highlights

Timeline in the history of communication, planar antennas, the effect of substrates on antennas, artificially engineered materials and the motivation for the work were described briefly in chapter 1.

A review of CPW fed antennas, different parameter extraction techniques, gain enhancement techniques and the effect of substrates on antennas are carried out in chapter 2.

The methodology used for experimental analysis of antenna, an introduction to simulation software used and antenna fabrication procedure were discussed in chapter 3.

Development of a single band antenna from an open ended CPW transmission line and further modifications to convert it into a dual band antenna were discussed in chapter 4.

Design of a periodic pattern which can be used as a superstrate and its effects on antennas developed in chapter 4 were described in chapter 5.

6.2 Inferences from CPW fed single band antenna

An open ended CPW transmission line is converted into an antenna by shorting the centre conductor to one of the ground planes and carving out a slot in the ground plane

The operating band width of the antenna can be varied by changing the position of the short and adjusting the length of the slot

Cross polar isolation of more than 10 dB is obtained along bore sight

Gain of the antenna observed at resonance frequency is 1.72 dB

6.3 Inferences from CPW fed dual band antenna

An asymmetric T shaped strip is added to the antenna developed in section 4.5 to generate additional resonances. These resonances are merged to form the upper frequency band for the antenna

The impedance matching of both upper and lower frequency bands are affected by the variation in the length of the slot

Cross polarization isolation is better for the lower frequency band compared to the upper frequency band

Gain observed at the resonance frequency for the lower frequency band is 3.24 dB and that of the upper frequency band is 2.4 dB

6.4 Inferences from effect of superstrates on performance characteristics of antennas

By proper design of the unit cell high value of effective permittivity can be attained for a superstrate printed with periodic pattern of unit cell

High value of effective permittivity helps in improving the gain of the antenna Gain can be increased by increasing array size of the antenna- superstrate combination

Antenna gain depends upon spacing between antenna and superstrate

When the spacing between array elements in the periodic pattern is increased, effective permittivity decreases

Effective permeability is not affected by spacing between array elements

Reflection /transmission characteristics of the artificial dielectric is a function of frequency. For the superstrate used, there is more reflection than transmission above 3.5GHz

6.5 Suggestions for future work

In the present work two CPW fed antennas were designed and their characteristics were analysed. Loading these antennas with superstrates were also discussed. Gain of these antennas were improved with the use of superstrates. In addition to that sperstrates provided a parasetic loading which helped in improving impedance matching.

One of the important parameters associated with an antenna is its polarization. In section 4.6.5 we discussed cross polar isolation of dual band antenna. We had excellent cross polar isolation for lower frequency band. The polarization purity associated with upper frequency band was not as good as the lower one. As a future work a new periodic pattern can be designed which when printed on the superstrate will provide all the salient features of the present pattern. At the same time it will improve the cross polarisation in the upper frequency band. A lot of applications are there where circular polarisation is preferred. Design of a periodic pattern which will help in improving the gain of an antenna and at the same time convert linear polarization to circular polarization will be an attractive one.

Chapter 7

List of publications

Journals

- [1] D. Tony, V. P. Sarin, M. S. Nishamol, C. K. Anandan, P. Mohanan, and K. Vasudevan, "Cpw-fed-slot planar antenna for wireless applications," *Microwave and Optical Technology Letters*, vol. 53, no. 11, pp. 2501–2504, 2011.
- [2] Tony D., Sarin V. P., Neeraj K. Pushkaran, Nelson K. J., Mohanan P. and Vasudevan K. Artificial Dielectric Superstrate Loaded Antenna for Enhanced Radiation Performance, *Progress In Electromagnetic Research Letters*(Communicated)
- [3] M. S. Nishamol, V. P. Sarin, D. Tony, C. K. Aanandan, P. Mohanan, and K. Vasudevan, "An electronically reconfigurable microstrip antenna with switchable slots for polarization diversity," *IEEE Transactions on Antennas and Propagation*, vol. 59, pp. 3424–3427, Sep. 2011.
- [4] M. S. Nishamol, V. P. Sarin, D. Tony, C. K. Anandan, P. Mohanan, and K. Vasudevan, "Varactor controlled frequency and polarization reconfigurable microstrip antenna," *International Journal of RF and Microwave Computer-Aided Engineering*, vol. 21, no. 6, pp. 680–686, 2011.
- [5] V. P. Sarin, M. S. Nishamol, D. Tony, C. K. Aanandan, P. Mohanan, and K. Vasudevan, "A broadband l-strip fed printed microstrip antenna," *IEEE Transactions on Antennas and Propagation*, vol. 59, pp. 281–284, Jan 2011.
- [6] V. P. Sarin, M. S. Nishamol, D. Tony, C. K. Aanandan, P. Mohanan, and K. Vasudevan, "A wideband stacked offset microstrip antenna with improved gain and low cross polarization," *IEEE Transactions on Antennas and Propagation*, vol. 59, pp. 1376–1379, April 2011.

- [7] Nishamol M S, Sarin V P, Tony D, C K Aanandan, P Mohanan and K Vasudevan Broadband printed V- slotted cross patch antenna for IEEE802.11a/WiMAX/HiperLAN2 applications, *Progress In Electromagnetic Research Letters*, Vol. 19, pp. 155-161, 2010.
- [8] .Nishamol M S, Sarin V P, Tony D, C K Aanandan, P Mohanan and K Vasudevan Design of Frequency and Polarization Tunable Microstrip Antenna *Microwave Review*, vol.16, No.2, pp.22-28, December 2010.
- [9] Nishamol M S, Sarin V P ,Tony D, C K Aanandan, P Mohanan and K Vasudevan Design of a circularly polarized rectangular microstrip antenna for GPS applications *Microwave and optical technology letters*, vol. 53, No.2, pp.468-470, February 2011.

RESUME

Tony D
Associate Professor
Department of ECE
Viswajyothi College of Engineering
and Technology
Vazhakulam
Muvattupuzha

Mob. : 9497680830
Email : pdtony@gmail.com

Education

M.TECH. Electronics, Department of Electronics, Cochin University of Science and Technology, Cochin, India, 2000.

M.Sc. Electronics Science, Department of Electronics, Cochin University of Science and Technology, Cochin, India, 1997.

Technical Skills

Simulation Software : CST, HFSS, MATLAB
Operating Systems : Windows, Linux
Office Packages : MS Office, LaTeX, LibreOffice

Teaching Experience

- Lecturer, Aquinas College Edacochin
- Lecturer on contract basis, Department of Electronics, CUSAT
- Lecturer, Sr. Lecturer, Assistant Professor and Associate Professor, Department of ECE, Viswajyothi College of Engineering and Technology, Muvattupuzha

Personal Details

Date of Birth : 30th May, 1973
Address : House No. B/1104
Satellite Township
Kakkanad
Cochin 682030
Kerala
Nationality : Indian

